BEHAVIOURAL AND NEURAL ALTERATIONS IN OFFSPRING OF MOUSE DAMS WITH ULCERATIVE COLITIS INDUCED DURING MID-TO-LATE GESTATION

WING YEUNG JIMMY LAM

MPhil

The Hong Kong Polytechnic University

2025

The Hong Kong Polytechnic University

Department of Rehabilitation Sciences

Behavioural and Neural Alterations in Offspring of Mouse Dams with Ulcerative Colitis Induced During Mid-to-Late Gestation

Wing Yeung Jimmy LAM

A thesis submitted in partial fulfilment of the requirements for the degree of Master of Philosophy

July 2025

CERTIFICATE OF ORIGINALITY

I hereby declare that this thesis is my own work and that, to the best of my knowledge and belief, it reproduces no material previously published or written, nor material that has been accepted for the award of any other degree or diploma, except where due acknowledgement has been made in the text.

Wing Yeung Jimmy LAM

Abstract

Rodent models have been pivotal in linking maternal immune activation (MIA) during pregnancy to schizophrenia- and autism-related behaviours in offspring, typically mimicking viral or bacterial infections. However, whether these findings extend to other maternal inflammatory conditions, such as ulcerative colitis (UC), a common inflammatory bowel disease (IBD) in women of childbearing age, remains unclear. This study establishes a chemical-induced UC model in pregnant C57BL/6J mice to investigate its impact on offspring psychological functioning from juvenile (postnatal days 31-40) to adult (postnatal days 73-105) stages.

UC-like pathology in the mouse was induced by administering 2.5% dextran sulphate sodium (DSS) in drinking water from gestational days (GD) 9 to 12, resulting in UC pathology by GD13, persisting through GD17, with elevated maternal inflammatory cytokines (TNF-α and IL-1β). Increased IL-1β in the foetal brain at GD13 indicated foetal brain inflammation, aligning with MIA mechanisms. Offspring behavioural assessments revealed both similarities and differences compared to viral/bacterial MIA models.

The gestational UC model impaired prepulse inhibition (PPI) in adult, but not juvenile, offspring, mirroring the age-dependent onset of schizophrenia-like sensory gating deficits and supporting a link between maternal immune activation and psychopathology. Spatial memory was impaired in juvenile and adult offspring, affecting familiarity discrimination but sparing working memory, suggesting a less severe hippocampal impact than in viral/bacterial MIA models. One plausible explanation for this discrepancy is that immune activation in the UC model may be weaker or more localised than in viral and bacterial infection models. This may also account for the lack of overt depression-like effect or social dysfunction in my model.

Unexpectedly, the UC model induced abnormal persistent latent inhibition (LI), contrasting with deficits seen in infectious MIA models, where disrupted LI is linked to schizophrenia's positive symptoms. The persistent latent inhibition may indicate cognitive rigidity, associated with negative symptoms, possibly tied to glutamatergic hypofunction via NMDA receptors. However, the offspring showed an attenuated psychostimulant response to the NMDA receptor antagonist MK-801, unlike the heightened response in viral/bacterial MIA models, highlighting distinct neurodevelopmental outcomes.

Post-mortem analyses found no increase in NMDA receptor synthesis but revealed elevated hippocampal brain-derived neurotrophic factor (BDNF) from juvenile to adult stages and increased synaptophysin expression in foetal brains at GD13 and GD17. These findings suggest early synaptic integrity changes and sustained BDNF elevation, potentially conferring resilience to NMDA receptor antagonism by supporting synaptic plasticity and mitigating excitotoxicity. This contrasts with synaptic protein deficits in MIA models, further distinguishing the impact of gestational UC.

This study establishes a gestational UC model, demonstrating its distinct impact on offspring neurodevelopment compared to infectious MIA models. It highlights synaptic and behavioural adaptations, challenging assumptions about uniform MIA effects and emphasising the variability of immune-driven psychiatric risks. The lack of social impairment and opposing effects on latent inhibition and NMDA sensitivity underscore UC's specific influence. Future research should explore mechanistic links between gestational UC and neurodevelopmental changes. To conclude, my study stresses the need of exploring diverse maternal inflammatory conditions to advance understanding of their impact on neurodevelopmental disorders and psychopathology.

Publications

Manuscripts

1. Lam, J. W. Y., Ng, M. H. F., Cheng, M. K., Sun, V. K. T., Lau, B. W. M, Cheng, A. S. K, Tai, W. C. S., & Yee, B. K. Behavioural alterations in offspring of mice with gestational ulcerative colitis: parallels and divergences with infection-like maternal immune activation model. *In preparation*

2. Ng, M.H.F., Lam, J. W. Y., Choi, Z. Y. K., Liu, H. F., Ho, P. W. L., Lau, B. W. M., Yee, B. K. (2025). Affective Phenotypes in Heterozygous LRRK2 R1441G Knock-In Mice. *Frontiers in Genetics*, *16*, 1629897. https://doi.org/10.3389/fgene.2025.1629897

3. Sun, V. K. T., Lam, J. W. Y., Ng, M. H. F., Wong, W. Y., Tai, W. C. S., Chow, D. H. K., Cheung, A. K. K., Lau, B. W. M., Cheng, A. S. K., & Yee, B. K. (2025). Early life environmental enrichment yields resilience to selected behavioural and brain responses to 5-fluorouracil in mice. *Brain, Behaviour, and Immunity*, *125*, 334–354. https://doi.org/10.1016/j.bbi.2025.01.009

4. Sun, K. T., Lam, J. W. Y., Tai, W. C. S., Lau, B. W. M., & Yee, B. K. (2022). Within-subjects vs between-subjects co-variation of prepulse-elicited reaction and the diminution of startle to the succeeding pulse stimulus in the prepulse inhibition paradigm. *Behavioural Brain Research*, *430*, 113924. https://doi.org/10.1016/j.bbr.2022.113924

Conference Presentations

1. Lam, J. W. Y., Ng, M. H. F., Cheng, M. K., & Yee, B. K. (2024). "Consequences of DSS-mediated maternal inflammatory bowel disease on brain development and behaviour in the offspring". Presented at PRSC 2024, Hong Kong SAR.

2. Lam, J. W. Y., Ng, M. H. F., Cheng, M. K., Sun, V. K. T., Lau, B. W. M, Cheng, A. S. K, Tai, W. C. S., & Yee, B. K. (2024). "Modification of cognitive development in offspring born to pregnant dams with IBD-like gut pathology induced at mid-gestation". Poster presented at FENS Forum 2024, Vienna, Austria.

Acknowledgements

I express my deepest gratitude to my chief supervisor, Prof Benjamin YEE, whose enthusiasm and expertise in animal behavioural research have been instrumental in shaping my research career. His guidance has instilled confidence and competence, enabling me to pursue my academic journey, and it is an honour to be his student. I am also sincerely grateful to my co-supervisors, Dr Benson LAU and Dr William TAI, for their invaluable technical expertise and steadfast support throughout this research.

Special appreciation goes to Dr Alex CHEUNG for his insightful feedback on foetal brain harvest techniques and to Dr Vic SUN for his valuable contributions to the experimental design of real-time PCR and molecular assay analysis. Their input has significantly enriched this work.

I am profoundly thankful to my dedicated teammates and colleagues, Mr Ka Ming CHENG, Mr Marcus NG, Ms Yvette YIP, Mr Jackie CHAN, and Mr Timothy FUNG, for their unwavering collaboration and support, which fostered an inspiring and productive laboratory environment. I also extend my gratitude to my former colleagues, Mr Victor MA, for his guidance on staining gut tissue with Alcian blue, and Mr Kelvin WONG and Mr Rax LAU, for their essential technical support. Additionally, I acknowledge Ms Zico LEUNG for sharing her expertise on DSS-induced colitis in non-pregnant mice models.

On a personal note, I am deeply grateful to my girlfriend, Ms Alice LEE, for her unwavering encouragement and support as I pursued my MPhil degree. My heartfelt gratitude also extends to my family, Mr and Mrs LAM, Ms Rebecca LAM, and Ms Oliver LAM, for their enduring patience and love, particularly during the challenging period of our father's bladder cancer treatment and surgery. Their strength has been my foundation.

This research was generously funded by The Hong Kong Polytechnic University (Prof Benjamin Yee) and supported by interdepartmental resources from the Mental Health Research Centre (MHRC) at The Hong Kong Polytechnic University (P0040606/1-BBCG). I am deeply appreciative of their support.

Table of contents

List of Figures

List of Tables

Abbreviations

DAB	3, 3'-diaminobenzidine
Abs	Absorbance
Ap3d1	Adaptor Related Protein Complex 3 Subunit Delta 1
ASD	Autism spectrum disorder
Ubc	Beta-2 microglobulin, component of MHC class I molecules
ACTB	Actin beta
BSA	Bovine serum albumin
BDNF	Brain-derived neurotrophic factor
CAF	Centralised Animal Facilities
CD	Crohn's disease
Ct/ dCt	Cycle of threshold/ delta cycle of threshold
°C	Degree Celsius
DNase	Deoxyribonuclease
dNTP	Deoxyribonucleotide mix
Oligo dT	Deoxythymidine oligomer
DSS	Dextran sulfate sodium
DTT	Dithiothreitol
DCX	Doublecortin
ddH2O	Double-distilled water
EPM	Elevated plus maze
ELISA	Enzyme Linked Immunosorbent Assay
FST	Forced swim test
GI	Gastrointestinal
GD	Gestational day
GAPDH	Glyceraldehyde 3-phosphate dehydrogenase
H&E	Hematoxylin and eosin
IHC	Immunohistochemistry
IBD	Inflammatory bowel disease
IFNγ	Interferon γ
IL-1β/ 6/ 10/ 17	Interleukin-1β/ 6/ 10/ 17
i.m	Intramuscular
i.p	Intraperitoneal
kDa	Kilodalton
LI	Latent inhibition
LPS	Lipopolysaccharide
Liq. N	Liquefied nitrogen

MIA	Maternal immune activation
MgCl2	Magnesium chloride
MW	Molecular weight
MWM	Morris water maze
NMDA	N-methyl-D-aspartate
NR	N-methyl-D-aspartate receptor
nPE	Non-pre-exposed
NSAIDs	Nonsteroidal anti-inflammatory drugs
OF	Open field
PFA	Paraformaldehyde
m/v	percentage mass per volume
v/v	percentage volume per volume
PBS	Phosphate buffer saline
Poly I:C	Polyinosinic:polycytidylic acid
Polr2a	Polymerase (RNA) II (DNA Directed) Polypeptide A
PCR	Polymerase chain reaction
PND	Postnatal day
PE	Pre-exposed
POIBD	pregnancy-onset inflammatory bowel disease
PPI	Prepulse inhibition
RIPA	Radioimmunoprecipitation assay buffer
RT-qPCR	Real-time quantitative PCR
RNase	Ribonuclease
RNasin	ribonuclease inhibitor
RNA/ mRNA	Ribonucleic acid/ messenger ribonucleic acid
RT	Room temperature
rpm	round per minute
SAT	Social approach test
SDS-PAGE	Sodium dodecyl sulfate-polyacrylamide gel electrophoresis
SPT	Sucrose preference test
Tbp	TATA-box-binding protein
TLR-2/ 4	Toll-like receptor-2/ 4
TNDS	Trinitrobenzene sulfonic acid
TBST	Tris-buffered saline plus 0.1% Tween 20
TNF or TNF-α	Tumor necrosis factor or tumor necrosis factor-α
UC	Ulcerative colitis
UV	Ultraviolet

Chapter 1 Introduction

1. Introduction

Over the past few decades, accumulating evidence has highlighted the critical role of maternal immune status during gestation in shaping the risk of psychiatric disturbances in offspring. The maternal immune activation (MIA) hypothesis suggests that a shift toward a pro-inflammatory cytokine profile during pregnancy may be particularly detrimental, potentially increasing the likelihood of schizophrenia and autism spectrum disorders in offspring (Brown & Meyer, 2018; Meyer, 2014, 2019). While inflammation is a common feature across various pathological conditions, the immune pathways implicated in the MIA hypothesis—primarily those triggered by infectious agents—differ from those involved in non-infectious inflammatory states (Meyer, 2019; Woods et al., 2021). To investigate the neurodevelopmental consequences of MIA, animal studies have predominantly relied on infection-based models to induce rapid systemic inflammation (Meyer, 2019), as well as localised inflammation models (Aguilar-Valles & Luheshi, 2011). These models have consistently demonstrated behavioural alterations in offspring, including heightened anxiety, impaired spatial recognition, reduced social interaction, depression-like symptoms, altered responses to psychotropic drugs, and deficits in learning and memory (Estes & McAllister, 2016; Kentner et al., 2019). However, these infection-driven and localised inflammation models may not fully capture the immunological complexity of maternal inflammatory bowel disease (IBD) during gestation. The cytokine imbalances and immune response associated with IBD suggest that its effects on offspring neurodevelopment may diverge significantly from those observed in traditional MIA models (Khatri & Kalyanasundaram, 2021). For instance, localised colon inflammation releases inflammatory cytokines (e.g., IL-1, TNF-α, and IL-10), TLR4 and TLR2 are extensively upregulated in IBD (Egger et al., 2000; Szebeni et al.,

2008). Consequently, relying solely on existing MIA frameworks may limit our ability to elucidate the specific neurodevelopmental impacts of gestational IBD, necessitating a more tailored investigative approach. In this study, we investigated for the first time the effects of gestational IBD on offspring, focusing on behavioural outcomes.

1.1. Animal models of maternal immune activation

Maternal immune activation (MIA) refers to the immune response elicited in a pregnant individual by various stimuli, including infections (Al-Haddad et al., 2019; Brown & Meyer, 2018; Mednick et al., 1988), allergens (Schwartzer et al., 2015; Schwartzer et al., 2017), toxins (Block & Calderón-Garcidueñas, 2009; Inoue et al., 2006), stress (Bronson & Bale, 2014; Fineberg et al., 2016; Hawes et al., 2015), and other environmental factors (Hawes et al., 2015; O'Reilly & Reynolds, 2013). Extensive research conducted in rodents and primates suggests plausible mechanisms linking maternal immune activation during pregnancy to schizophrenia. These include downstream events such as cytokine release (Deverman & Patterson, 2009; McAfoose et al., 2009; Patterson, 2009), oxidative stress (Bitanihirwe & Woo, 2011; Sertan Copoglu et al., 2015), apoptosis (Fankhauser et al., 2000; Rath & Aggarwal, 1999), vitamin D status (McGrath et al., 2010), as well as disruptions in zinc (Coyle et al., 2011) and iron metabolism (Aguilar-Valles et al., 2020).

Focusing on cytokine imbalance, the release of inflammatory cytokines and mediators that cross the placental barrier may influence foetal development (Smith et al., 2007; Woods et al., 2023). During critical neurodevelopmental windows, the foetal brain is particularly susceptible to these inflammatory signals, which may disrupt normal processes and contribute to neurological disorders with developmental origins (Meyer, Nyffeler, et al., 2008; Smith et al., 2007). To investigate the association between prenatal immune challenges and such disorders, researchers have developed various animal models that simulate immune activation during pregnancy. These models, encompassing viral (Meyer et al., 2005; Zuckerman & Weiner, 2005), bacterial (Gayle et al., 2004; Glass et al., 2019), toll-like receptor (TLR) signalling in mimicking autoimmune conditions (Missig et al., 2020), and localised inflammatory paradigms

(Aguilar-Valles & Luheshi, 2011; Aguilar-Valles et al., 2007), engage distinct immune mechanisms and consistently induce behavioural alterations in offspring.

Infection-Based MIA Models

The viral mimetic model utilises polyinosinic:polycytidylic acid (Poly I:C), a synthetic double-stranded RNA (dsRNA) compound, to elicit a maternal antiviral inflammatory response (Patterson, 2009). Poly I:C activates toll-like receptor 3 (TLR3) in a manner analogous to dsRNA from live viruses, triggering a signalling cascade that activates nuclear factor kappa B (NFκB) and sustains an acute immune response for approximately three days, as evidenced by elevated maternal rectal temperature (Arsenault et al., 2014). This response rapidly increases maternal serum levels of pro- and anti-inflammatory cytokines, including interleukin (IL)-1, IL-6, tumour necrosis factor-alpha (TNF-α), and type I interferons (e.g., IFN-α and IFN-β)—which peak within three to six hours post-administration (Boksa, 2010; Cunningham et al., 2007; Meyer et al., 2005; Meyer et al., 2009; Meyer, Nyffeler, et al., 2006). These cytokines either stimulate downstream pathways or directly traverse the placenta, influencing foetal brain development with potential long-term consequences, including behavioural impairment (Kwon et al., 2022; Meyer et al., 2009; Smith et al., 2007).

Lipopolysaccharide (LPS), a component of the outer membrane of Gram-negative bacteria, serves as a well-established immunogenic agent for modelling MIA and simulating bacterial infection in animal studies (Matsuura, 2013). Recognised by TLR4, LPS is a potent stimulator of the host's innate immune system, playing a critical role in bacterial pathogen clearance (Park & Lee, 2013). Its administration triggers a robust inflammatory response characterised by fever, cytokine production, and systemic inflammation (Zetterstrom et al., 1998), involving a rapid and significant upregulation of pro-inflammatory cytokines and chemokines (Kentner et al., 2019). LPS-induced

MIA has also been shown to trigger oxidative stress during foetal brain development (Lante et al., 2007; Noworyta-Sokolowska et al., 2013).

The Poly I:C and LPS models have successfully recapitulated core behavioural features of mental disorders suspected to have neurodevelopmental origins, including schizophrenia and autism spectrum disorder (Kentner et al., 2019; Meyer, 2019). These findings have been consistently replicated across studies (Meyer, 2014; Patterson, 2009), reinforcing the model's reliability in studying these conditions. Key behavioural alterations observed in offspring include impairments in PPI, reduced social interaction, and heightened sensitivity to the locomotor-activating effects of psychostimulant drugs such as amphetamine and MK-801(Kentner et al., 2019). While the Poly I:C and LPS models focus on TLR3 and TLR4 activation, respectively, effectively replicating the neurodevelopmental impacts of viral and bacterial prenatal immune challenges, their scope for exploring other immunogenic pathways remains limited. To expand this framework, studies have investigated alternative TLR-stimulating agents, such as imiquimod (TLR7) and resiquimod (TLR7/8), to broaden the understanding of immune-mediated neurodevelopmental effects (Maelfait et al., 2008; Sheng et al., 2024; Sheng & Tobet, 2024). This expanding research on diverse TLR agonists paves the way for investigating non-infectious mimic models, shedding light on the impact of non-infectious immune challenges on neurodevelopmental outcomes.

Localised Inflammation Mimic Model: Turpentine (TURP)

This model involves an intramuscular (i.m.) injection of turpentine, an inflammatory agent that induces localised necrotic damage and activates the host's immune response. Unlike infection-based models, TURP does not introduce a pathogen but instead causes localised necrotic damage (Wusteman et al., 1990). This localised insult initiates a rapid inflammatory cascade, including a febrile response within 24

hours, accompanied by the production of cytokines such as TNF-α and IL-1β at the injury site, followed by the release of IL-6 into the maternal circulation (Aguilar-Valles et al., 2007; Turnbull et al., 2003). Maternal exposure to TURP also alters placental cytokine expression, notably increasing mRNA levels of IL-1β and IL-6, which may influence foetal development. Behavioural outcomes in offspring of TURP-treated dams include impairments in prepulse inhibition (PPI), heightened sensitivity to the locomotor effects of amphetamine, and deficits in cognitive function, as evidenced by performance in the cued version of the Morris water maze (Aguilar-Valles & Luheshi, 2011). These findings underscore the TURP model's utility in exploring the neurodevelopmental consequences of localised maternal inflammation, paving the way for further investigation into its long-term behavioural implications.

1.1.1. Limitations of MIA Models and Transition to Non-Infectious Inflammation

Infectious and non-infectious maternal immune activation (MIA) models, such as those using turpentine (TURP), polyinosinic:polycytidylic acid (Poly I:C), and lipopolysaccharide (LPS), effectively link acute maternal inflammation during pregnancy to offspring behavioural abnormalities relevant to schizophrenia and autism spectrum disorder (ASD) (Kentner et al., 2019; Meyer, 2019; Meyer, Nyffeler, et al., 2006). These models, however, induce transient inflammation through single toll-like receptor (TLR) pathways (e.g., TLR3 for Poly I:C, TLR4 for LPS), failing to reflect the chronicity and complexity of non-infectious inflammatory conditions. Maternal conditions, such as obesity (Kong et al., 2020) and famine (Susser & St Clair, 2013), as well as vitamin D deficiency (Kovacs, 2013; McGrath et al., 2010), are associated with heightened neurodevelopmental risks. However, it remains uncertain whether findings from acute MIA models extend to these chronic states. Inflammatory bowel disease (IBD) characterised by prolonged inflammation, activation of TLR2 and TLR4, and distinct cytokine profiles (e.g., elevated IL-1β, TNF-α), differs markedly from acute infectious responses (Abraham & Cho, 2009; Balding et al., 2004; Maeda et al., 1992).

Epidemiological studies provide inconclusive evidence regarding the link between maternal IBD and neurodevelopmental outcomes in offspring. While some studies report no increased risk of neurodevelopmental disorders associated with maternal IBD, others suggest an association, particularly when IBD is active during pregnancy. The precise relationship remains unclear, but maternal IBD-related risk factors, such as distinct inflammatory profiles (Rogler & Andus, 1998), vitamin D deficiency (Ananthakrishnan, 2016; Yang et al., 2024), and altered gut microbiota (Shan et al., 2022), may elevate the risk of neurodevelopmental disorders in offspring (Jasarevic,

Rodgers, et al., 2015; Vuillermot et al., 2017). Maternal IBD is plausibly a significant risk factor for conditions such as schizophrenia and ASD in offspring. The limited ability of existing MIA models to capture non-infectious inflammation underscores the need for an IBD-specific model to elucidate its impact on neurodevelopmental disorders. Therefore, the present study employs an animal model to investigate the association between maternal IBD and its neurodevelopmental implications for offspring.

1.2. Inflammatory bowel disease

1.2.1. Prevalence of inflammatory bowel disease

Inflammatory bowel disease is characterised by inflammation of the gastrointestinal (GI) tract, and ulcerative colitis (UC) is a common subtype that primarily affects the colon (Liu et al., 2022). The global rise in IBD prevalence is a significant public health issue (Chen et al., 2023; Kappelman et al., 2013; Pedersen et al., 2013). Notably, IBD commonly affects women during their reproductive years (Abhyankar et al., 2013; Cornish et al., 2007; Kim et al., 2021), necessitating further research into its impact on fertility as well as the medical management of IBD during pregnancy (Hashash & Kane, 2015). A distinct subpopulation of women who experience the first onset of IBD symptoms and diagnosis during pregnancy, or pregnancy-onset IBD (POIBD), has been identified as predominantly presenting with UC, and were mostly diagnosed during the first trimester of pregnancy (Yu et al., 2021). If validated, POIBD and/or flare-ups associated with IBD during pregnancy may represent additional risk factors for neurodevelopmental disorders in offspring through disruptions of early brain developmental processes. This would further support the generality of the MIA hypothesis, regarding foetal inflammation *in utero* during early gestation.

Although the exact mechanism and cause of UC are still unclear, it involves

multiple toll-like receptors (TLRs)-mediated innate immune signalling pathways in the pathogenesis (Lu et al., 2018), including TLR2/6 promoting colitis and TLR3 causing intestinal tissue destruction and ulceration (Levin & Shibolet, 2008; Pierik et al., 2006). Also, upregulation of inflammatory cytokines is a hallmark of IBD. The upregulation of pro-inflammatory cytokines, notably tumor necrosis factor-alpha (TNF-α), with elevated levels detected in both serum and colon of affected individuals (Murch et al., 1991). Anti-TNF-α therapies, such as monoclonal antibodies, effectively reduce inflammation and induce remission in many IBD patients (Nielsen et al., 2013; Su et al., 2002). These immune responses, driven by TLR activation and cytokine imbalances during pregnancy, align with the MIA hypothesis, potentially influencing offspring's neurodevelopmental trajectories and increasing risks for disorders like ASD and schizophrenia (Estes & McAllister, 2015; Meyer, 2014).

Although several studies have explored the effects of IBD on pregnancy outcomes, the long-term neurodevelopmental impact on offspring remains largely unexplored, with epidemiological findings still inconclusive (Dotan et al., 2013; Norgard et al., 2019; Prentice et al., 2024). Dotan et al. (2013) observed a trend towards increased motor and neurological problems, such as epilepsy, among children born to mothers with IBD. Similarly, Shero and Pandeya (2022) proposed a plausible link between maternal Crohn's disease (CD), a subtype of IBD, particularly in cases complicated by iron deficiency anaemia, and an increased risk of attention deficit hyperactivity disorder (ADHD) in offspring. More recent research has also suggested an association between maternal IBD and neurodevelopmental disorders, including autism spectrum disorder (ASD) (Sadik et al., 2022). However, findings from two Danish nationwide studies by Andersen et al. (2014) and Jolving et al. (2017) did not indicate an overall increased risk of ASD or schizophrenia in offspring with maternal IBD. These inconsistencies

may be attributed to various confounding factors in human studies, such as medication use, the lack of differentiation between IBD subtypes (ulcerative colitis vs Crohn's disease), and the failure to analyse POIBD subpopulations separately. To minimise these confounding variables, the mouse IBD model has been employed as an initial step to clarify the association between maternal IBD and the long-term neurodevelopmental implications for offspring.

This study is the first to address a critical research gap by examining whether IBD-like pathology in mice leads to long-term behavioural changes in offspring. Using a gestational UC-like face validity model (Yang & Merlin, 2024), we compare its outcomes with infection-like and localised inflammation MIA models. This investigation explores whether transient gut-derived inflammation produces neurodevelopmental effects on offspring similar to those triggered by infection-like stimuli during a comparable gestational window (see **Table 1.1**). By expanding beyond MIA infection-based paradigms, this approach seeks to clarify the neurodevelopmental consequences of non-infectious maternal inflammatory conditions in offspring.

1.2.2. Review of animal models of IBD

Animal models are critical for studying the pathogenesis of IBD, developing novel therapeutics, and understanding histopathological changes in the GI tract. These models replicate key pathological hallmarks of human IBD—including inflammation, epithelial damage, and immune dysregulation—offering a controlled framework for mechanistic and therapeutic studies (Goyal et al., 2014). Additionally, the animal model minimises confounding variables, such as the growth environment in humans, and enables detailed monitoring of foetal development. Various IBD animal models have been established, encompassing chemically induced, cell-transfer, spontaneous, congenital, and genetically engineered approaches (Mizoguchi, 2012; Randhawa et al.,

2014). Selecting an appropriate model for this study requires meeting specific criteria: the ability to induce ulcerative colitis (UC), minimal trauma during administration, reduced confounding effects on foetal development, and sufficient face validity to reflect human IBD pathology.

Among these, chemically induced models are the most widely utilised due to their reproducibility, ease of induction, and capacity to mirror gut histopathological changes observed in human IBD, particularly in the colon (Kiesler et al., 2015). Next, I reviewed four commonly employed chemically induced IBD rodent models—dextran sodium sulphate (DSS), trinitrobenzene sulphonic acid (TNBS), oxazolone, and acetic acid—to inform the selection process for investigating gestational IBD.

Dextran Sodium Sulphate (DSS)

The DSS-induced colitis model closely mimics human UC, producing reproducible morphological and symptomatic features. DSS, a sulphated polysaccharide, exerts direct toxic effects on colonic epithelial cells, disrupting mucosal integrity and increasing permeability to large molecules (See **Fig. 1.1**). This leads to acute colitis characterised by hyperaemia, ulcerations, submucosal oedema, and granulocyte infiltration, often manifesting as bloody diarrhoea. DSS also elevates pro-inflammatory cytokines (e.g., IL-1β, IL-6, and TNF-α) in the distal colon (Egger et al., 2000). Typically, colitis is induced by administering 2–5% DSS (w/v) in drinking water to mice for 3–8 days (Chassaing et al., 2014; Wirtz et al., 2017), followed by histological and cytokine analyses to confirm disease induction.

Trinitrobenzene Sulphonic Acid (TNBS)

TNBS induces transmural inflammation and cell-mediated immune responses, closely resembling features of Crohn's disease. In murine models, Crohn's disease-like pathology is triggered by the rectal administration of low-dose TNBS in ethanol under

anaesthesia, following a 12–24-hour fasting period (Antoniou et al., 2016; Fuss et al., 2004). This procedure induced chronic colitis, characterised by severe diarrhoea, weight loss, and rectal prolapse, mirroring key aspects of human Crohn's disease

Oxazolone

The oxazolone model replicates ulcerative colitis (UC) by inducing mucosal inflammation and microulceration in the distal colon (Randhawa et al., 2014). It is administered rectally in ethanol following skin pre-sensitisation, though responses vary across mouse strains—for example, C57BL/6 mice exhibit resistance (Pal-Ghosh et al., 2008). This model is particularly useful for investigating UC-specific immunological processes and assessing the Th2-mediated immune response (Heller et al., 2002).

Acetic Acid

Acetic acid induces non-transmural inflammation through intrarectal administration, replicating key aspects of human IBD histopathology and inflammatory mediator profiles (Dieleman et al., 1996; Randhawa et al., 2014). It facilitates neutrophil infiltration into intestinal tissue, providing a simple yet effective model for studying acute inflammation (Lee et al., 2023).

1.2.3. Selection of the DSS Model for Maternal IBD Studies

Among the chemically induced models reviewed, the DSS-induced colitis model is considered the most suitable for investigating gestational IBD. Its advantages include non-invasive administration via drinking water, which eliminates the trauma and procedural complexity associated with intrarectal methods (e.g., TNBS, oxazolone, and acetic acid). Furthermore, DSS reliably induces UC-like pathology in the colon within a short timeframe, characterised by reproducible histopathological changes, including inflammation and epithelial damage. This model also minimises potential confounding effects on foetal development due to its straightforward delivery and lack of additional

agents like ethanol (Chen et al., 2003; Guerri et al., 2009). Consequently, I selected to use the DSS model to establish a robust framework for examining gestational IBD and its neurodevelopmental implications.

1.2.4. Introduction DSS-induced colitis

The DSS model's origins trace back to the 1960s, when extracts of red seaweed (containing sulphated polysaccharides like carrageenan) were found to induce UC in guinea pigs, rabbits, and rodents (Marcus & Watt, 1969). Subsequent research identified carrageenan's hydrolysis products (molecular weight ~40–50 kDa) as particularly ulcerogenic. In 1985, Ohkusa's group demonstrated that DSS administration in hamsters produced colitis symptoms akin to human IBD (Ohkusa, 1985). By 1990, they refined the model in mice, showing that 2–5% DSS in drinking water for a few days induced acute, reproducible colonic inflammation—characterised by erosions, crypt loss, ulcers, and granulocyte infiltration (Okayasu et al., 1990).

The severity and localisation of DSS-induced colitis depend on its molecular weight: 40-kDa DSS causes diffuse colitis in the middle and distal colon by forming lipid complexes with medium-chain fatty acids, whereas 5-kDa DSS targets the cecum and upper colon (Kitajima et al., 1999; Okayasu et al., 1990). This controllability makes DSS a valuable tool for studying UC-like pathology (see **Fig. 1.1**, adapted from Yang and Merlin (2024)). The mechanism involves: (1) DSS disrupting the mucus and epithelial layers, allowing bacterial penetration into underlying tissues; (2) triggering innate lymphoid responses and pro-inflammatory cytokine release (e.g., IL-1β, IL-6, TNF-α); and (3) recruiting macrophages and neutrophils to the colon.

The innate immune response to mucosal injury in the DSS-induced IBD model involves toll-like receptors (TLRs) in its pathogenesis. DSS, a sulphated polysaccharide, disrupts colonic epithelial layers, increasing permeability and exposing the underlying mucosa to luminal microbiota and their associated pathogen-associated molecular patterns (PAMPs) (Chassaing et al., 2014; Eichele & Kharbanda, 2017; Yang & Merlin, 2024). TLRs, expressed on epithelial cells, macrophages, and dendritic cells within the

gut, recognise these PAMPs—such as lipopolysaccharides, flagellin, and bacterial DNA—triggering a signalling cascade that activates NFκB and mitogen-activated protein kinases (MAPKs) (Cario, 2010; Rakoff-Nahoum et al., 2004). This leads to the upregulation of pro-inflammatory cytokines, including IL-1β, IL-6, and TNF-α, further amplifying colonic inflammation (Coccia et al., 2012; Egger et al., 2000). Unlike lipopolysaccharide (LPS), which primarily stimulates TLR4, both TLR4 and TLR2 play key roles in DSS-induced colitis. Studies have shown that TLR4-deficient mice experience exacerbated inflammation due to impaired mucosal repair (Gibson et al., 2010), whereas TLR2-deficient models exhibit attenuated colitis and promote mucosal integrity, highlighting their distinct regulatory roles (Cario, 2010; Rakoff-Nahoum et al., 2004). This TLR-mediated immune activation underpins the histopathology observed in DSS-induced colitis.

DSS administration induces not only localised gut inflammation (e.g. shortened gut length) but also systemic effects, including splenomegaly and significant weight loss. The enlarged spleen reflects heightened immune activation and lymphocyte proliferation, while the shortened gut—spanning the caecum, colon, rectum, and anus—results from epithelial loss and tissue remodelling (Chassaing et al., 2014). Body weight loss, often exceeding 10–20% of baseline, correlates with disease severity and is a widely used indicator of successful IBD induction (Wirtz et al., 2017). Some studies employ the disease activity index (DAI), a composite score based on weight loss, stool consistency, and rectal bleeding, to assess colitis progression. However, the DAI's subjective nature—relying on observational assessments—limits its reliability relative to objective measures such as body weight loss (Cooper et al., 1993).

For robust validation of the DSS-induced IBD model, histological analysis and quantification of localised inflammatory cytokine gene expression in the colon is

preferred (see **Method section**). Histological changes—including crypt distortion, ulceration, and inflammatory cell infiltration—provide a direct and quantifiable assessment of tissue damage (Chassaing et al., 2014). Concurrently, increased mRNA expression of cytokines such as IL-1β, IL-6, and TNF-α in colonic tissue, measured via quantitative PCR, can confirm the inflammatory state and align with TLR-driven responses (Egger et al., 2000). Body weight change serves as an additional practical metric, reinforcing successful induction and complementing these molecular and histological endpoints. Collectively, these objective measures validate the DSS model's efficacy in replicating UC-like pathology in this study.

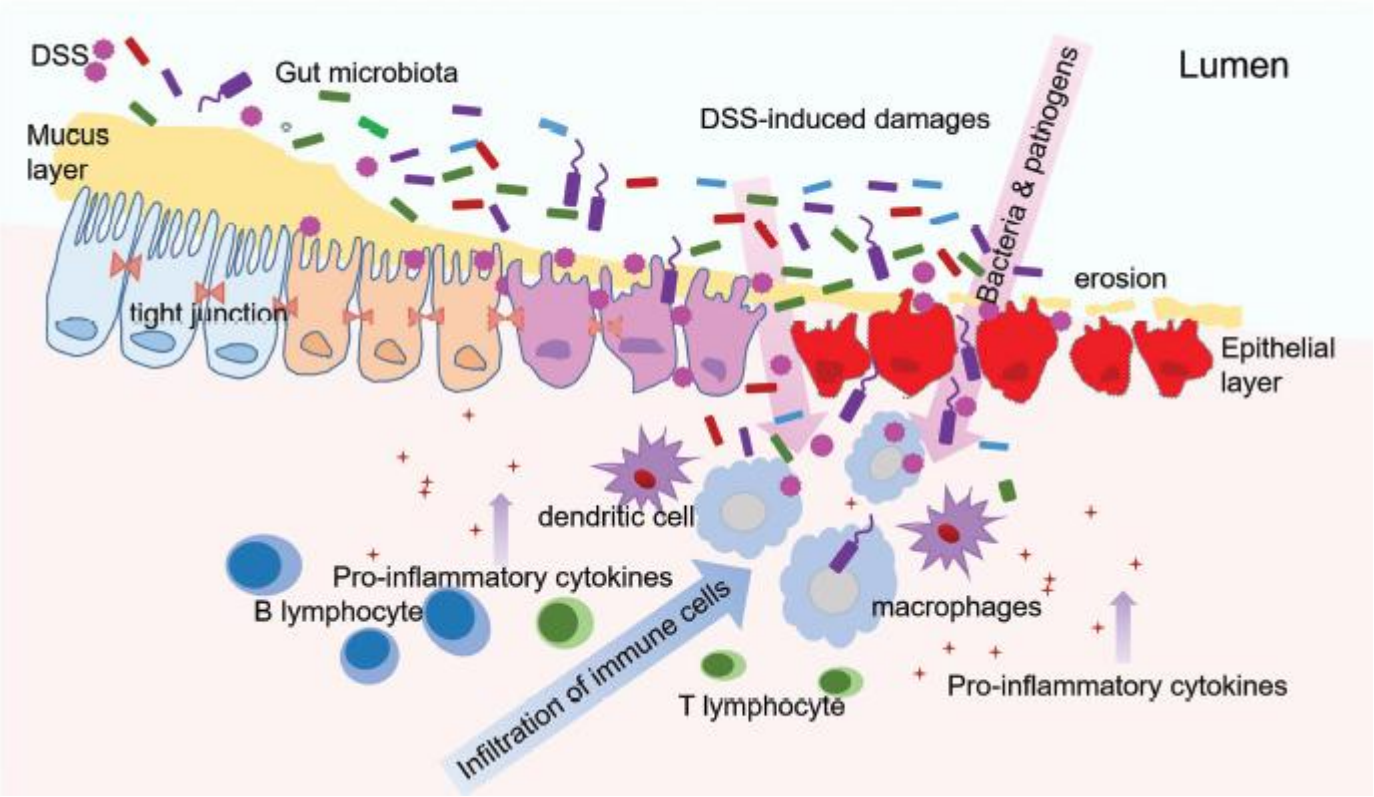

Figure 1.1. The schematic diagram of DSS-induced colitis.
The diagram is adapted and modified from Yang and Merlin (2024). (1) The DSS could disrupt the mucus layers and damage the epithelial layer. Afterwards, the damaged layer allows bacteria and/or intestinal content to penetrate underlying tissues. (2) These pathogens stimulate the innate lymphoid response to secrete pro-inflammatory cytokines and chemokines. (3) Thereby, an influx of inflammatory macrophages and neutrophils occurs in the colon area.

1.2.5. Establishing the gestational DSS model: Preliminary experiments

Although the DSS-induced colitis model has been extensively studied in non-pregnant animals, its application in gestational contexts remains unexplored (Yang & Merlin, 2024). Therefore, optimising the dose and duration of DSS in pregnant mice is essential. This study is the first to develop and implement a gestational DSS treatment protocol to investigate the effects of maternal IBD on offspring neurodevelopment. To ensure the model's feasibility for subsequent behavioural analyses, three preliminary experiments were conducted to optimise DSS dosage, treatment duration, and survival outcomes in pregnant mice.

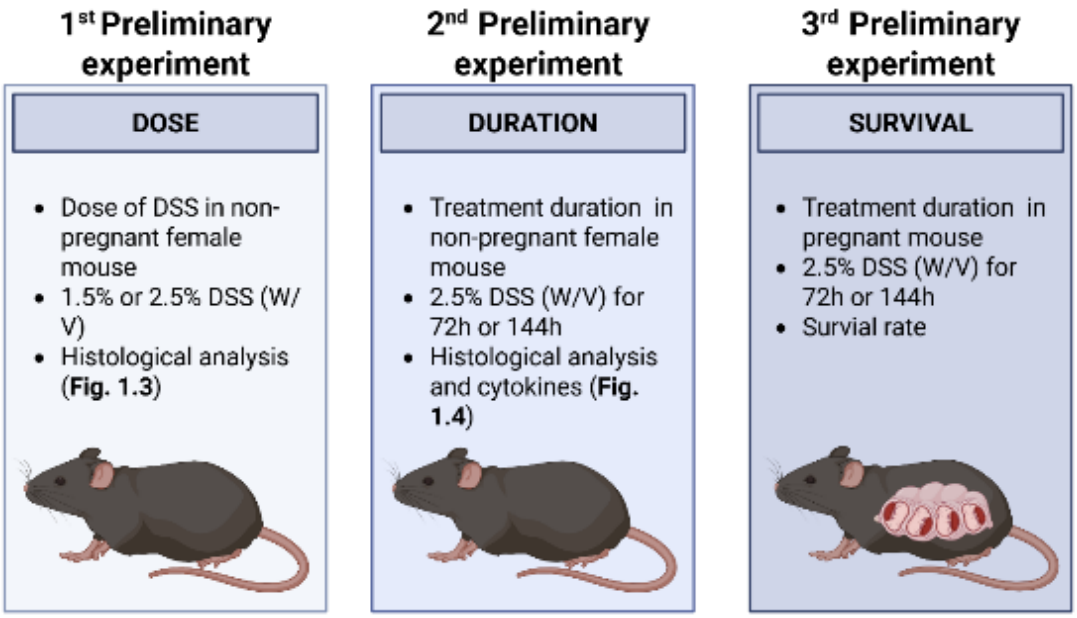

Figure 1.2 The schematic diagram of preliminary experiments.
The preliminary experiment consists of three parts. The first experiment involved non-pregnant female mice to evaluate the DSS dose using histological assessment. The second experiment involved non-pregnant female mice to evaluate the treatment duration of the 2.5% DSS. The third experiment involved pregnant mice to evaluate the survival rate in 2.5% DSS for 72h or 144h.

The first experiment aimed to determine an effective DSS concentration using non-pregnant female mice. Various concentrations were tested to identify a dose that reliably induces UC-like pathology, characterised by histopathological changes (**Fig. 1.3**) and without excessive mortality. As DSS sensitivity varies by strain and laboratory conditions, the optimal concentration was selected accordingly. Comparing 2.5% and 1.5% DSS (w/v), a concentration of 2.5% DSS in drinking water was chosen, as it consistently induced colonic inflammation while maintaining animal viability, aligning with standard IBD induction protocols (Chassaing et al., 2014).

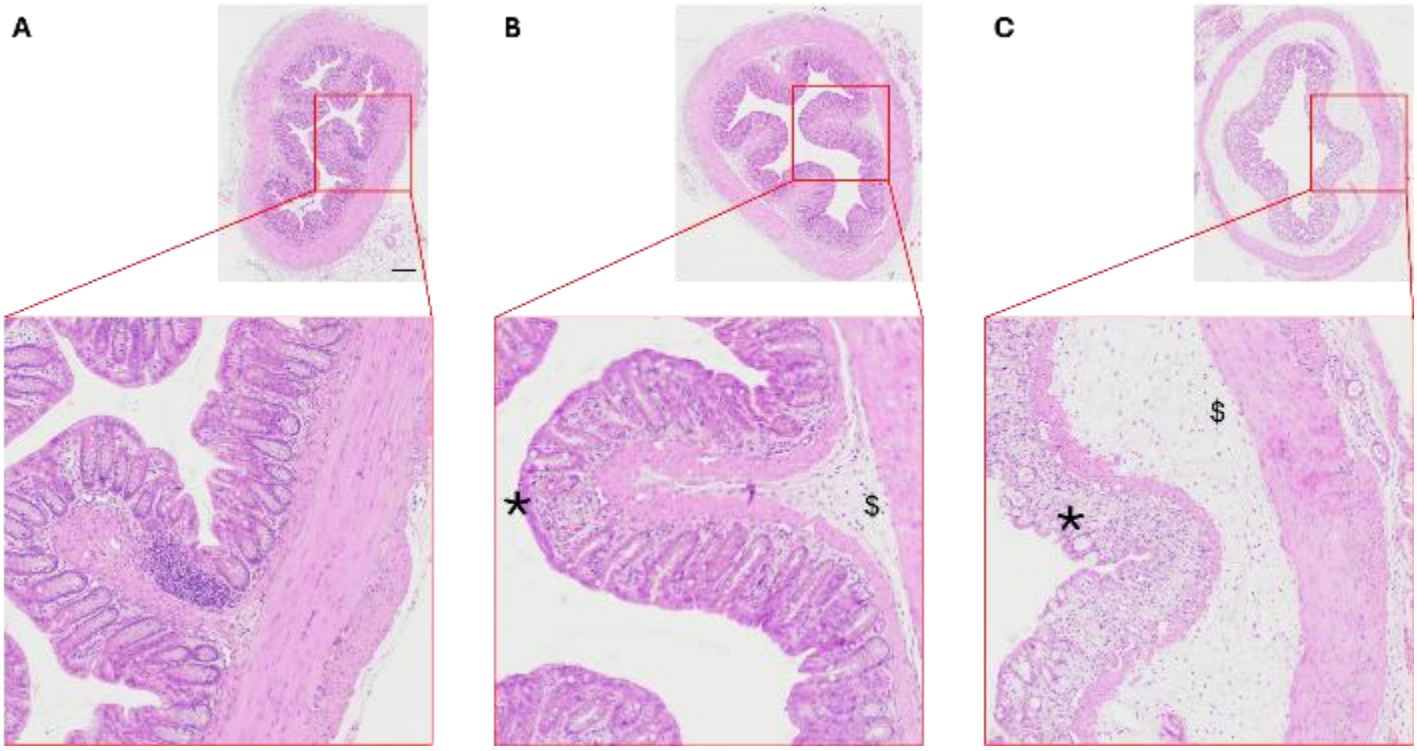

Figure 1.3. Representative images of colon sections stained with H&E from non-pregnant female mice treated with vehicle, 1.5% DSS, and 2.5% DSS for 6 days. **(A)** Colon section from the vehicle-treated group. **(B)** and **(C)** Colon sections from mice treated with 1.5% and 2.5% DSS, respectively. All images were captured at 10X magnification. The lower images show magnified views of the regions marked by red squares in the upper images. The **($)** symbol indicates submucosal oedema, while the (*) symbol marks infiltrated cells. Scale bar = 250 µm

The second experiment focused on determining the appropriate treatment duration, either 3 days or 6 days, using non-pregnant female mice. Animals received 2.5% DSS and were harvested after 3 or 6 days to evaluate colitis severity via histological analysis and cytokine expression in the colon. Results showed that the 6-day treatment significantly elevated pro-inflammatory cytokines, including IL-1β, IL-17, interferon (IFN)-γ, and TNF-α, compared to the control group (see **Fig. 1.4**), suggesting a more pronounced inflammatory response with longer exposure. Additionally, the 3-day treatment significantly increased both the pro-inflammatory cytokine TNF-α and the anti-inflammatory cytokine IL-10. However, as this experiment was conducted in non-pregnant mice, further validation in a gestational context was necessary.

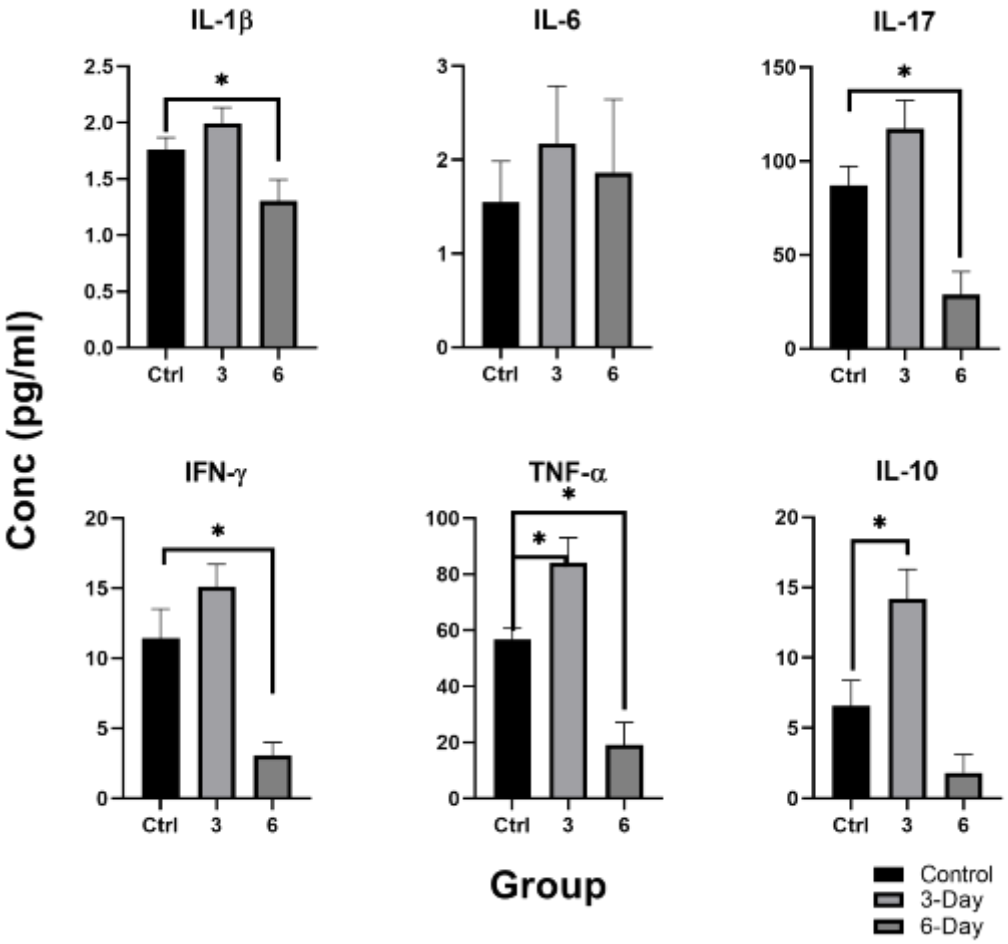

Figure 1.4. The effect of IBD administration on pro- or anti-inflammatory cytokines in serum from non-pregnant mice.
The bar plots show the concentration of multiple cytokines in the serum of adult female mice following exposure to 2.5% DSS for 3 days or 6 days (light and dark grey bars, respectively) for the induction of IBD pathology. Data are presented as mean ± SEM (n = 9 in the control condition (black bars) and DSS treatment for 3 days; n = 8 in DSS treatment for 6 days). Symbol (*) indicates a statistically significant difference of $p < 0.05$ compared with the control group (one-way ANOVA, Tukey HSD post-hoc test).

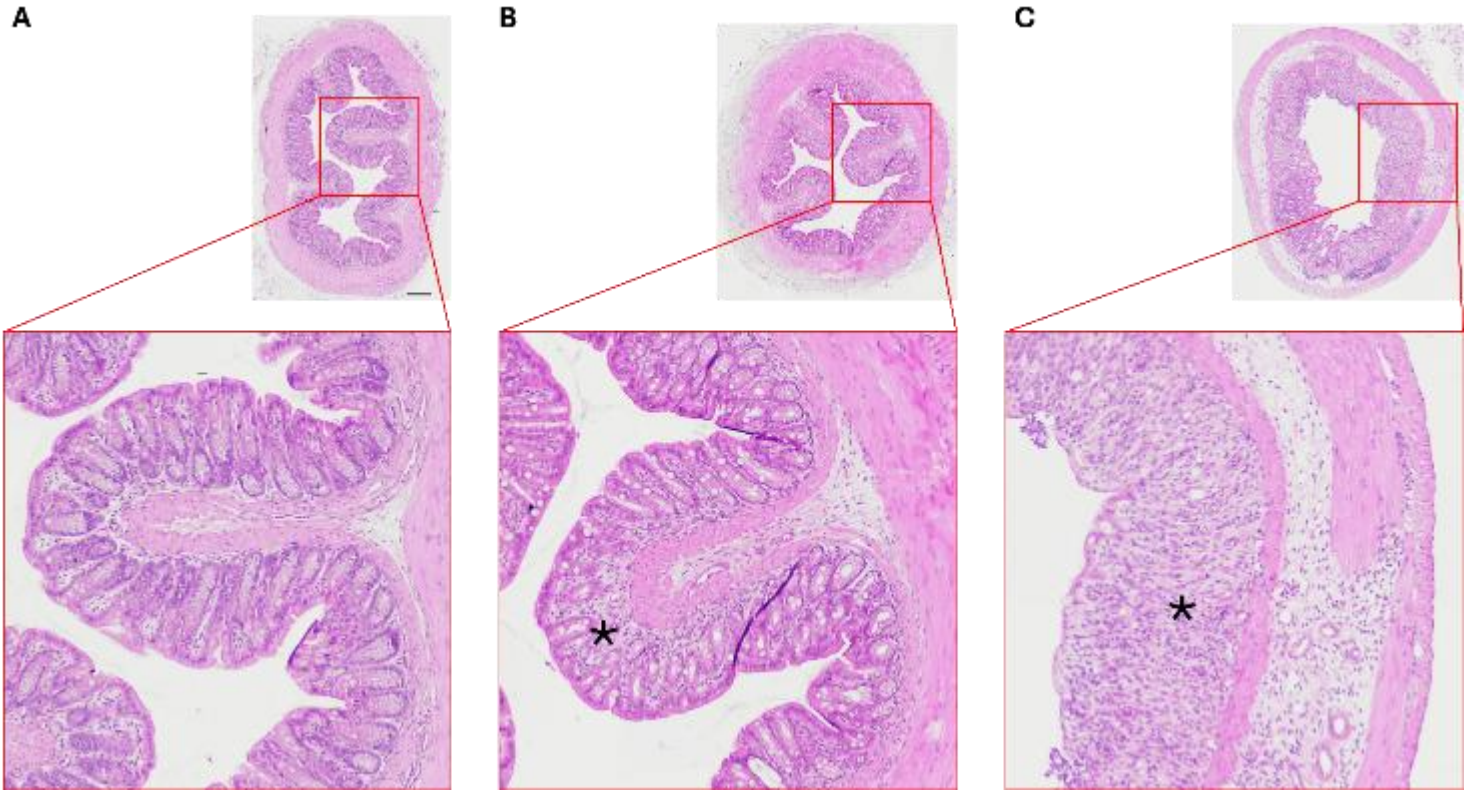

Figure 1.5. Representative images of colon sections stained with H&E from non-pregnant female mice treated with vehicle and 2.5% DSS for 3 and 6 days.
(A) Colon section from the vehicle-treated group. **(B)** and **(C)** Colon sections from mice treated with 2.5% DSS for 3 days and 6 days, respectively. All images were captured at 10X magnification. The lower images present magnified views of the regions marked by red squares in the upper images. The symbol (*) denotes infiltrated cells. Scale bar = 250 μm.

The third experiment assessed the effects of 2.5% DSS treatment in pregnant dams to evaluate survival and suitability for gestational studies. Dams were exposed to DSS for either 3 or 6 days, starting at gestational day 9 (GD9), and monitored for mortality and overall health. The 6-day treatment significantly increased maternal mortality, posing practical challenges for subsequent experiments. Higher mortality rates reduced the number of viable offspring available for behavioural analysis and disrupted postpartum maternal care, introducing potential confounding factors in neurodevelopmental outcomes. Additionally, the 6-day treatment resulted in greater severity of symptoms compared to the 3-day treatment, as illustrated in **Figs 1.6 and 1.7.** To balance the need for sufficient acute inflammation to model IBD with maternal and offspring survival, the 3-day treatment period was deemed optimal.

Based on these preliminary findings, a gestational DSS protocol using 2.5% DSS in drinking water for 72 hours (GD9–GD12) was deemed the most practical approach. This regimen effectively induces UC-like pathology (**Fig. 1.8**) in pregnant dams while minimising mortality, ensuring sufficient litter survival for behavioural experiments. With this validated model established, the following section details the behavioural tests used to evaluate the long-term neurodevelopmental impact on offspring exposed to gestational IBD.

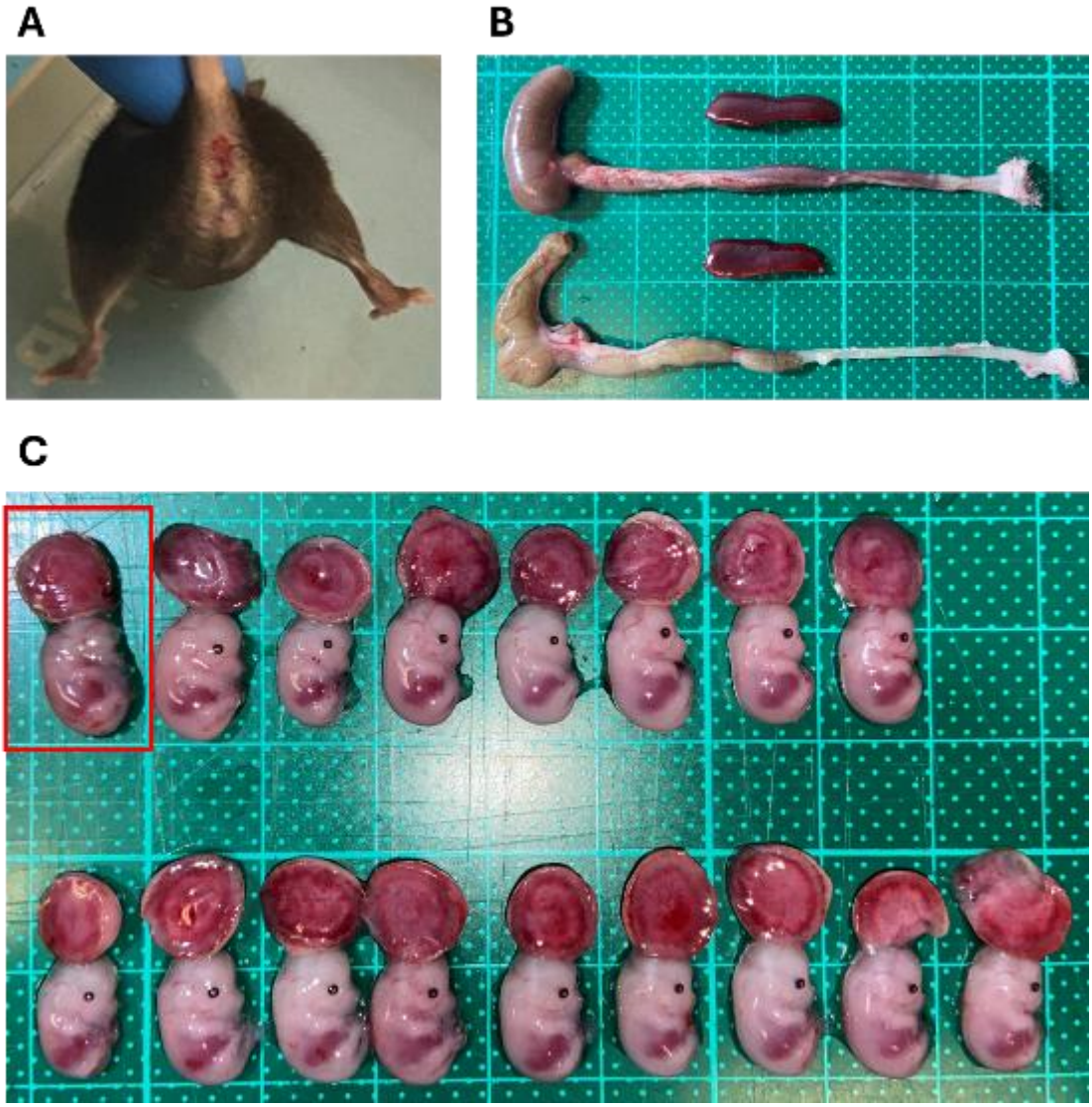

Figure 1.6. Representative images of pregnant mice and their tissues following 2.5% DSS treatment (via drinking water) from GD9 to GD12 (i.e., for a total of 72 hours), harvested at GD13.
(A) Representative image of the rectal area of a DSS-treated dam after 3 days of exposure. **(B)** Representative images of the gut and spleen from DSS-treated (upper panel) and control (lower panel) dams, harvested on GD13. Compared with controls, DSS-treated dams exhibit shorter gut segments, including the caecum, colon, rectum, and anus. **(C)** Representative images of the foetus and placenta from DSS-treated (upper panel) and control (lower panel) dams, harvested on GD13. Foetuses from DSS-treated dams appear smaller and show signs of deformation. A deformed foetus, highlighted with a red square, is visible in the left corner of the control panel. The green square provides a scale reference of 1 cm × 1 cm.

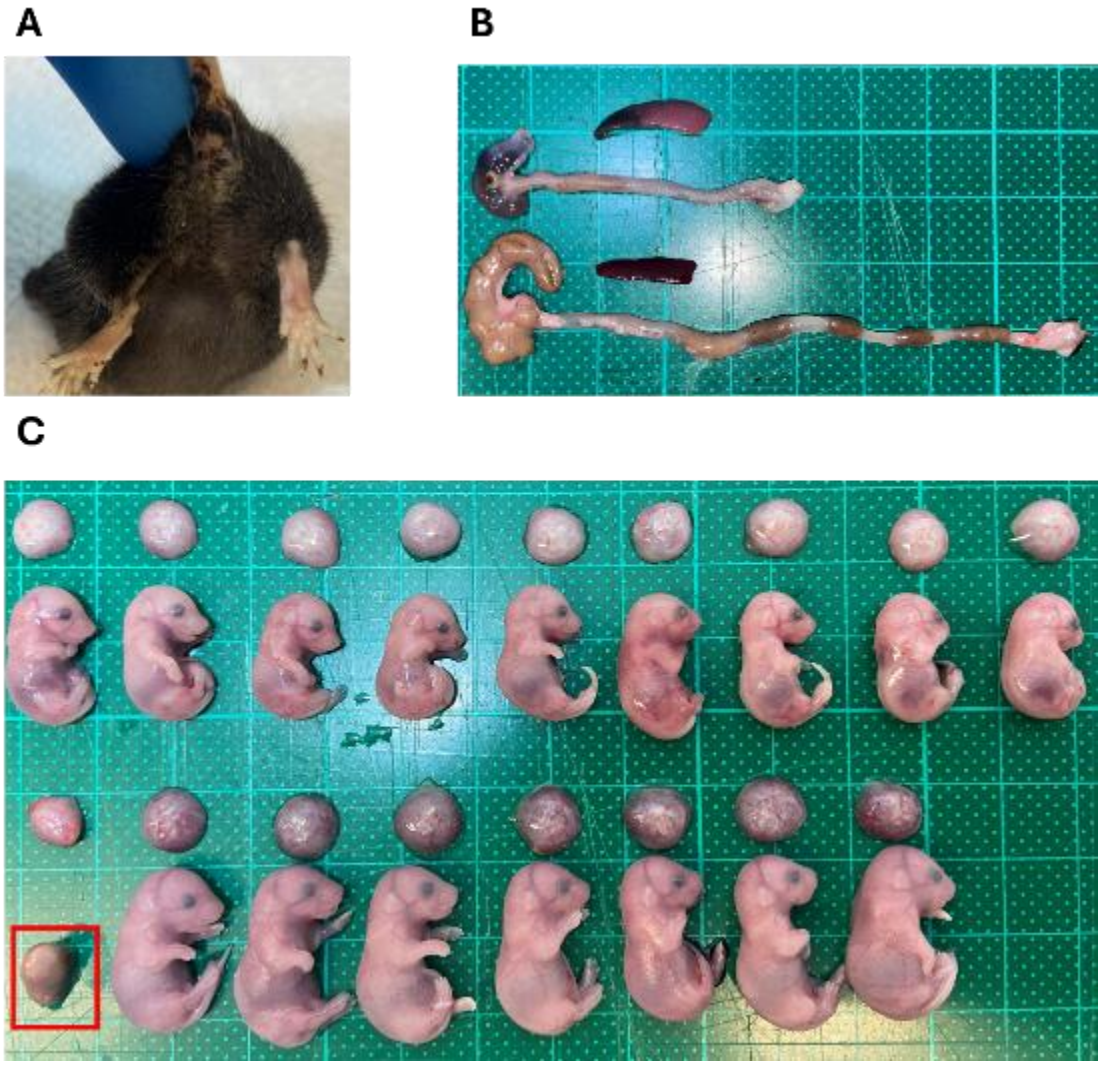

Figure 1.7. Representative images of pregnant mice and their tissues following 2.5% DSS treatment (via drinking water) from GD9 to GD15 (a total of 144 hours), harvested at GD17.

(A) Representative image of the rectal area of a DSS-treated dam after 6 days of exposure. **(B)** Representative images of the gut and spleen from DSS-treated (upper panel) and control (lower panel) dams. DSS-treated dams exhibit a shorter gut—including the caecum, colon, rectum, and anus—as well as an enlarged spleen. **(C)** Representative images of the foetus and placenta from DSS-treated (upper panel) and control (lower panel) dams. DSS-treated foetuses appear smaller compared to controls. A resorbed foetus, highlighted with a red square, is visible in the left corner of the control panel. The green square provides a scale reference of 1 cm × 1 cm.

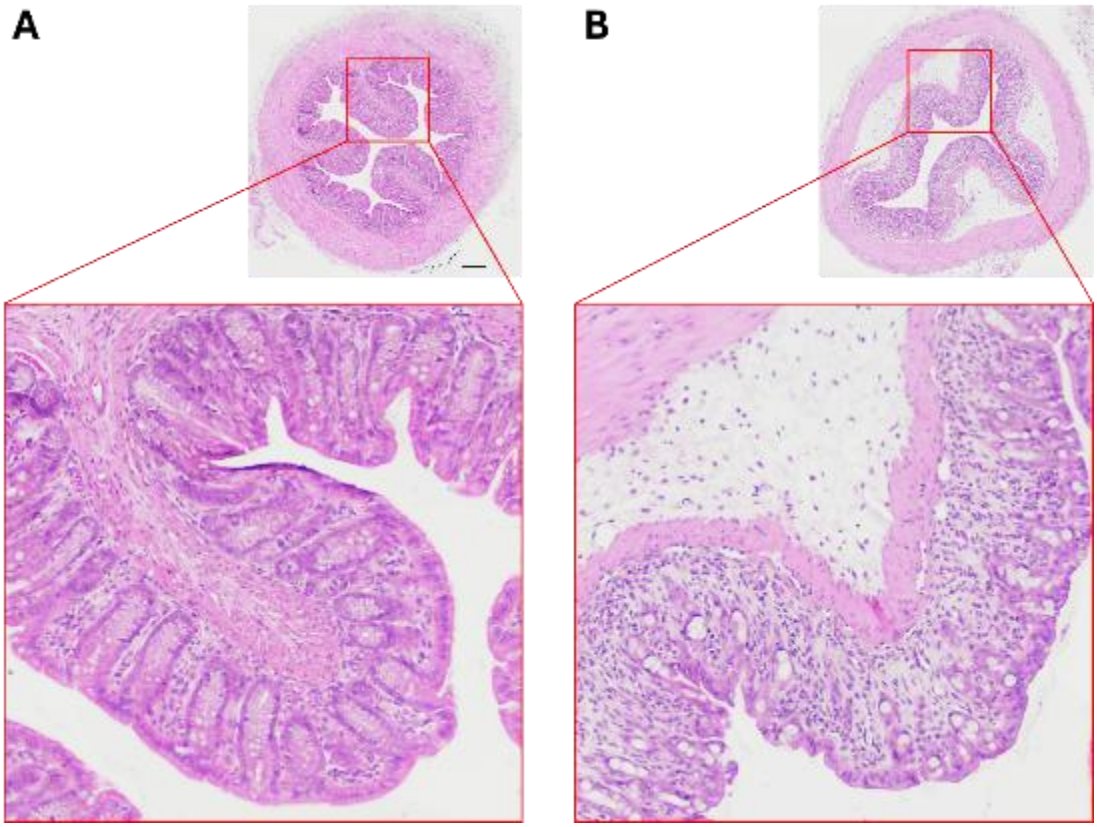

Figure 1.8. Representative images of colon sections stained with H&E from pregnant mice treated with vehicle or 2.5% DSS for 3 days.
(A) Colon section from the vehicle-treated group. **(B)** Colon section from mice treated with 2.5% DSS for 3 days. All images were captured at 10X magnification. The lower images show magnified views of the regions marked by red squares in the upper images. Scale bar = 250 µm.

1.3. Animal behavioural tests:

In the current study, the behavioural tests were designed to evaluate endophenotypes, a concept first introduced by Gottesman and Shields in the 1970s. Endophenotypes are internal, heritable, and quantifiable traits, such as neurophysiological, biochemical, cognitive, or neuropsychological characteristics, that are less observable than clinical diagnostic symptoms but may underlie complex psychiatric disorders (Gottesman & Gould, 2003).

Although endophenotypes are classically heritable, environmental stimuli can produce analogous intermediate phenotypes in animal models that mimic the human endophenotypes seen in patients. In the MIA paradigm, prenatal inflammation causes quantifiable and repeatable behavioural alternation in offspring that are associated with deficits of schizophrenia and ASD. Therefore, I refer to these induced traits as model endophenotypes to emphasise their translational value while acknowledging that the proximal cause is developmental rather than genetic.

Modelling of human psychiatric disorders such as schizophrenia and ASD in animals is extremely challenging because animals cannot self-report symptoms like hallucinations and social communication deficits. The present study, therefore, focused on behavioural changes in offspring of dams with gestational IBD. **Table 1.1** summarises a selection of behavioural paradigms commonly used to assess schizophrenia and ASD-related abnormalities in offspring exposed to MIA in rodent models.

This study established a gestational IBD model and subjected the offspring to behavioural tests at two time points. These tests, categorised by their purpose, included emotional responses, cognitive function, social interaction, and sensitivity to psychotropic drugs (**Table 1.2**). The following section outlines the principles and

methodologies of the selected behavioural tests.

Behavioural tests	Neuropsychological/chemical process involved
EPM	Anxiety-like behaviour
Y-maze	Novelty preference and spatial recognition
Social interaction	Social interaction
PPI	Sensorimotor gating and short-term attention
Morris water maze	Spatial working memory
Forced swimming test	Despair behaviour
Sucrose preference test	Anhedonia
Latent inhibition	Selective attention
Motor response to the psychostimulant	Glutamate associated neurotransmission

Table 1.1. Overview of the selected experimental paradigms used to investigate behavioural and neurochemical abnormalities in infectious MIA models.

	EPM	Y-maze	SI	PPI	MWM	FST	SPT	LI	MK-801	Reference
PolyI:C (early-mid)	↑/=	↓	↓	↓ [d]	↓ [g]	↑	=	↓	↑	Vuillermot et al., (2017); Meyer et al., (2010), Smith et al., (2007), Meyer et al., (2006)
PolyI:C (late)	=	↓	↓	↓	↓ [f]		↓	↑/=	↑/↓	Meyer et al., (2007); Bitanihirwe et al., (2010), Nakamura et al., (2021)
LPS	↑		↓/= [e]	↓		↑		↓	↑	Kaim et al., (2011); Abu-Ata et al., (2023), A M Depino et al., (2015), Fernández de Cossío et al., (2017), Water house et al., (2016), Imai et al., (2018)
Cytokines				↓				↓		Smith et al., (2007)
TURP			↓	↓ [b]						Aguilar-Valles et al., (2011)
SEA	↑		↓	=	↓ [a]					Glass et al., (2019)
SEB	↑		=	=	=					Glass et al., (2019)
Imiquimod	=		↑	=						Missig et al., (2020)
STAg	↑ [g]		↓							Spini et al., (2020)

Table 1.2. Overview of experimental paradigms for investigating behavioural and neurochemical abnormalities in infectious MIA models
This table lists the nine behavioural tests performed on offspring of dams with infectious MIA stimuli. Each test measures a specific deficit seen in schizophrenia or autism spectrum disorder, grouped into four domains: emotional reactivity, cognition, social behaviour, and response to antipsychotic drugs. The term "=" indicates no significant effect from the prenatal immune challenge. Poly I:C, polyinosinic:polycytidylic acid; LPS, lipopolysaccharide; TURP, turpentine; SEA and SEB, staphylococcal enterotoxin A and B; STAg, soluble *T. gondii* antigen. The symbols "↑" and "↓" denote a decrease/disruption or increase/persistence in the behavioural effect, respectively. Empty cells (filled black) indicate no relevant literature cited. Annotations:
a = age-dependent effect; b = significant difference observed with longer inter-trial intervals (ITI, 60 s to 10 min); c = social deficit observed in rats; d = impairment dependent on the timing of immune induction; e = decreased learning rate in females and increased short-term memory; f = significant difference observed with longer inter-trial intervals (ITI, 60 s to 10 min); g = only in the early gestation.

1.3.1. Elevated plus maze:

The elevated plus maze (EPM) is a widely used behavioural assay for assessing anxiolytic and anxiogenic effects in rodents. Introduced by Handley and Muthani in the mid-1980s, this test evaluates psychotropic agents' influence on fear and anxiety in rats (Handley & Mithani, 1984). The EPM is based on an approach-avoidance conflict, exploiting the natural tension between a rodent's drive to explore new environments and its aversion to open, exposed spaces, proposed by Montgomery (1955).

The maze consists of two opposing open arms and two enclosed arms, positioned at an elevation. The open arms lack protective walls, triggering anxiety due to the rodent's instinctive fear of heights and exposure, whereas the enclosed arms provide a sense of security (Handley & Mithani, 1984). Anxiety is assessed by measuring either the proportion of time spent in the open arms or the ratio of entries into open arms compared to total arm entries. Since its inception, the EPM has been widely adopted beyond pharmacological research, including investigations on strain differences, transgenic models, brain lesions, and environmental influences. The first adaptation of the EPM for mice, described by Stephens et al. (1986), involved a scaled-down version of the rat maze constructed from grey plastic

Several methodological factors influence EPM results, including maze wall structure (Hagenbuch et al., 2006), maze height (Falter et al., 1992; Treit et al., 1993), lighting conditions (Falter et al., 1992), arm flooring texture (Benjamin et al., 1990; Falter et al., 1992; Morato & Castrechini, 1989) prior handling of subjects (Pellow et al., 1985), and testing time of day (Griebel et al., 1993). The EPM is the first in our series of behavioural tests, as its novel environment allows the assessment of anxiety-like behaviours without confounding effects from previous testing. Maintaining

consistency in apparatus setup is essential for reliable results.

To further examine anxiety-like behaviours, some studies have assessed maternal immune activation using the open field test, which measures reduced entries into an open field's central zone (Meyer et al., 2005). Research has shown that mice born to dams infected with human influenza virus or Poly I:C exhibit diminished exploratory behaviour in the open field (Meyer et al., 2005; Shi et al., 2003), though significant treatment effects in the EPM have been inconsistently observed (Vuillermot et al., 2017). This discrepancy suggests the EPM may offer a more direct assessment of anxiety-like behaviours (Lister, 1987; Pellow et al., 1985).

Thus, this experiment utilises the EPM to evaluate anxiety-like behaviours in offspring subjected to prenatal DSS treatment (see Chapter 2: Method).

1.3.2. Spatial memory in Y-maze

The Y-maze is a widely used behavioural paradigm for assessing short-term spatial memory in mice, particularly in the context of recognition memory, which is crucial for distinguishing between familiar and novel stimuli (Ennaceur & Delacour, 1988). This form of memory enables mice to differentiate between previously visited and unvisited arms of the maze, relying on spatial cues processed by the hippocampus, a brain region essential for spatial navigation and memory formation (Sanderson et al., 2006). The Y-maze test is hippocampus-dependent, engaging spatial working memory during spontaneous alternation tasks and spatial reference memory in rewarded paradigms (Sanderson et al., 2007). Hippocampal lesions or dysfunction impair performance in this test (Sanderson et al., 2006). Mice navigate the maze using both internal cues, such as proprioceptive and vestibular signals for egocentric navigation, and external cues,

such as visual landmarks for allocentric navigation. External cues, in particular, rely heavily on hippocampal processing (Save & Poucet, 2000).

Recognition memory deficits are commonly observed in patients with schizophrenia (Coleman et al., 2002; Gabrovska et al., 2003; Shipman et al., 2009), and animal models have been used to demonstrate similar impairments using tests originally designed for object or spatial recognition memory (Grayson et al., 2007; Karasawa et al., 2008). Researchers assess memory retention over time by manipulating the delay interval between the sample and test phases, allowing for the evaluation of "forgetting." However, the Y-maze test is susceptible to confounding factors, including novelty-seeking behaviour and anxiety (Yee & Singer, 2013). For example, poor performance may result from neophobia—the fear of unfamiliar environments—rather than impaired familiarity judgment. Additionally, a lack of motivation, characterized by avolition or apathy, may hinder exploration of novel stimuli, affecting performance. The reliance on internal versus external cues further influences outcomes, as external cues improve spatial discrimination but may also heighten anxiety in aversive conditions.

To ensure validity, it is crucial to account for these confounding variables. One approach is to measure total distance travelled during the sample and test phases to assess motivation for exploration. MIA studies have utilised the Y-maze paradigm to investigate spontaneous alternation and spatial recognition memory in offspring exposed to prenatal MIA (Giovanoli et al., 2015; Mueller et al., 2021). Most studies indicate that offspring exposed to prenatal MIA exhibit impairments in working or spatial recognition memory, potentially linked to hippocampal dysfunction. Accordingly, this study employs the Y-maze test to evaluate spatial recognition in the offspring of DSS-treated mothers, focusing on spatial cue utilisation and hippocampal

processing.

In summary, the Y-maze serves as a valuable tool for investigating short-term memory and recognition capabilities in mice. Controlling for confounding variables is essential to ensure reliable results, particularly when examining hippocampal-dependent spatial navigation and its implications for offspring development in maternal immune activation models.

1.3.3. Social interaction test

Social withdrawal, often viewed as an expression of reduced social motivation, is a key feature of several psychiatric disorders, including schizophrenia, depression, and autism spectrum disorder (ASD) (Crespi & Badcock, 2008). Early social interaction tests in rodents, developed to study social phobia and screen anxiolytic drugs, highlighted the confounding role of anxiety and fear toward unfamiliar conspecifics in assessing social behaviour (File & Hyde, 1978). To address the need for paradigms relevant to psychiatric disorders characterised by social deficits, an automated high-throughput three-chamber social interaction test was developed (Nadler et al., 2004). In this test, the tendency to approach a compartment containing a conspecific—measured by time spent and number of entries—serves as an index of social motivation, while a social novelty phase, where the animal's preference for an unfamiliar conspecific over a familiar one is assessed, provides a measure of social recognition memory, akin to the preference for novel arms in the hippocampus-dependent spontaneous Y-maze test (Lalonde, 2002). This paradigm has been widely adopted due to its ease of implementation and has been used to assess social deficits in models of ASD (Silverman et al., 2010). MIA-related studies also have utilised Crawley's three-chamber test as a paradigm to evaluate autism-like behaviour in offspring exposed to prenatal MIA (Bitanihirwe et al., 2010; Missig et al., 2020). Therefore, this study employs a similar setting to evaluate social withdrawal in the offspring of mothers with inflammatory bowel disease (IBD), focusing on social motivation and recognition memory.

1.3.4. Prepulse inhibition

Prepulse inhibition (PPI) of the acoustic startle reflex refers to the reduction of startle reactions in response to a startle-eliciting pulse stimulus when it is shortly preceded by a weak prepulse stimulus (Hoffman & Searle, 1965). PPI was initially developed in human psychophysiological research and subsequently translated into non-human subjects. Almost identical procedures and stimuli are used in both humans and animals (Swerdlow et al., 1999). Thus, PPI can be reliably demonstrated across a variety of species.

Theoretical expositions of PPI consistently attribute it to competition between the prepulse and pulse stimuli for limited processing resources (Graham, 1975). PPI has been considered an operational measure of sensorimotor gating, and its deficit has been consistently reported in both acute and chronic schizophrenia patients, as well as in psychosis-prone individuals (Braff, Geyer, Light, et al., 2001; Braff et al., 1992). Swerdlow and colleagues first proposed that deficiencies in PPI constitute a model of information processing deficiency in the realm of early (within 100 ms) attentional control in schizophrenia patients (Braff & Geyer, 1990; Geyer & Swerdlow, 2001; Swerdlow et al., 1994).

However, PPI disruption is not exclusively associated with schizophrenia; it has also been reported in obsessive-compulsive disorder (Swerdlow et al., 1993), Huntington's disease (Swerdlow et al., 1995), Tourette's syndrome (Castellanos et al., 1996), and attention-deficit hyperactivity disorder (ADHD) in children (Braff, Geyer, & Swerdlow, 2001; Castellanos et al., 1996; Swerdlow et al., 1995). Other conditions, such as post-traumatic stress disorder (PTSD) (Grillon et al., 1996), autism spectrum disorder (ASD) (Perry et al., 2007) and bipolar mania with psychosis (Perry et al., 2001), have also been linked to PPI deficits.

Although the Prepulse Inhibition (PPI) test is straightforward to conduct, its data analysis and interpretation require careful attention to several critical factors. Firstly, PPI is commonly indexed by percent inhibition, calculated as %PPI = [(pulse-alone startle – prepulse + pulse startle) / pulse-alone startle] × 100 (Yee et al., 2005). This measure is sensitive to independent changes in startle reactivity, derived from the pulse-alone condition in rodents, which can influence the interpretation of PPI deficits

(Swerdlow et al., 2000). To avoid spurious conclusions, startle magnitude should be analysed as a function of increasing prepulse intensity, ensuring that changes in PPI reflect sensorimotor gating rather than altered baseline reactivity. Secondly, body weight is a potential confounding factor in rodent PPI tests, as startle reactions are measured by whole-body motion, in contrast to the startle eye-blink reflex used in human PPI studies (Swerdlow et al., 2000; Valls-Sole et al., 1999). Since this study examines sex and age as between-subject factors in the context of offspring exposed to maternal IBD, body weight was included as a covariate in the analysis to control for its influence on startle responses (Yee & Singer, 2013).

Prior MIA studies have demonstrated that PPI disruption is a robust behavioural phenotype in the MIA models (Poly I:C and LPS), highlighting the impact of prenatal immune activation on schizophrenia-like behaviours (Aguilar-Valles & Luheshi, 2011; Meyer et al., 2005; Smith et al., 2007). These studies have also captured the age-dependent nature of PPI disruption, with deficits often becoming more pronounced during adolescence and young adulthood, emphasising the importance of developmental timing in neurobehavioural assessments (Vorhees et al., 2015; Zhao et al., 2022). Since schizophrenia-like behavioural symptoms typically emerge during these developmental stages, this study employs the PPI test to evaluate sensorimotor gating deficits in offspring of mothers with IBD at two time points (juvenile and adult) to investigate the impact of maternal inflammation on neurodevelopmental outcomes.

1.3.5. Morris water maze of working memory

The Morris water maze is a widely used paradigm for assessing spatial working memory. Deficits in this cognitive domain are commonly observed in individuals with schizophrenia and autism spectrum disorder (ASD). Working memory refers to the system responsible for actively maintaining and manipulating information within a transient, limited-capacity memory buffer. It plays a critical role in supporting ongoing behaviour, enabling complex reasoning and problem-solving processes (Baddeley, 2003; Baddeley & Hitch, 1974).

The theoretical framework of working memory function, as established by (Baddeley, 1992), is primarily based on human data. Consequently, some of its finer distinctions—such as the separation between verbal and visual buffers—may not directly apply to animal studies. The concept of "working memory," first introduced by Baddeley and Hitch (1974), was later adapted by Olton and Samuelson (1976) in their research using the radial arm maze to assess spatial working memory in rats. In this task, each arm of the maze was baited, and rats completed multiple trials per day, requiring them to remember which arms they had previously visited to optimise rewards. As the Morris water maze gained popularity, many studies favoured its use over the radial arm maze for evaluating working memory due to its simpler implementation (Hodges et al., 1996).

The Morris Water Maze (MWM) test is a widely used escape task conducted in a large circular water tank, where animals are motivated to learn to locate a hidden escape platform submerged just below the water's surface to escape the aversive water environment (Morris, 1981). The aversive nature of swimming in water increased the animals' motivation to retrieve the platform, enhancing spatial learning as they rely on

distal spatial cues to form a cognitive map of the platform's location(Vorhees & Williams, 2006). By changing the position of the escape platform daily, the task challenges working memory, requiring animals to adapt to new spatial configurations, which further enhances learning through flexible memory updating and consolidation (Steele & Morris, 1999). On each day's first trial, animals typically locate the platform by chance, as its position is unknown. Subsequent trials within the same day allow for improved escape performance, measured by reduced escape latency and shorter path distance. This improvement from trial 1 to trial 2 reflects rapid one-trial learning, serving as a measure of the working memory buffer's function. Normal rats or mice typically show significant learning improvements from trial 1 to trial 2 within 4–5 days of training (Yee & Singer, 2013). As animals rely on environmental spatial cues to remember a single escape location, the task does not allow manipulation of memory span but supports assessment of temporal retention by varying the delay between trial 1 and trial 2.

The Morris water maze has been widely used to evaluate working memory in MIA studies, often as a cognitive symptom of schizophrenia and ASD like behaviour (Meyer et al., 2005; Zuckerman & Weiner, 2005). In the present study, the Morris water maze was used to assess working memory in offspring with gestational IBD.

1.3.6. Sucrose preference test

The sucrose preference test (SPT) quantifies the hedonic response to a sweet solution, serving as a robust measure of anhedonia, a core negative symptom of schizophrenia and a hallmark feature of depression in rodent models (Horan et al., 2006; Willner et al., 1987). Anhedonia, characterized as a reduced capacity to experience pleasure from typically rewarding stimuli, is a key feature of psychiatric disorders (Der-Avakian & Markou, 2012). The SPT, a straightforward two-bottle choice paradigm, is widely used to assess anhedonia by measuring the preference for a sucrose solution over plain water, reflecting the rewarding properties of sucrose (Papp et al., 1991).

The SPT evaluates this reward sensitivity by allowing animals to freely choose between two identical drinking tubes—one containing a sucrose solution and one with water in a controlled setting (detailed in Chapter 2, Methods). To ensure accurate individual consumption and minimise stress, the SPT is optimally conducted in the home cage with single-housing conditions (Yee & Singer, 2013). Consistent with the glutamate hypothesis of schizophrenia, blockade of NMDA receptors can reduce the preference for sucrose in rats and the atypical antipsychotic, clozapine, can reverse this effect (Vardigan et al., 2010).

In MIA studies, the SPT has been instrumental in assessing anhedonia in offspring, with models such as Poly I:C demonstrating reduced sucrose preference following late prenatal immune activation, indicative of schizophrenia-like negative symptoms (Bitanihirwe et al., 2010). Building on these findings, the present study employed the SPT to evaluate anhedonia in offspring exposed to gestational IBD, as part of a comprehensive investigation.

1.3.7. Forced Swimming Test

The Forced Swim Test (FST), developed by Porsolt et al. (1977) as a streamlined alternative to the learned helplessness paradigm Seligman and Maier (1967), is a widely used rodent model to assess depressive-like behaviour by inducing behavioural despair. Originally designed to screen antidepressant efficacy, the FST has become a standard tool in preclinical studies of psychiatric disorders, including schizophrenia and depression (Porsolt et al., 1978). In the FST, rats or mice are placed in an inescapable cylinder filled with water, where initial escape attempts (e.g., swimming or climbing) transition to immobility—defined as floating with minimal movements to keep the head above water—reflecting a state of behavioural despair akin to learned helplessness (Porsolt et al., 1978). This immobility is interpreted as a resignation to the aversive, inescapable situation, mirroring despair-like responses.

In MIA studies, the FST has been extensively employed to evaluate depressive-like behaviour, often as a negative symptom of schizophrenia-like phenotypes, with models such as Poly I:C showing increased immobility in offspring (Khan et al., 2014). Building on these findings, the present study also used the FST to assess depressive-like behaviour in offspring exposed to gestational IBD.

1.3.8. Learned inattention for attentional learning

Latent inhibition (LI), first described by Lubow and Moore (1959) in animal studies, is a selective learning paradigm observed in animals, reflecting reduced associability with a previously inconsequential stimulus. In LI, a conditioned stimulus (CS), like a tone, is pre-exposed without consequence, then paired with an unconditioned stimulus (US), such as food or shock, to elicit a specific conditioned response (CR), like salivation or freezing, with pre-exposure attenuating the CR. Distinct from conditioned inhibition (Pavlov, 1927), LI is widely regarded as a form of salience (attentional) learning, reflecting the ability to ignore stimuli that predict no significant consequences from prior experiences.

Theoretical accounts of LI emphasise different mechanisms. Attentional theories (A-theory) propose that LI results from reduced attention to the pre-exposed CS, diminishing its salience during conditioning (Lubow et al., 1981; Mackintosh, 1975). Conversely, retrieval-based theories (R-theory) suggest that LI arises from competition between pre-exposure memories and new associations during retrieval (Bouton, 1993; Kraemer & Spear, 1992; Mackintosh, 1975). Additionally, contextual processing is critical for LI expression, as contextual cues modulate the retrieval of pre-exposure memories (Grahame et al., 1994; Lubow & Gewirtz, 1995; McLaren & Mackintosh, 2000; Miller & Matzel, 1988; Wagner & Brandon, 1981). These perspectives highlight LI as a multifaceted construct involving attention, memory, and context.

In schizophrenia, disrupted LI is a well-documented cognitive deficit, linked to an inability to ignore irrelevant stimuli, contributing to symptoms like delusions (Baruch et al., 1988; Gray, 1992). This aligns with the neuropsychological model of Gray et al. (1991), which posits that LI deficits reflect impaired attentional and contextual processing, driven by dopaminergic dysregulation. While attentional accounts dominate LI research in schizophrenia, contextual and retrieval-based accounts are equally relevant to understanding its neuropsychological basis (Escobar et al., 2002).

In maternal immune activation models, the latent inhibition test was utilized to assess cognitive impairments relevant to positive symptoms of schizophrenia. Most MIA studies report disrupted LI in mice Meyer et al. (2005) or rats Zuckerman and Weiner (2005), mirroring LI deficits observed in schizophrenia patients (Baruch et al.,

1988; Gray, 1992; Williams et al., 1998). This study investigates LI in offspring exposed to gestational DSS treatment, using a conditioned freezing paradigm adapted from Meyer et al. (2005), to evaluate whether LI is enhanced or disrupted compared to controls, contributing to the understanding of LI's role in schizophrenia-related cognitive deficits.

1.3.9. Sensitivity to MK-801-induced hyper locomotor activity

MK-801, also known as dizocilpine, is a potent non-competitive antagonist of the N-methyl-D-aspartate (NMDA) receptor, widely utilised in research as a pharmacological model for schizophrenia-like behaviour, like PPI disruption and LI disruption (Gaisler-Salomon & Weiner, 2003; Pothuizen et al., 2006). The administration of MK-801 has been demonstrated to induce hyperlocomotor activity and impair cognition in rodents (Dai & Carey, 1994). These behaviours correlate well with the hyperactivity exhibited by negative symptoms of schizophrenia in humans (Rung et al., 2005).

By blocking NMDA receptors, MK-801 disrupts glutamatergic transmission, supporting its use as a preclinical model to study NMDA receptor hypofunction (Krystal et al., 2003). This model is relevant in maternal immune activation (MIA) studies, where offspring exhibited heightened sensitivity to MK-801, reflecting neurodevelopmental deficits associated with schizophrenia-like phenotypes (Meyer, Murray, et al., 2008; Meyer, Nyffeler, et al., 2008).

To investigate the hyperlocomotor effects of MK-801, dose selection is critical. Higher doses (e.g., 0.5 mg/kg) induce a motor syndrome characterized by ataxia, head weaving, and salivation, whereas lower doses (0.15–0.2 mg/kg) elicit robust locomotor stimulation, ideal for studying schizophrenia-like hyperactivity (Liljequist et al., 1991). In infectious MIA models using Poly I:C or lipopolysaccharide (LPS), adult offspring show enhanced locomotor responses to low-dose MK-801 (0.2 mg/kg), indicative of NMDA receptor hypofunction and schizophrenia-like phenotypes (Meyer, Murray, et al., 2008; Meyer, Nyffeler, et al., 2008; Zuckerman & Weiner, 2005). Building on these findings, the present study administers MK-801 at 0.2 mg/kg to evaluate NMDA receptor-mediated responses in offspring exposed to gestational IBD.

1.4. Aims and outline of the thesis

In the past two decades, rodent models have been instrumental in exploring the connection between maternal immune activation and the emergence of abnormal behaviours relevant to schizophrenia and autism in the resulting offspring. However, whether neurodevelopmental disruptions observed in infectious MIA models extend to maternal IBD remains unclear. Building on the suggested link between maternal IBD and neurodevelopmental disorders, the present thesis aims to model the association in animals. Specifically, it established a chemical-induced ulcerative colitis (UC) model in pregnant C57BL/6J mice and investigated its impact on the psychological functioning of offspring from juvenile stages to adulthood.

The first part of this thesis focuses on characterizing changes in maternal immune status using the established IBD model. It confirms the alteration of maternal immune status through the face validity of dextran sulfate sodium (DSS)-induced UC-like pathology.

The second part involves the behavioural characterisation of offspring in the established IBD model. It assesses the extent to which maternal immune activation by mimicking an immune response to viral or bacterial infections during pregnancy can induce schizophrenia or autism like behavioural phenotypes in the offspring. Clinical observation indicate that male schizophrenics typically have an earlier onset age and exhibit a more severe clinical profile, especially in terms of negative symptomatology (Aleman et al., 2003; Goldstein et al., 2013; Roy et al., 2001) and cognitive deficits (Angermeyer & Kuhn, 1988; Eranti et al., 2013). However, the behavioural effects of infectious MIA models were consistently comparable between sexes (Meyer et al., 2005; Zuckerman & Weiner, 2003). This thesis determines whether the DSS-induced maternal IBD model during early/mid gestation may result in a cluster of age and sex dependent

behavioural changes.

The third part examines the chemical and structural changes in the offspring and foetus resulting from the DSS-induced gestational IBD model. It investigates how gestational IBD influences developmental trajectories by assessing alterations in brain chemistry, including neurotransmitter levels, inflammatory markers, and other molecular changes in the offspring and foetus. These findings elucidate the potential mechanisms through which maternal IBD may disrupt neurodevelopmental processes.

Chapter 2 Methodology and Material

2. Methodology and Materials

The experimental work presented in this thesis was conducted within the Department of Rehabilitation Sciences at The Hong Kong Polytechnic University. This study utilised C57BL/6J mice to investigate the research objectives. To establish a gestational inflammatory bowel disease (IBD) model, pregnant mice were administered water containing dextran sulphate sodium (DSS). The rationale for selecting this animal model, the design of experimental protocols, and an overview of the general procedures is detailed in **section 2.2**.

2.1. Subjects

All mice in this study were descended from breeders of the inbred C57BL/6J strain originating from Jackson Laboratory (ME, USA). They were bred and housed in the Central Animal Facilities of The Hong Kong Polytechnic University. Offspring were weaned and sexed on postnatal day (PND) 23. Littermates of the same sex were caged in groups of 2 to 4 in Makrolon® cages (Tecniplast, Italy) in a climatized (22±1ºC and 55±5% RH) vivarium maintained under a 12h/12h light-dark cycle with lights off from 2000 to 0759 hrs. Food and water were available ad libitum unless otherwise stated.

All experimenters were licensed by the Department of Health in accordance with the Animals (Control of Experiments) Ordinance (Cap. 340) under the Laws of Hong Kong. Institutional approval for the present study was granted by the University's Animal Subjects Ethics Committee (#22–23/328-RS-R). All procedures were further ensured to comply with the European Union Directive 2010/63/EU on the protection of animals used for scientific purposes, as well as relevant guidelines from the U.S. National Academies (2011).

2.2. Timed mating, breeding, and gestation DSS treatment

Virgin females, 10 weeks old, were selected from our C57BL/6J colony and housed five to a cage for 10 days prior to the induction of the Whitten effect by introducing bedding soiled with male urine, which synchronised their oestrous cycles in preparation for timed mating (Ma et al., 1998). During oestrus, individual females were paired with one breeding male in separate cages overnight. The presence of a vaginal plug the following morning confirmed successful mating. This day was designated as gestational day (GD) 0. The males were then removed, while the females remained in the breeding cage, and their body weight was recorded. The weight of the mated females was monitored daily from GD 5 to GD 9, and an increment exceeding 2 g relative to GD 0 weight indicated pregnancy.

On GD 9, pregnant dams were randomly assigned to either the DSS or control groups, and autoclaved nesting materials (110 mm × 125 mm) were provided. Dams in the DSS group received drinking bottles containing a freshly prepared 2.5% (w/v) DSS solution (MW: 36–50 kDa, Cat. #160110, MP Biomedicals, Canada), while those in the control group received filtered water. The initial weights of all drinking bottles and the pregnant dams in both the DSS and control groups were recorded (at 1500 hr, on GD 9) and monitored every 24 hr (at 1500 hrs on GD 10 to GD12). After 72 hr of DSS exposure, dams in the DSS group were switched back to filtered water bottles.

The pregnant dams were then left undisturbed (except for daily weighing till GD 17) until parturition or euthanised earlier on GD 13 or GD 17 for the collection of foetal and placental tissues, as well as blood, spleen, and colon samples from the maternal hosts (see **Fig 2.1**).

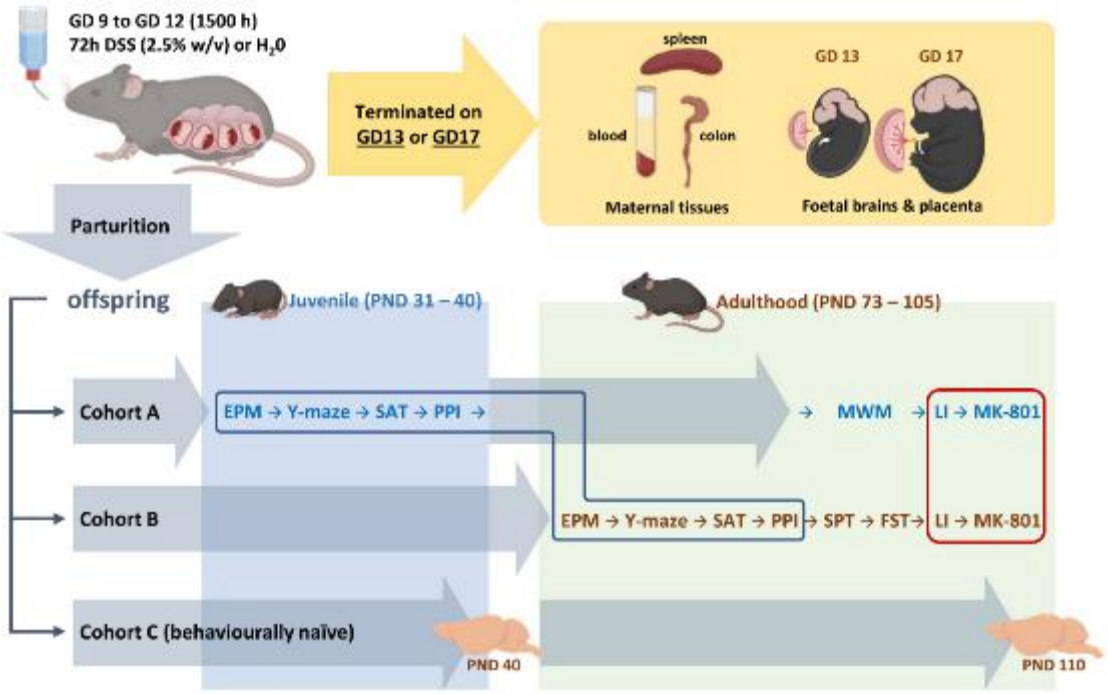

Figure 2.1. The schematic diagram of the experimental design
The study comprises two experiments to evaluate the effects of DSS-induced colitis in pregnant mice, focusing on foetal and placental changes and the subsequent long-term behavioural outcomes in their offspring. In the initial experiment, pregnant mice were administered a 2.5% DSS solution in their drinking water from gestational day 9 (GD9) to GD 12. Maternal organs, including the colons, spleens, and serum, as well as foetal brains and placentas, were collected on GD13 (from 11 DSS-treated dams and 10 control dams) or GD17 (from 8 DSS-treated dams and 9 control dams) for further analysis. In the second experiment, aimed at assessing long-term effects on offspring, female and male littermates were from 11 litters of DSS-treated dams and 14 litters of control dams and were divided into three cohorts at PND 23. Cohorts A and B commenced behavioural testing at PND 31 and PND 73, respectively. Meanwhile, cohort C was subjected to brain harvest for molecular and histological assessments at PND 40 or PND 110.

2.3. Allocation of Offspring and Pregnant Dams

Male and female offspring were collected from 11 independent litters of DSS-treated dams and 14 litters of control dams to minimise potential litter effects, as recommended by Zorrilla (1997). After parturition, the dams and their pups were left undisturbed until weaning on PND 23. At weaning, the pups were moved to same-sex group cages, with 2-4 mice per cage. The pups were then distributed between three cohorts, two for planned behavioural experiments (Cohorts A and B) and one cohort remained behaviourally naïve until harvesting of brain tissues (Cohort C). Behavioural testing as well as tissues harvesting was performed at two developmental periods: juvenile (from PND 31 to PND 40) and adulthood (from PND 73 to PND 105) (see **Fig. 2.1**), which aligns with the gradual attainment of sexual maturity and age-specific behavioural discontinuities from younger to older animals, as described by (Spear, 2000), who defined PNDs 28-40 as juvenile and PND 65 onward as adulthood.

Cohort A underwent the first four tests as juveniles between PND 31 and PND 40. These included the elevated plus maze (EPM) test of anxiety, the Y-maze test of spatial familiarity, the social approach test (SAT), and prepulse inhibition (PPI) of the acoustic startle reflex. These four tests were conducted in Cohort B when the mice reached adult age from PND 73 onwards. The same sequence was followed for an age comparison (juvenile vs. adulthood) for these four tests (as indicated by the "⌐|_"-shaped box in **Fig. 2.1**). The other five behavioural tests were only conducted in adulthood.

Afterwards, Cohort B adults were evaluated on two tests related to depression-related behaviour: anhedonia in the sucrose preference test (SPT) and cognitive despair in the Porsolt forced swim test (FST), whereas Cohort A adults underwent the Morris water maze (MWM) test of spatial working memory. Due to its duration, the MWM test was not performed in the juvenile period. To avoid confounding effects on

swimming, we refrained from including Cohort B adults in the MWM who had experienced the FST.

Next, latent inhibition (LI) of classical conditioning was evaluated using mice from both Cohort A and Cohort B, as it required further subdivision of animals into pre-exposed (PE) and non-pre-exposed (nPE) subgroups. LI is a form of learned inattention where the subject learns to ignore irrelevant stimuli (Mackintosh, 1973), and its aberrant expression has been linked to both positive and negative symptoms of schizophrenia (Gray et al., 1991; Gray et al., 1995; Gray et al., 1992; Weiner, 2003). The LI experiment was performed in two balanced replications since we were limited to two conditioning chambers. Finally, the acute psychomotor reaction to NMDA receptor (NMDAR) blockade by MK-801 (0.2 mg/kg, i.p.) was assessed in all adult mice from Cohorts A and B.

Given that Cohorts A and B were subjected to multiple behavioural tests, including systemic exposure to a psychoactive substance, the behaviourally naïve Cohort C was prepared for the harvesting of offspring brain tissues.

2.4. Behavioural Procedures

Behavioural change in offspring from DSS treatment was evaluated by a series of behavioural tests, including emotional, cognitive function, sensorimotor gating, and sensitivity to psychiatric stimulants (see **Table 2.1**). In general, to avoid interference by olfactory cues from the opposite sex, male and female mice were evaluated on separate days. As a result, all animals were left undisturbed for at least 24 hr between tests. All tests were conducted between 0900 and 1900 hr during the light phase under dim lighting to avoid bright illumination. The animals were always acclimatised to the testing room for at least 30 min before testing. The numbers of mice used in each behavioural test are summarised in **Table 2.1.**

	Readout	Gestational Condition:	DSS				Control			
		Age:	Juvenile		Adult		Juvenile		Adult	
		Sex:	F	M	F	M	F	M	F	M
Cohort A & B	Elevated pluse maze		10	11	10	11	14	14	14	14
	Y-maze of spatial recognition		10	11	10	11	14	14	14	14
	Social approach test		10	11	10	11	14	14	14	14
	Prepulse inhibition		10	11	10	11	14	14	14	14
	Morris water maze				10	11			14	14
	Sucrose preference test				10	11			14	14
	Forced swim test				10	11			14	14
	Latent inhibition									
	NPE				10	11			14	14
	PE (CS)				10	11			14	14
	MK-801 induced locomotor activity				20	22			28	28
Cohort C	**Body weight**		9	6	12	8	11	12	7	11
	Histological assessment									
	DCX				2	1			2	1
	Molecular assessment									
	BDNF		5	5	5	5	5	5	5	5
	NR-1, NR-2a and NR-2b				3	2			3	2

Table 2.1. The number of subjects in the experiment pods-parturition.
All experimental subjects in Cohort A and Cohort B participated in behavioural tests. Cohort A underwent the Morris water maze test, while Cohort B was subjected to the sucrose preference test and the forced swim test. All subjects from Cohort C were monitored for body weight until harvest. Histological and molecular assessments were conducted on brain tissue from Cohort C. The histological assessment of DCX and NR-1 targets was performed in the left dorsal hippocampus region (see section 2.10). Additionally, the molecular assessment of BDNF in the right hippocampus was evaluated using ELISA (see section 2.8). The expression levels of NR-1, NR-2a, and NR-2b were measured from total RNA in the right hippocampus using real-time PCR (see section 2.12).

2.4.1. Elevated Plus Maze

The maze was constructed from grey acrylic and consisted of four 30-cm long arms radiating from a central square measuring 5 cm in width. It was elevated 65 cm above the floor. Two opposing arms were enclosed by 30-cm high walls, while the other arms had only a 5-mm border. The mouse was placed in the centre, facing an open arm, and allowed to explore freely for 5 min. Ethovision XT (v11.5, Noldus, NL) tracked the animal's movement to calculate the proportion of time spent in the open arms and the number of open arm entries (relative to total time in and entries into all arms) as measures of anxiety. The total distance was measured to confirm mobility. The setting of the apparatus is shown in **Figure 2.2.**

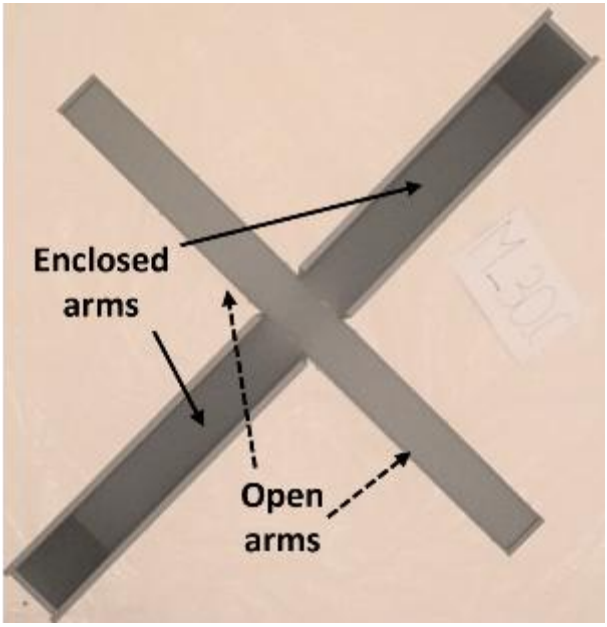

Figure 2.2. The top view of the elevated plus maze apparatus.
This view illustrates the layout of the four arms (two open and two enclosed) of the elevated plus maze used for assessing anxiety-like behaviour in mice. Solid line and dotted line indicated the enclosed arms and open arms in the figure.

2.4.2. Y-maze test of spatial familiarity

The Y-maze, constructed from grey acrylic, was situated in the centre of a room unfamiliar to the animals and enriched with a variety of extra-maze cues (see **Fig 2.3.C**). It featured three identical arms, each measuring 5 cm in width and 30 cm in length, converging at a triangular central region with adjacent arms set 120° apart. The maze's outer perimeter was enclosed by 5-cm-high walls. Access between the central region and each arm was regulated by a manually operated, 15-cm high opaque sliding door, recessed 5 cm into each arm (see the apparatus **Fig 2.3.A & B**). The arm closest to the room door was designated as the start arm, while the other two arms served as the familiar (F) and novel (N) arms (see **Fig 2.3.A**). The relative positions of the F and N arms were counterbalanced between subjects. The test was composed of a sample phase and a test phase, separated by a 35-min interval during which the animals were housed in a waiting cage in a secluded area of the test room. To start the sample phase, the N arm was blocked, and the mouse was placed at the far end of the S arm, with the entrance to the central area also blocked. The sliding door controlling the S arm was then lifted, allowing the mouse to freely explore the F and S arms for 3 min after exiting the S arm. The test phase was conducted similarly, except that access to the assigned N arm was not blocked. Ethovision XT (v11.5, Noldus, NL) tracked the mouse's location in both phases. Based on the recorded time spent in the arms, the ratio (N - F) / (N + F) was calculated as a proxy measure for the preferential exploration of the N arm relative to the F arm in the test phase.

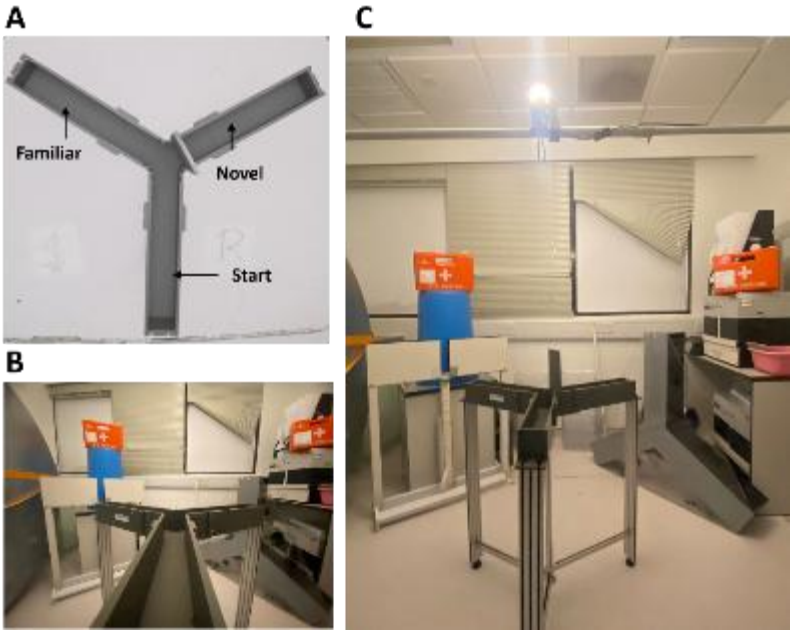

Figure 2.3. Top view of the y-maze apparatus with extra-maze cues.
This figure presents an overhead view of the Y-maze apparatus, highlighting its three arms arranged at 120° angles. Surrounding the maze, extra-maze cues (e.g., distinct landmarks or visual markers) are strategically positioned to facilitate spatial orientation during behavioural testing. **(A)** A top view image of the Y-maze during the sample phase shows that novel arm was blocked by a partition, while the start arm is positioned closest to the room door to ensure consistent orientation. **(B)** This picture shows the side view of the Y-maze apparatus, the Y-maze's 5-cm high walls. These walls allowed the mice to perceive extra-maze cues, aiding in their familiarization with the test environment. **(C)** This picture illustrates the overall height of the Y-maze setup and highlights the design of the extra-maze cue used to orient the mice spatially.

2.4.3. Social preference test

The test was based on modifications by Willi et al. (2010) to the original design described by Crawley and her colleagues (see Nadler et al. (2004)). The apparatus consisted of a rectangular opaque Plexiglas box measuring 60 × 40 cm, divided by transparent walls into three parallel chambers, each measuring 20 × 40 cm. The partition walls had a 9 × 6 cm opening, allowing access from the two side chambers into the middle chamber (**Fig 2.4**). In the centre of each side chamber was a cylindrical metal mesh container, measuring 9.8 cm in height, 9 cm in diameter, with a 5-mm mesh aperture all around. The container was placed upside down, with its bottom facing upwards, and a weight was fixed on top to prevent it from being toppled or climbed on by the mouse during the test. The test procedure included three 10-minute phases: habituation, social interaction, and social novelty. In the habituation phase, each mouse was placed in the central compartment of a three-chamber apparatus and allowed to explore the entire box freely. The mouse was then briefly removed and returned to the apparatus later for the social interaction phase. In this phase, an unfamiliar same-sex, age-matched C57BL/6J mouse and a plastic toy mouse were placed in separate meshed containers in the side chambers to assess the mouse's preference for social interaction. In the social novelty phase, the toy was replaced with another unfamiliar same-sex, age-matched mouse to evaluate social novelty detection. The positions of the stimuli in the social interaction and social novelty phases were counterbalanced across test subjects. The time spent in each of the three chambers was recorded using Ethovision XT software. For the social interaction phase, the ratio (mouse)/(mouse + toy) was calculated to measure sociality. For the social novelty phase, the ratio (unfamiliar)/(unfamiliar + familiar) was calculated to measure preferential exploration. These ratios served as proxy measures for the mouse's preference for the real mouse

over the toy in the social interaction phase and for the unfamiliar mouse over the familiar mouse in the social novelty phase.

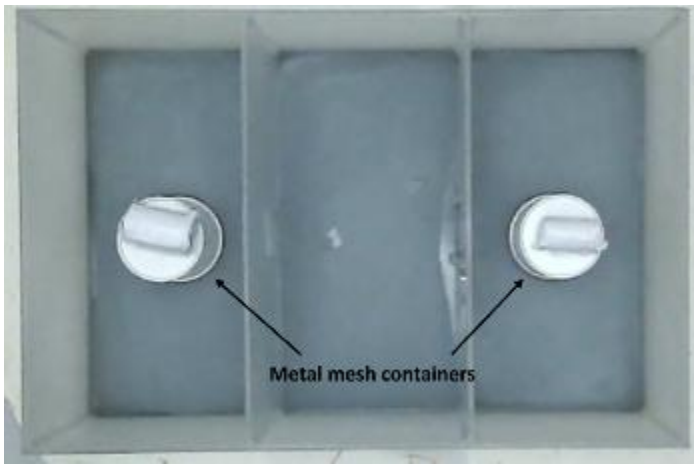

Figure 2.4. Top view of the social interaction test apparatus.
The top view of the apparatus shows two inverted metal mesh containers in the middle of the two side chambers during the social novelty phase. The placement of the familiar or unfamiliar mice in the two containers was counterbalanced.

2.4.4. Prepulse inhibition of acoustic startle

The test was conducted with a SR-LAB-Startle Response System (San Diego Instruments, CA, USA) equipped with two mouse test chambers as previously described (Sun et al., 2022). Each sound-attenuated chamber contained a non-restrictive cylindrical acrylic enclosure (inner ⌀ = 3.8 cm, length = 8.9 cm) that held the mouse during the test (**Fig 2.5**). The enclosure was fixed horizontally onto a lightweight acrylic platform, and the whole assembly rested on a heavy block fixed to the chamber's base. The startle response was detected by a piezoelectric sensor attached to the enclosure assembly at 1-ms intervals. A high-frequency loudspeaker mounted above the enclosure maintained the 65-dB background noise and delivered acoustic stimuli in the form of white noise at the desired intensity and duration with a 0.2~1.0 ms rise/fall time. A constant house light mounted in the ceiling provided ambient lighting inside. The intensity of the noise was calibrated in decibels (dB using the A-scale) before the experiment.

The test commenced with a 2-min acclimatisation period, followed by the 108 discrete trials that were administered at a 15-s variable (10-20 s) inter-trial interval. All trials followed the same basic temporal structure consisting of a 20-ms prepulse period, an 80-ms inter-stimulus interval, and then a 40-ms pulse period. Therefore, the stimulus onset asynchrony (SOA) between the prepulse and pulse was 100 ms. Readings were recorded during two response windows of 65 ms duration for each trial: one starting from the beginning of the prepulse period and the other from the start of the pulse period. The average of the 65 piezoelectric outputs (in mV) at 1-ms intervals within the respective response windows was taken as a measure of the motor reaction to the prepulse (prior to pulse onset), and the startle reaction in response to the pulse stimulus, respectively.

During the prepulse period, the noise level was set at one of three different intensities: 71, 77 and 83 dB, corresponding to prepulse stimuli at +6, +12 and +18 decibel units, above the 65 dB background noise, respectively. The 65 dB prepulse condition represented the "pulse-only" condition. During the pulse period, the noise level was set at three different intensities: 100, 110 and 120 dB, representing the pulse stimuli. In total, there were 12 possible combinations of prepulse and pulse intensities.

The session began with 6 pulse-only trials (+0 dB prepulse) to stabilize the startle response. Following these, the middle 96 trials were organised into 8 blocks, with each block containing all 12 counterbalanced prepulse–pulse combinations presented in pseudorandom order. The initial and final six trials, which had the prepulse set at +0, were used to stabilise the startle response at the beginning and assess the habituation of the startle response throughout the entire test session.

Percent prepulse inhibition (%PPI) was calculated using only the middle 96 trials, as a function of prepulse intensity (+6, +12, or +18 dB above background) and pulse intensity (100, 110, or 120 dB). %PPI reflects the attenuation of the startle response with increasing prepulse intensity, expressed as percent inhibition relative to the baseline startle response elicited by the pulse alone (i.e., without a perceptible prepulse).

At the session’s end, the animals were removed from the chambers and the apparatus cleansed with 70% ethanol.

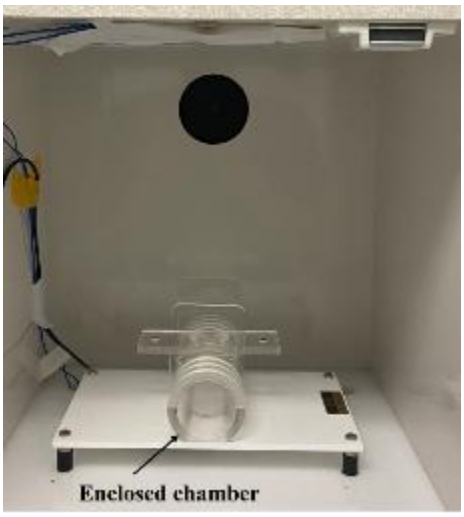

Figure 2.5. Prepulse inhibition test apparatus.
The figure illustrates the setup for the prepulse inhibition (PPI) test. A centrally positioned enclosed chamber was situated within a larger testing box. During the test, a dim light was maintained and a fan operated continuously to provide a consistent background environment. Each animal was placed in a non-restrictive, enclosed container within the chamber, allowing for free movement while ensuring standardized testing conditions.

2.4.5. Morris's water maze test of working memory

A galvanized steel circular tank measuring 170cm in diameter and 36cm high was positioned in the middle of the testing room with adequate light and enriched with distal visual cues. At the beginning of each day, the water maze was refreshed and filled with water to a level of 31 cm at 23±1°C. A stable transparent Plexiglas cylinder (⌀ = 12 cm, 30 cm high) served as the escape platform. It had a rough top surface to allow the mouse to climb onto easily it once its presence was detected. Four points, equally spaced along the circumference of the pool, were designated as N, E, S and W. These points served as the starting position at which the mouse was lowered gently into the water, with its head facing the wall of the water maze at the trial began. The area of the pool was conceptually divided into four quadrants (NE, SE, SW, and NE) of equal size by two imaginary orthogonal lines running through the centre of the water tank. A camera (FDR-X3000, Sony, Japan) was mounted directly above the water maze tank to record the swim path of the mouse for subsequent analysis by Ethovision XT.

Prior to the visible platform phase, mice underwent pre-training in a small water bucket (31 cm in diameter) equipped with a platform (7 cm in diameter) to assess their swimming ability (see **Fig 2.6**.**A**). The following day, the mice were pre-trained in the water maze using a visible platform positioned at the centre of the maze. This comprised three consecutive trials to familiarize the animals with the water maze and to reduce the stress associated with swimming. At the beginning of each trial, the animals were gently placed in the water maze against one of the four cardinal positions (North, East, South, West) (see **Fig 2.6.B**). They were given a maximum of 60 s to locate the escape platform. If they failed to find the platform within this time, they were guided to it by the experimenter. Once on the platform, animals were allowed to remain for 15 s before the next trial began, giving them the opportunity to explore the extra-maze cues (see **Fig.**

2.6.C & D). The inter-trial interval was approximately 15-20 s (minimal inter-trial interval). All mice successfully acquired the swimming response and climbed onto the escape platform.

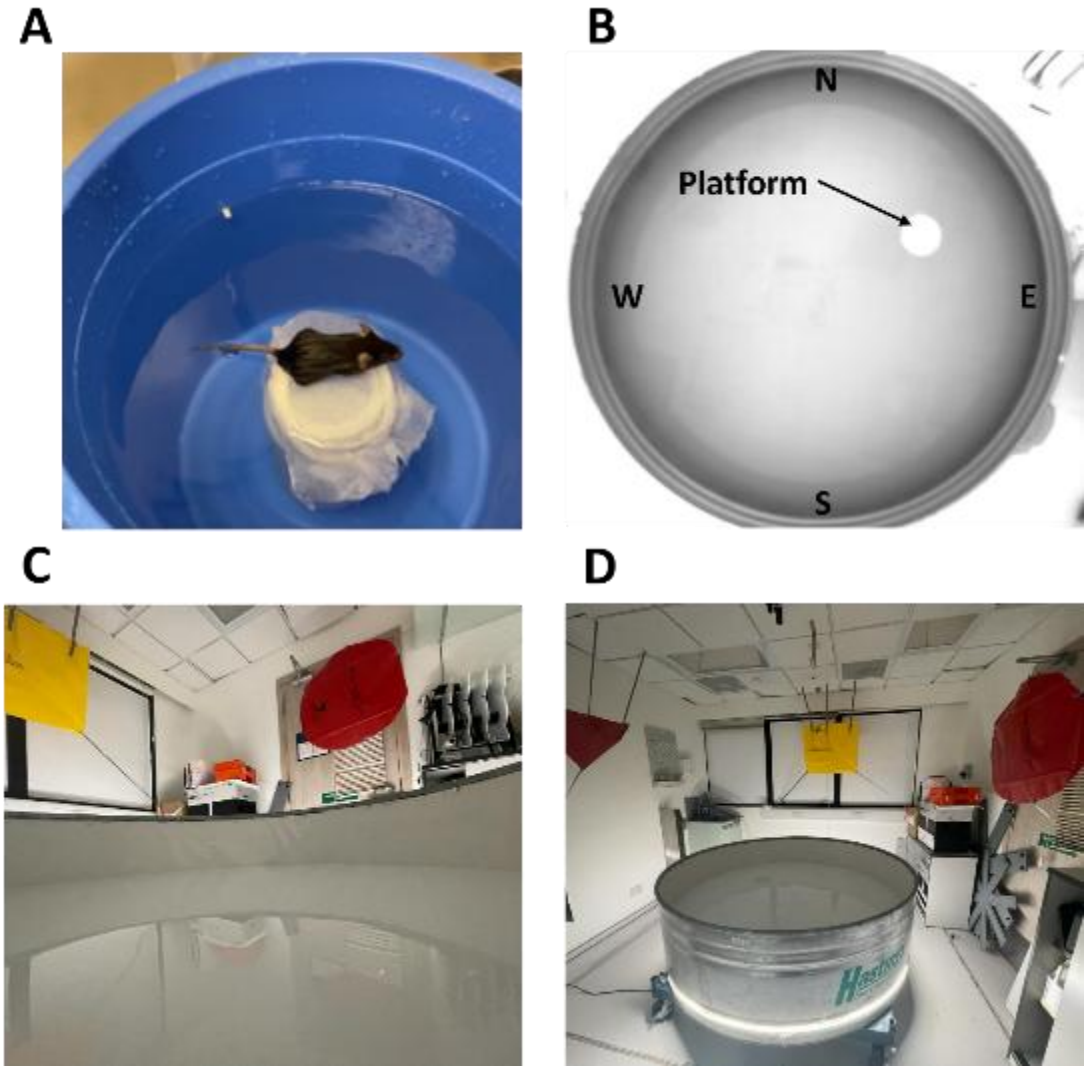

Figure 2.6. The apparatus of the pre-training test and water maze.
(A) illustrates the setup of the pre-training test for all mice before the water maze test. Each mouse was allowed to swim into a small water bucket and locate and climb onto the mini platform to assess its swimming ability. **(B)** shows the top view of the water maze captured by a digital camera. The water tank was designed with four distinct entry positions (N, E, S, and W) for the animals. **(C)** displays the platform view with the extra-maze cues. **(D)** presents the side view of the apparatus, highlighting the extra-maze cues that the animals used to locate the hidden platform.

The assessment of working memory spanned over the next 11 days. During this period, the escape platform was rendered invisible by setting it 1 cm below the water surface, and its location was changed from one day to the next. The platform always assumed a new position in the water maze (selected from 12 possible locations (see **Fig 2.7**), counterbalanced between mice) but remained in the same position between the two consecutive trials on a given day. The 12 positions are centred at 30 cm and 55 cm away from the maze centre in the four cardinal directions, and 45 cm from the maze centre in the four intercardinal directions (see **Fig 2.7**). Memory of its location learned from the first trial (*sample trial*) was expected to facilitate the return to the same position in the second trial *(test trial)*. After being released from the designated starting position, the mouse had 60 s to locate the hidden platform; otherwise, the experimenter would guide the mouse to the platform and leave it there for 15 s before the second trial.

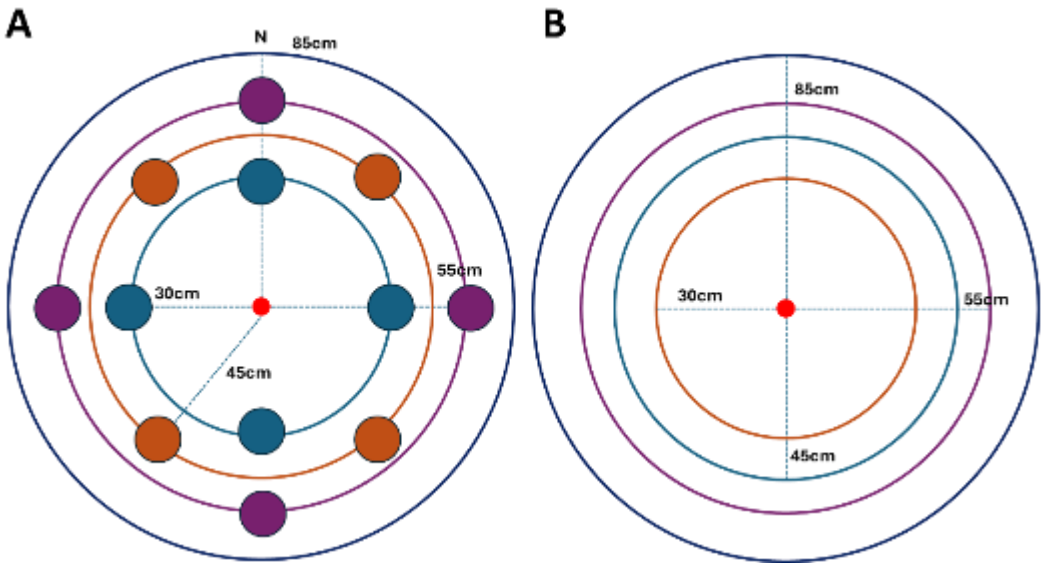

Figure 2.7. The platform positions of the water maze test.
(A) Shows the positions of 12 platforms in the water maze tank. **(B)** Illustrates the distribution of platforms across three concentric circles, with diameters of 30 cm (to centre), 45 cm, and 55 cm, used to structure platform placement within the tank.

2.4.6. Porsolt swim test

The test was performed with four glass cylinders, 9 cm in diameter and 24 cm high. They were filled with clean water to a depth of 15 cm and left at RT (~23°C). Partition walls were set to prevent visual contact between the mice during the test (See **Fig. 2.8**). The mice were individually placed in the water-filled cylinders and observed for 10 min. A video camera was positioned to provide a clear side view of all four cylinders. The 10 min of the test were analysed by Ethovision XT to compute the time of immobility based on validated image processing parameters verified against manual scoring by two independent observers.

Figure 2.8. The setting of Porsolt swim test.
This figure illustrates the setup of the Porsolt swim test. To prevent animals from seeing each other during the test, partitions were placed between individual subjects. The arrangement ensures minimal visual interaction, reducing potential external influences on behaviour. The camera was positioned to ensure the entire body of the animal was captured during the test, allowing for accurate observation and analysis of swimming behaviour.

2.4.7. Sucrose preference test

The mice were caged singly in this test, and the standard drinking bottle was replaced by two 15-mL conical tubes (Thermo Fisher Scientific, USA) with their conical end cut to create an opening of 2.5 mm in diameter. When the tubes were securely placed on the top of the cage, the mouse could access the liquid inside the pair of drinking tubes with their opening set 5 cm above the cage's bedding floor. The two drinking tubes were set 4 cm apart, allowing the mouse to easily switch drinking from one tube to the other (**Fig. 2.9**).

Following habituation to single housing and training to drink from 15mL conical tubes (as outlined by Yee et al. (2006)), a 3–4-day baseline period was conducted. During this period, body weight and fluid consumption from two water-filled tubes were measured daily at 1600 hr. This ensured that all mice consumed approximately 5.75 mL of water over the previous 24 hr and confirmed no significant side bias in drinking preference. Sucrose preference was assessed over the following 8 days, with one bottle containing a sucrose solution and the other filtered water. The initial position of the two drinking tubes was counterbalanced within each group and swapped between days. The concentration of the sucrose solution was changed from 1.0%, 0.5%, 0.25% to 0.06% w/v every two days. Daily measurement of fluid consumption was conducted at 1600 hr when the tubes were weighed and refilled daily. Sucrose consumption expressed as percent of total fluid intake [sucrose/ (sucrose + water)] × 100% was computed as a proxy for sucrose preference.

Figure 2.9. The setting of sucrose preference test.
This figure illustrates the setup of the sucrose preference test. Each animal was housed in an individual cage to prevent interference from other subjects. Two 15-mL conical tubes, positioned at a height of 5 cm above the cage floor, were used as containers for sucrose solution and water, ensuring easy access for the animals during the test.

2.4.8. Latent inhibition (LI) of conditioned freezing

The apparatus consisted of the Med Associates mouse fear conditioning system equipped with two conditioning chambers (MED-VFC-USB-M, Med Associates, VT, USA. Detailed descriptions of their construction and dimensions are accessible at https://med-associates.com/product/nir-video-fear-conditioning-vfc-system-for-general-use. Briefly, each chamber was equipped with a grid floor made from stainless-steel rods (4 mm in diameter, spaced 10 mm apart centre-to-centre), through which scrambled electric shocks could be administered. The conditioned stimulus (CS) was a 30-s tone (5000 Hz) at 86 dB delivered from a speaker mounted on the chamber wall. An incandescent light bulb mounted on the wall serves as the house light. All sessions were video recorded by an infrared camera. Freezing was estimated by immobility time detected by image analysis software provided by Med Associates with the manufacturer's recommended settings for mice. The test was conducted at the adult age from mice in Cohort A and Cohort B to accommodate the additional between-subject variable, Stimulus Pre-exposure. To control for litter effects, littermates were distributed across the two pre-exposure conditions as evenly as possible. All mice were derived from dams that contributed at least 2 male and 2 female pups, with exactly one male and one female from each litter assigned to each cohort. Chamber allocation was counterbalanced with respect to groups, sex, and pre-exposure conditions. The test procedures comprised four phases as described by Meyer et al. (2005).

• Pre-Exposure: After the mice were placed in the designated chamber, mice allocated to the pre-exposed (PE) condition received 40 presentations of the to-be-conditioned CS delivered with a variable inter-stimulus interval (40 ± 30 s), while mice in the non-pre-exposed (nPE) condition were confined to the chamber for an equivalent period without any tone.

• Conditioning: This phase commenced immediately at the end of pre-exposure without any interruption, with the animals remaining in the chambers. All mice received three discrete trials of CS-US pairings. Each pairing began with the 30-s tone followed immediately by a 1-s, 0.25 mA foot shock. The house light was kept on throughout the test (**Fig 2.10.A**). Each trial was preceded and followed by a 180-s inter-trial interval. At the end, the mice were returned to their home cages.

• Context-freezing test: the mice were returned to the conditioning chambers 24 hr after conditioning and left undisturbed for 4 min. This served to gauge conditioned freezing in response to the context in which the CS-US pairings took place.

• 24 hr later, to better isolate the conditioned freezing response specific to the CS, the chamber's context was modified. A curved opaque Plexiglas back wall was added, and the metal grid was covered with a Plexiglas floor. The house light was kept off throughout the test (**Fig 2.10.B**). Additionally, a distinct odour was introduced by placing 10 g of commercial freeze-dried coffee powder (UCC The Blend 117 Instant Coffee, Ueshima Coffee Co., Ltd., Japan) under the ventilation fan 30 min before the start of the CS test. Two minutes after the mice were placed inside the modified chamber, the tone CS was activated continuously for 8 min. No shock was delivered. CS-freezing was indexed by the increment of % time freezing over the first 2 min after CS onset relative- to the % time freezing recorded over the 2-min pre-CS baseline period.

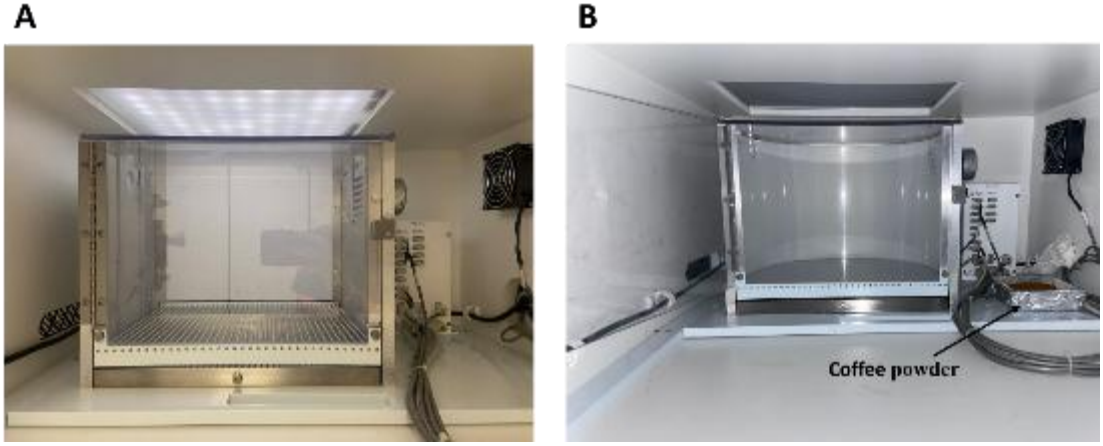

Figure 2.10. The setting of latent inhibition test under conditioning freezing paradigm.
(A) shows the context environment during the pre-exposure, conditioning phases and context-freezing test, with the light turned on in the freezing box. **(B)** illustrates the environmental setup for assessing the CS test 24 hours after the context-freezing test. In this phase, a Plexiglas back wall was added, and the metal grid was covered with a Plexiglas floor to modify the test environment. The house light remained off throughout the test. Additionally, coffee powder was placed under the ventilation fan 30 minutes before the start of the CS test to create a distinct contextual cue.

2.4.9. Sensitivity to MK-801-induced hyper-locomotor activity

Locomotor activity was assessed using eight identical open-field arenas made of grey acrylic, each with floor dimensions of 40 × 40 cm and 30-cm high perimeter walls (**Fig 2.11**). The test consisted of three consecutive phases. First, the mice were placed in the centre of their designated arena without any injection for 15 min to acclimatize them to the environment. Following a habituation phase, the mice were briefly removed from their arenas and injected intraperitoneally (i.p.) with a vehicle solution of 0.9% NaCl (0.1 mL per 10 g body weight). They were then returned to their respective arenas for an additional 30 min of observation. In the final phase, the mice received an i.p. injection of (+)-MK-801 (2.5 mg/kg, 5 mL/kg), sourced from Sigma-Aldrich (Germany) and freshly dissolved in sterile 0.9% saline solution. After this administration, the animals were observed for 120 min.

Locomotion was tracked using EthoVision XT, with video recordings by a camera (FDR-X3000, Sony, Japan) mounted above each set of four arenas. The distance traversed in the arena was quantified in successive 5-min bins. Thigmotaxis tendency was evaluated by computing the average vertical distance from the nearest arena walls per 5-min bin.

Figure 2.11. The apparatus of the open-field box
This figure illustrates the setup of the open-field, consisting of four boxes used for the MK-801 motor activity test. A camera was positioned at the top centre to capture the entire testing area. Animals were counterbalanced across the four boxes to ensure unbiased assessment of motor activity.

2.5. Tissue harvesting

In Experiment 1, maternal tissues, including colon, spleen, and blood, were collected from dams treated with gestational DSS or vehicle controls (see **Fig. 2.1**). The collected colon and spleen were analysed to validate colitis-like pathology, while the serum was examined to assess the maternal immune response. Moreover, the foetuses and placentas from the dams were weighed to assess weight changes. Specifically, foetal brains were isolated and collected for further molecular analyses. In Experiment 2, the left hemisphere and the hippocampus from the right hemisphere were collected from behaviourally naïve offspring exposed to gestational DSS or vehicle controls for molecular and histological assessments. The following sections detail the tissue harvesting procedures.

2.5.1. Maternal, foetal and placental tissues

The collection of maternal blood for cytokine assays, the spleen and colon were also collected from pregnant dams on GD13 (11 DSS-treated and 10 control dams) or GD17 (8 DSS-treated dams and 9 control dams) (See **Fig. 2.1**) under deep non-surviving anaesthesia induced by sodium pentobarbital (150 mg/kg, i.p.) (Dormminal, Alfasan international, Holland) since splenomegaly and colonic shortening are gross pathological hallmarks of DSS-induced colitis (Chassaing et al., 2014; Yang & Merlin, 2024)

Maternal blood was first collected by cardiac puncture after thoracotomy. The sample was left at room temperature (RT) for 30 min, then centrifuged at 2,000 × g and 4°C for 30 min, after which the separated serum was stored at -80°C until analysis. Next, the abdominal cavity was incised, and two experimenters worked together to extract the uterine horn, spleen, and colon.

After separation from the surrounding tissues, the uterine horns were dissected, photographed, and the number of intact and reabsorbed (calcified) foetuses was noted (see **Fig. 2.12**). Individual conceptuses (comprising the embryo, umbilical cord and placenta as a single unit) were carefully extracted one by one. Placed under ice-cold PBS, the embryo and placenta were separated. The foetal brain was then dissected *in toto* under a dissection microscope. After removal of the facial tissue, a midline incision was made along the skull, which was gently peeled back to expose the brain. The meninges were removed, and the brain was detached from the spinal cord. Harvested foetal brains and placentas were either immersed immediately in 4% PFA for 24 hr at 4°C before being transferred to 30% sucrose for cryoprotection at 4°C until sectioning, or placed inside an Eppendorf tube, snap-frozen in liquid nitrogen and stored at -80°C until molecular assays.

At the same time, the spleen was isolated *in toto* from the connective tissues by blunt forceps, weighed and photographed.

Next, the colon was carefully grasped with forceps and gently lifted until the cecum was exposed. The colon, together with the cecum and rectum, was resected *in toto*, from the ileocecal junction to the anus. The entire length of the colon was carefully straightened alongside a ruler and photographed. Colonic length was measured from the junction between the cecum and the ascending colon to the end of the rectum. To remove faecal matter and blood, the colon was flushed with cold PBS delivered via a blunt 18G needle connected to a syringe. Then two 1-cm fragments from the distal end of the colon adjoining the rectum were excised. One fragment destined for subsequent histological processing was post-fixed in 10% neutral formalin. The other fragment was placed inside an Eppendorf tube, snap-frozen in liquid nitrogen, and stored at -80°C until molecular assays.

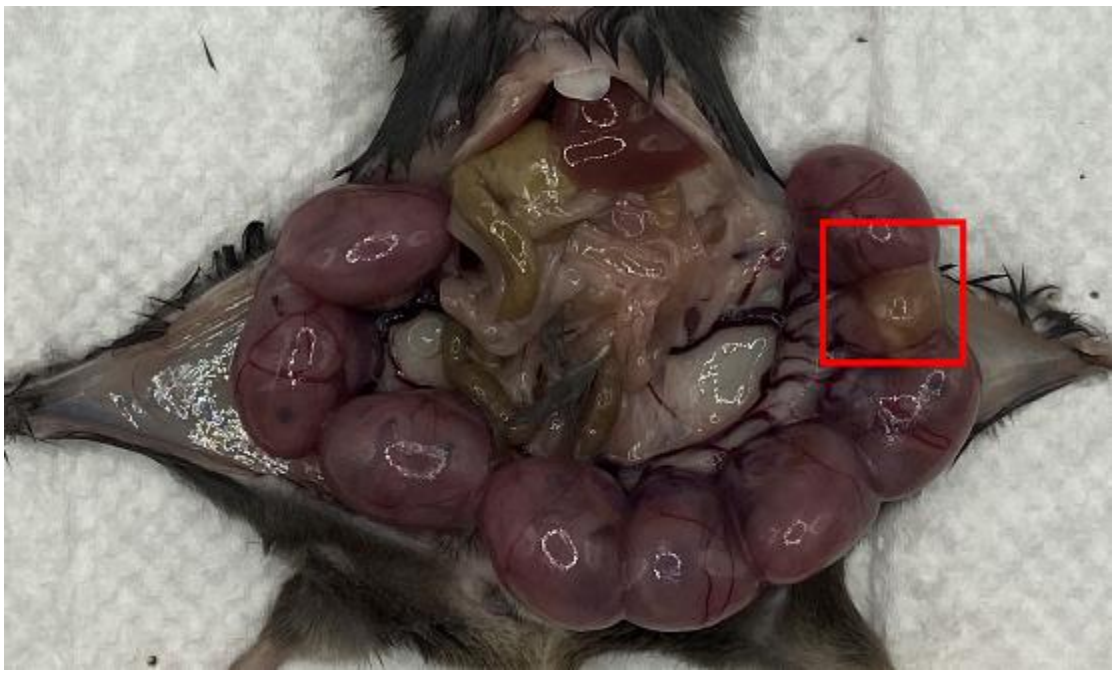

Figure 2.12. Representative Image of the Dissection Procedure.
This photograph captured the abdominal cavity of a DSS-treated dam on GD 17. The resorbed foetus, indicated within the red box, is highlighted to provide a clear visual reference for the dissection process.

2.5.2. Brains from behaviourally naïve offspring Cohort C

Under deep pentobarbital euthanasia, offspring of Cohort C (see **Fig. 2.1**) were killed by decapitation on either PND 40 as juvenile mice (DSS: 9 females, 6 males; Ctrl: 11 females, 12 males) or on PNDs 110~113 as adult mice (DSS: 12 females, 8 males; Ctrl: 7 females, 11 males), and their brain quickly removed *in toto*. The left hemisphere was separated and post-fixed in 4% PFA for 72 h before being immersed in 30% sucrose for cryoprotection and storage at 4°C until immunohistochemistry. The hippocampus was extracted in toto from the right hemisphere, snap-frozen in liquid nitrogen immediately and stored at -80°C until molecular assays: ELISA for BDNF, and RT-PCR for synthesis of NR1 and NR2A/B subunits.

2.6. Evaluation of transcription expression

To examine the impact of gestational DSS on tissue transcript expression, total RNA was extracted from the colon, foetal brain, placenta, and brain samples in experiment 1 and 2 respectively. After purification, the RNA was reverse-transcribed into cDNA for probe-based real-time quantitative PCR (RT-qPCR) analysis. Gene expression levels were quantified using TaqMan assays.

2.6.1. Total RNA extraction:

All RNA-related procedures were conducted in a dedicated molecular biology workspace. Work surfaces and instruments were disinfected with 70% ethanol, followed by commercial ribonuclease (RNase) decontamination reagents (Thermo Fisher Scientific, USA). All consumables were nuclease-free. Pestles and mortars used for tissue disruption were treated overnight with 1% diethyl pyrocarbonate (DEPC; Sigma-Aldrich, USA) in ultrapure water and autoclaved at 120°C for 20 min to eliminate RNase activity. Rigorous precautions were implemented to prevent sample contamination with exogenous DNA and RNA degradation by RNases or elevated

temperatures. These included wearing fresh masks and gloves, avoiding movement of objects over uncapped samples or reagents, and keeping RNA-containing tubes on ice. Following these measures, total RNA was extracted in high yield and quality. RNA purification, including removal of contaminating genomic DNA and proteins, was performed using commercial kits, such as the ReliaPrep RNA Tissue Miniprep System (Promega, USA). All RNA samples were treated with deoxyribonuclease (DNase), supplied with the kit, during purification to eliminate genomic DNA.

Total RNA was extracted from isolated colon, foetal brain, and placenta tissues using TRIzol Reagent (Invitrogen, USA), followed by purification with the ReliaPrep RNA Tissue Miniprep System (Promega, USA). The manufacturer's protocols for reagent preparation and RNA purification were strictly followed. Briefly, tissues were lysed in 500 µL of TRIzol Reagent per sample and homogenised using a homogeniser. The homogenate was incubated for 5 min at RT to ensure complete dissociation of nucleoprotein complexes. Subsequently, 50 µL of BCP phase separation reagent (Molecular Research Center, USA) was added, and the mixture was incubated for 3 min, followed by centrifugation at 12,000 × g for 15 min at 4°C. The aqueous phase containing RNA was transferred to a new tube, mixed with 250 µL of isopropanol, and incubated for 10 min at 4°C to precipitate RNA. The mixture was then applied to a ReliaPrep mini-column and centrifuged at 14,000 × g for 30 s at RT (this centrifugation condition was used for subsequent steps unless otherwise specified). The RNA was washed with 500 µL of RNA wash solution (prepared with ethanol) and centrifuged. To remove contaminating genomic DNA, the sample was treated with DNase (supplied with the kit) for 30 min at RT, followed by the addition of 200 µL of column wash solution to inactivate DNase and centrifugation. The RNA was further washed with 500 µL of RNA wash solution and centrifuged. A final wash with 200 µL of RNA wash

solution was performed, followed by centrifugation for 2 min to remove residual buffer. Purified RNA was eluted in 10 µL of nuclease-free water to maximise concentration, as lower elution volumes could reduce total RNA yield, per the manufacturer's recommendations. The quality of the extracted total RNA was evaluated by the RNA electrophoresis in TAE agarose gels.

2.6.2. First-standard cDNA synthesis:

The concentration and purity of purified total RNA samples isolated from tissues were determined by spectrophotometry using a NanoDrop™ One/OneC Microvolume UV-Vis Spectrophotometer (Thermo Fisher Scientific, USA). RNA purity was assessed by calculating the A260/A280 and A260/A230 absorbance ratios. The A260/A280 ratio, which measures absorbance at 260 nm relative to 280 nm, serves as an indicator of RNA purity, with a value of approximately 2.0 considered indicative of pure RNA. The A260/A230 ratio evaluates contamination by organic compounds, such as TRIzol, phenol, guanidine HCl, or guanidine thiocyanate, with acceptable values typically ranging from 2.0 to 2.2.

To synthesise first-strand cDNA, 1 µg of total RNA was reverse-transcribed using the GoScript Reverse Transcription System (Promega, USA). The constituents of the reaction mixes were summarised in **Table 2.2**. For reverse transcription, reaction mix 1 was incubated at 42°C for 5 min. After 5 min incubation, reaction mixes 1 and 2 were then combined into a final mix, which underwent reverse transcription through incubation at 25°C for 5 minutes, 42°C for 60 min, and 70°C for 15 min. The reverse transcription reaction was performed using a T100 Thermal Cycler (Bio-Rad, USA). To confirm the absence of genomic DNA contamination in total RNA samples, a no-reverse-transcriptase (NRT) control was prepared for each sample, in which reverse transcriptase was replaced with nuclease-free water. The resulting cDNA samples were

stored at -20°C prior to RT-qPCR analysis or at -80°C for storage.

Reaction mixes 1 (per sample)	**Reaction mixes 2 (per sample)**
*Total RNA (1 μg) = X μL	GoScript 5X reaction buffer = 4 μL
Random primer (0.5 μg) = 1 μL	$MgCl_2$ (2 mM) = 2 μL
Oligo dT (0.5 μg) = 1 μL	PCR Nucleotide mix (0.5 mM) = 1 μL
Nuclease-free water = (8 – X) μL	RNasin = 0.5 μL
	GoScript reverse transcriptase = 1 μL
	Nuclease-free water = 1.5 μL
Total volume = 10 μL	Total volume = 10 μL

Table 2.2. **Reaction mixes of the reverse transcription reaction.**
Total RNA was isolated from tissue samples. * For a less abundant cell sample, X was about 9, which was the volume of RNA eluted. The GoScript reverse transcription system provided all the listed components. Abbreviation: oligo-dT = deoxythymidine oligomer; $MgCl_2$ = magnesium chloride; RNasin = ribonuclease inhibitor.

2.6.3. RT-qPCR data processing and analysis:

To quantify transcript levels in cDNA samples, probe-based real-time quantitative PCR (RT-qPCR) was performed using a CFX opus 96 Real-Time PCR System (Bio-Rad, USA). All probes were TaqMan assays targeting the mouse genome (Thermo Fisher Scientific, USA), as listed in **Table 2.3**. The SsoAdvanced Universal Probes Supermix (Bio-Rad, USA) was used, containing all necessary components for probe-based RT-qPCR. The reaction mixes recipe and PCR cycling conditions were summarised in **Table 2.4**.

Housekeeping genes were selected and validated using NormFinder, an algorithm for assessing expression stability (Andersen et al., 2004). NormFinder ranks candidate housekeeping genes based on their stability within a given sample set and experimental design. In this study, the candidate housekeeping genes were GAPDH, ACTB, TBP, POLR2A, and AP3D1. The cycle threshold (Ct) values from these housekeeping gene candidates were analysed using NormFinder to identify the most stable gene or combination of genes for normalisation.

To ensure consistency across experimental batches, the fluorescence threshold was set at relative fluorescence units (RFU) of 100, 200, 300, 400, or 500, empirically determined to lie within the exponential phase of the PCR amplification curves. Ct values were calculated for each gene and sample. Genes with Ct values exceeding 35 cycles were considered not expressed in the respective sample. To account for variations in starting material, Ct values of target genes were normalised to those of the selected housekeeping gene(s). Relative gene expression changes between groups were calculated using the $2^{-\Delta\Delta Ct}$ method (Livak & Schmittgen, 2001), where $\Delta\Delta Ct$ represented the difference in normalised Ct values. Statistical analyses were conducted on delta Ct (ΔCt) values, calculated as Ct (target gene) − Ct (housekeeping gene(s)).

Description	Symbol	Assay ID
Glyceraldehyde 3-phosphate dehydrogenase	GAPDH	Mm4352932E
Beta-actin	ACTB	Mm02619580_g1
TATA-box binding protein	TBP	Mm01277042_m1
RNA polymerase II subunit A	POLR2A	Mm00839502_m1
Adaptor-related protein complex 3 subunit delta 1	AP3D1	Mm00475961_m1
Glutamate Ionotropic Receptor NMDA Type Subunit 1	Grin1	Mm00433790_m1
Glutamate Ionotropic Receptor NMDA Type Subunit 2A	Grin2a	Mm00433802_m1
Glutamate Ionotropic Receptor NMDA Type Subunit 2B	Grin2b	Mm00433820_m1
Interleukin 1 Beta	IL1b	Mm00434228_m1
Interleukin 6	IL6	Mm00446190_m1
Interleukin 10	IL10	Mm01288386_m1
Tumor Necrosis Factor	TNF	Mm00443258_m1

Table 2.3. TaqMan Assays used for RT-qPCR analysis.
This table lists the TaqMan assays employed for RT-qPCR to quantify gene expression in cDNA samples derived from mouse tissues. The table includes housekeeping genes used for normalisation and target genes of interest. Columns detail the gene name, gene symbol, TaqMan assay ID in the study.

A

Components	Volume per reaction (µL)
2X Universal probes supermix	10
cDNA	1
Taqman assay 1	1
Nuclease-free water	8
Total Volume	20

B

Steps	Temperature and duration	
Activation	95°C, 30 sec	
Denaturing	95°C, 15 sec	Cycles: 40
Annealing, Extension and Measurement	60°C, 30 sec	
End	25°C, forever	

Table 2.4. Protocol of probe-based RT-qPCR.
A) Reaction mix recipe for a single reaction; B) qPCR conditions

2.7. Protein expression

In Experiment 1, maternal serum was analysed for inflammatory cytokines, including interleukin (IL)-1β, IL-6, and tumor necrosis factor (TNF)-α, using enzyme-linked immunosorbent assay (ELISA) **(see Section 2.7.3).** This assessed the maternal immune response to gestational dextran sulfate sodium (DSS). In Experiment 2, hippocampal brain-derived neurotrophic factor (BDNF) levels in juvenile and adult offspring were measured via ELISA to evaluate neurodevelopmental impacts in the offspring. To explore immune markers activated in response to the induction of inflammatory bowel disease (IBD), and synaptic neuron markers in the foetal brain were evaluated at gestational days (GD) 13 and 17 in Experiment 1. Antibodies for the proteins of interest are listed in **Table 2.6**. Protein extraction and Western blotting procedures, adapted from Cheung et al. (2011) and the Bio-Rad Western Blotting Guide (Bio-Rad, USA), are described below.

https://www.bio-rad.com/webroot/web/pdf/lsr/literature/Bulletin_6376.pdf

2.7.1. Protein extraction

The total protein was extracted from two different tissues, one the right hippocampus of behaviourally naïve offspring in juvenile and adult (Cohort C in Experiment 1) and the foetal brain on GD13 and GD17 (Experiment 2). These tissues were lysed in radioimmunoprecipitation assay (RIPA) buffer (Thermo Fisher Scientific, USA). The RIPA buffer composition is listed in **Table 2.5.** The buffer was supplemented with phosphatase and protease inhibitors to prevent protein dephosphorylation and degradation by endogenous phosphatases and proteases, respectively. Precautions were taken to use autoclaved, protease-free consumables and to keep protein samples on ice to minimise degradation.

For protein extraction, frozen foetal brain (Experiment 1) and hippocampus tissue (Cohort C in Experiment 2) were homogenised using a KIMBLE® Pellet Pestle® homogeniser for 30 s. The tissue was then lysed in 100 µL (hippocampus) and 250 µL

(foetal brain) of ice-cold RIPA lysis containing cOmplete™ Mini Protease Inhibitor Cocktail (Roche, Switzerland) and a protease and phosphatase inhibitor cocktail (Abcam, UK). The homogenate was further processed by passing it through a 25-G needle until smooth (typically fewer than 20 passages), taking care to avoid bubble formation. The lysate was incubated on ice for 30 min and centrifuged at 12,000 × g for 30 min at 4°C. The supernatant, containing total protein, was aliquoted, snap-frozen in liquid nitrogen, and stored at -80°C until analysis.

Components	Volume (µl) per 1 ml buffer
10X RIPA lysis buffer	100
10X PhosSTOP phosphatase inhibitor	100
10X cOmplete™, Mini Protease Inhibitor Cocktail	100
ddH2O	700

Table 2.5. Composition of protein lysis buffer for protein extraction.
Tablet of cOmplete™, Mini Protease Inhibitor Cocktail was dissolved in double-distilled water (ddH2O) at 10 times the concentration. The protein lysis buffer mix was freshly prepared before the protein extraction.

2.7.2. Protein concentration determination

Stored aliquot protein samples were thawed on ice, and total protein concentration was determined using the Bio-Rad Quick Start™ Bradford Protein Assay (Bio-Rad, USA) with bovine serum albumin (BSA) standards (Bio-Rad, USA), following the manufacturer's protocol. Briefly, samples were diluted to minimise interference from the lysis buffer matrix. Pooled protein extracts from each group were diluted 50-fold for hippocampus and 25-fold for foetal brain with ddH_2O and loaded in duplicate into a 96-well plate containing 250 µL of Bradford reagent per well. Similarly, BSA standards were serially diluted to four concentrations and loaded in duplicate per concentration into the same plate. The plate was scanned for absorbance at 595 nm using a Varioskan LUX Multimode Microplate Reader (Thermo Fisher Scientific, USA). Absorbance values for duplicates were averaged and blank-subtracted. A standard curve was generated by plotting absorbance at 595 nm against BSA standard concentrations (0, 0.125, 0.25, 0.5, 0.75, 1 mg/mL), and sample protein concentrations were calculated using the linear slope of the standard curve.

Sample dilution factor = n (Hippocampus= 50× ; Foetal brain= 25×)

Sample protein concentration ($\mu g \cdot \mu l^{-1}$) = (Blank subtracted sample Abs 590 nm/ M_{BSA}) x Sample dilution factor

After determining protein concentrations, hippocampal samples from Experiment 2 were analysed via ELISA to quantify BDNF levels, while foetal brain samples from Experiment 1 were prepared for Western blotting to assess inflammatory and synaptic markers.

2.7.3. ELISA for hippocampal BDNF (Cohort C)

Brain-derived neurotrophic factor (BDNF) levels were quantified in hippocampal protein extracts using the BDNF ELISA Kit (R&D Systems, DY248) and DuoSet Ancillary Reagent Kit (R&D Systems, DY008B). All plate preparation and assay procedures were performed at RT following the manufacturer's instruction. Briefly, 100 µL of diluted capture antibody was added to each well of a 96-well plate and incubated overnight. The plate was then washed with the provided wash buffer and blocked with reagent diluent at the working concentration for 1 hr. Total protein extracts were diluted 50-fold in reagent diluent based on optimisation data to minimise matrix effects. BDNF standards were serially diluted in reagent diluent containing 2% lysis buffer to account for matrix interference. After blocking, the plate was washed, and 100 µL of samples or standards was added to each well and incubated for 2 hr. Subsequently, 100 µL of the detection antibody was added, followed by a 2-hr incubation. The plate was then incubated with streptavidin-horseradish peroxidase (HRP) for 30 min, with washing steps performed between each stage. Finally, 100 µL of tetramethylbenzidine (TMB) substrate was added per well, and the plate was incubated with shaking at 25°C. Absorbance was monitored at 652 nm for 1 min until reaching approximately 1.0, at which point 50 µL of stop solution was added per well, followed by shaking at 600 rpm for 30 s. The plate was read at 450 nm and 540 nm using a Varioskan LUX Multimode Microplate Reader (Thermo Fisher Scientific, USA). Absorbance values at 540 nm were subtracted from those at 450 nm and fitted to a four-parameter logistic function to determine BDNF concentrations. All samples and standards were measured in duplicate wells.

2.7.4. Quantification of cytokines in maternal serum on GD 13 and 17

Pro-inflammatory cytokine levels in maternal serum, collected on GD 13 and 17, were quantified by ELISA kits. Serum concentrations of TNF-α and IL-1β were measured using high-sensitivity ELISA kits (R&D Systems, USA; TNF-α: MHSTA50, sensitivity 0.295 pg/mL; IL-1β: MHSLB00, sensitivity 0.312 pg/mL). IL-6 levels were determined using an ELISA kit (Abcam, UK; ab222503, sensitivity 11.3 pg/mL). All assays were performed at RT following the manufacturers' protocols.

For TNF-α and IL-1β quantification, 50 µL of assay diluent and 50 µL of standard or serum sample were added to each well of a 96-well plate, mixed, and incubated for 2 hr. Plates were washed three times with the provided wash buffer. Subsequently, 100 µL of mouse TNF-α high-sensitivity conjugate or IL-1β conjugate was added, followed by a 1-hour incubation and three additional washes. Then, 200 µL of streptavidin-polymer-horseradish peroxidase (HRP) was added, incubated for 30 min, and washed three times. Finally, 200 µL of substrate solution was added, and plates were incubated until sufficient color development. Absorbance was measured at 450 nm and 540 nm using a Varioskan LUX Multimode Microplate Reader (Thermo Fisher Scientific, USA). Absorbance values at 540 nm were subtracted from those at 450 nm to correct for background noise.

For IL-6 quantification, 50 µL of antibody cocktail and 50 µL of standard or serum sample were added to each well, mixed, and incubated for 1 hour on a plate shaker (400 rpm). Plates were washed three times with wash buffer, followed by the addition of 100 µL of TMB development solution. Incubation time was optimized by monitoring absorbance at 600 nm until an optical density of 1.0 was reached, as measured by the microplate reader. Subsequently, 100 µL of stop solution was added, and absorbance was measured at 450 nm.

For all cytokines, absorbance values were fitted to a four-parameter logistic function to determine concentrations. Samples and standards were analysed in duplicate to ensure reproducibility, and results were expressed as pg/mL.

2.7.5. SDS-PAGE protein separation for foetal brain on GD 13 and 17

Unless otherwise specified, all reagents and materials for sodium dodecyl sulphate-polyacrylamide gel electrophoresis (SDS-PAGE) were purchased from Bio-Rad (USA). Tris-glycine-SDS running buffer was freshly prepared by diluting 10× stock with double-distilled water (ddH_2O). A commercial 4–15% gradient Mini-PROTEAN TGX Stain-Free precast gel was used. The gel was assembled in an electrophoresis apparatus, with the inner and outer chambers filled with running buffers. The comb was removed from the gel, and any bubbles in the wells were dislodged by gently flushing with running buffer.

For sample preparation, 100 µg of total protein was mixed with 5× Laemmli buffer supplemented with 500 mM dithiothreitol (DTT; Sigma-Aldrich, USA) and topped up to 40 µL with ddH_2O. The sample-buffer mixtures were denatured at 95°C for 5 min and briefly centrifuged. Denatured protein samples, along with dual-colour and kaleidoscope protein ladders (10–250 kDa; Bio-Rad, USA) for molecular weight reference, were loaded into the wells. Empty wells were filled with an equivalent volume of working loading buffer to prevent edge effects during electrophoresis. Gels were running at 120 V for 30 min. For runs involving more than two gels, higher voltage or extended running time was applied as needed. Electrophoresis was stopped when the dye front reached approximately 1 cm from the gel bottom, after which the gel was removed from the cassette for subsequent Western blotting. After electrophoresis, the stain-free gel was placed in the chamber of a ChemiDoc Imaging System (Bio-Rad, USA) and exposed to ultraviolet (UV) light for 5 min to activate the stain-free

technology for total protein visualisation.

2.7.6. Western Blotting transfer for foetal brain on GD 13 and 17

Following SDS-PAGE, proteins were transferred to a (polyvinylidene difluoride) PVDF membrane (Bio-Rad, USA) using a wet transfer system. The gel holder cassette, containing sponge pads, blotting filter papers, and the PVDF, was pre-soaked in transfer buffer composed of 20% methanol (Sigma-Aldrich, USA) and 1× Tris-glycine buffer diluted from 10× stock (Bio-Rad, USA) with ddH_2O.

The activated gel was equilibrated in transfer buffer and assembled in the gel holder cassette for wet transfer. The sandwich arrangement, from cathode (−) to anode (+), consisted of a sponge pad, filter papers, gel, nitrocellulose membrane, filter papers, and a sponge pad. This configuration facilitated the migration of negatively charged proteins from the gel to the membrane under an electric field. The cassette was placed in a transfer tank filled with transfer buffer and maintained at 4°C. Transfer was performed at a constant voltage of 80 V overnight. Successful transfer was confirmed by the complete migration of coloured ladder markers to the membrane. The membrane was then imaged using the ChemiDoc Imaging System to verify total protein loading and ensure complete protein transfer. Subsequently, the membrane was prepared for blocking and primary antibody incubation.

2.7.7. Membrane blocking and primary antibody incubation

Following protein transfer, the nitrocellulose membrane was washed twice with Tris-buffered saline containing 0.1% Tween 20 (TBST; Tween 20, Sigma-Aldrich, USA) for 5 min each. The membrane was then blocked with 5% non-fat dry milk in TBST for 4 hr at 4°C. After replacing the blocking solution, the membrane was incubated with primary antibodies (listed in **Table 2.6**) diluted in fresh blocking solution at 4°C overnight with continuous rolling.

2.7.8. Secondary antibody incubation and detection

The membrane was washed three times with TBST for 5 min each and incubated with horseradish peroxidase (HRP)-conjugated secondary antibodies against mouse immunoglobulin G (IgG; 1:3,000; Cell Signaling Technology, USA) in 5% non-fat dry milk in TBST for 2 hr at RT. Following three additional 5-min TBST washes, the membrane was treated with enhanced chemiluminescent (ECL) substrate (Bio-Rad, USA) or SuperSignal™ West Femto Maximum Sensitivity Substrate (Thermo Fisher Scientific, USA) and imaged using a ChemiDoc Imaging System to visualise chemiluminescence. Images captured at various exposure times were analysed qualitatively.

Primary antibody	MW(kDa)	Dilution
ASC/TMS1	22	1:1000
Cleaved IL-1β	17	1:500
NLRP3	110	1:500
p-NF-κB	65	1:1000
Complexin-1/2	14-16	1:1000
SHANK3	220	1:1000
Synapsin-1	77	1:1000
Synaptophysin	38	1:1000
Synaptotagmin-1	60	1:1000
ZO-1	220	1:1000

Table 2.6. The primary antibodies were used for western blotting.
The primary antibodies contained three categories of markers: inflammasome markers, synaptic neuron markers and the tight junction protein marker. All antibodies were purchased from Cell Signalling Technology, except for NLRP3 and ZO-1, which were obtained from Abcam.

2.8. Histological analysis of the maternal colon and hippocampus (Cohort C)

2.8.1. Hematoxylin and eosin staining of maternal colon sections

Formalin-fixed maternal colon tissues were dehydrated through a graded ethanol series (70%, 90%, 100%) and cleared in xylene. The samples were embedded in paraffin using two 90-min cycles followed by one 180-min cycle at 62°C under vacuum. Embedded colon tissues were sectioned coronally at 5 μm using a rotary microtome (Leica, Germany). Paraffin sections were mounted onto IncuPLUS adhesive glass slides (IncuPath™, China) and air-dried overnight. The paraffin sections were dewaxed in xylene, rehydrated through a descending ethanol series (100%, 90%, 70%), and running water for 2 min. For H&E staining, rehydrated sections were incubated in Gill's 2 Hematoxylin (Cancerdiagnostics, USA) for 10 min, destained with acid alcohol for 5 s, and differentiated with bluing reagent for 1 min. Sections were then stained with Shandon Eosin Y aqueous solution (Thermo Fisher Scientific, USA) for 1 min. Between each step, slides were rinsed in running tap water for 1 min to remove excess solution. After staining, sections were dehydrated through an ascending ethanol series (70%, 90%, 100%, three times each) for 5 min per step, followed by clearing in xylene (three times, 5 min each). Stained sections were mounted on coverslips with DPX mounting medium (Sigma-Aldrich, USA) and left to air-dry at RT before being examined under a microscope.

2.8.2. Alcian blue staining of maternal colon sections

To evaluate goblet cells in paraffin-embedded colon sections, slides were stained with Alcian blue solution (pH 2.5) (Cancerdiagnostics, USA) for 30 min. Sections were then rinsed in running tap water for 2 min, followed by counterstaining with nuclear fast red solution (Cancerdiagnostics, USA) for 5 min. Slides were washed again in

running tap water for 2 min. Dehydration, clearing, and mounting were performed as described for H&E staining

2.8.3. Immunohistochemistry

Formalin-fixed left-brain hemispheres from behaviourally naïve cohort C offspring were embedded in paraffin and sectioned coronally at 30 µm using a rotary microtome (Leica, Germany) following the method described in **2.8.1**. After rehydration, slides were then immersed in running water for 2 min, followed by incubation in preheated (95°C) EnVision Flex Target Retrieval Solution (Dako, K800421-2, Denmark) for 30 min for antigen retrieval. After cooling to RT for 45 min, slides were rinsed in phosphate-buffered saline (PBS). To inhibit endogenous peroxidase activity, sections were treated with Dako Peroxidase-Blocking Solution (S202386, Denmark) for 10 min at RT. Sections were then incubated for 1 h at RT with primary antibody, anti-doublecortin (DCx; 1:1000; Abcam, UK), diluted in Dako Antibody Diluent (S302283, Denmark). After washing with buffer (Dako, K800721-2, Denmark), sections were incubated with horseradish peroxidase (HRP)-labelled polymer-conjugated secondary antibody (EnVision® System, Peroxidase/DAB, Rabbit/Mouse; Dako, K5007, Denmark) for 30 min. Immunoreactivity was visualised using 3,3'-diaminobenzidine (DAB) chromogen, with the reaction stopped by immersion in deionised water for 1–2 min once optimal staining intensity was achieved.

2.8.4. Microscopic imaging

All the prepared paraffin sections were observed under our Eclipse Ni microscope (Nikon Instruments, USA) equipped with 4x to 40x objectives. DS-Qi2 (Nikon Instruments, USA) and NIS-Elements Basic Research (Nikon Instruments, USA) imaging software were used for image capturing. For bright-field imaging, white balance was adjusted using the imaging software. The noise or background signal, including non-specific antibody binding, was identified by no primary control staining during optimisation. For quantitative measurement, large images at 20x magnification were captured from the whole hemisphere section.

2.8.5. Counting of DCx- immunoreactive cells in the hippocampus

Cell counting and morphometric analysis of DCx-immunoreactive (DCx-ir) cells in the dorsal hippocampus were performed on three coronal sections (180 μm apart) taken approximately at 1.82 to 2.18 mm posterior to bregma according to Franklin and Paxinos (2008). High-resolution stitched images of the hippocampal formation from selected sections were acquired using a light microscope equipped with a 10× objective, a motorized stage, and DS-Qi2 (Nikon Instruments, USA). DCx-ir cells within the dentate granular cell layer, characterized by a stained soma and an identifiable apical dendrite extending toward the molecular layer, were manually counted under blind conditions and expressed in counts per mm^2.

2.9. Statistical analyses

All data were analysed using SPSS version 26, employing parametric analysis of variance (ANOVA) where applicable. Before conducting ANOVAs, the normality of individual datasets was assessed using the Shapiro-Wilk test, along with visual inspections of QQ plots, skewness, and kurtosis. To correct deviations from normality, a logarithmic transformation was applied to the TNF-α dataset.

In the foetal experiment (see **Fig 2.1**), ANOVAs included the between-subject factors Group (DSS vs Control) and Harvest time point (GD13 vs GD17) to assess potential interactions between treatment and developmental timing. In the offspring experiment (see **Fig. 2.1**), behavioural data collected from the elevated plus maze (EPM), Y-maze, social interaction test, and prepulse inhibition (PPI) task were analysed using ANOVAs, incorporating the between-subject factors Group (DSS vs Control), Sex (Male vs Female), and Age (Juvenile vs Adult). For additional behavioural measures collected in adulthood, ANOVAs were conducted with Group (DSS vs Control) and Sex (Male vs Female) as between-subject factors. Specifically, the latent inhibition test included pre-exposure (PE vs NPE) as an additional factor.

Within-subject factors, including time bins (1-min and 5-min), prepulse intensity, pulse intensity, trials, and sucrose concentration, were integrated into the analyses depending on the nature of the dependent variables. To account for potential confounding effects of body weight, ANCOVAs were employed in the analysis of whole-body startle magnitude. Statistical significance was determined at a Type-I error rate of 0.05, and effect sizes were reported as ηp^2.

To further interpret significant interactions involving Treatment, Sex, and Age, Fisher's LSD post-hoc comparisons were conducted. For the analysis of circulating IL-1β and IL-6 levels in maternal hosts, nonparametric Mann–Whitney U tests were used.

Additionally, independent t-tests were applied to evaluate outcomes from real-time PCR analyses.

Pregnant dams were considered the unit of manipulation for statistical analysis. Statistical significance thresholds were denoted as (*) $p < 0.05$* and (***) $p < 0.001$. All data are presented as means ± standard error (SE), obtained either directly from ANOVA outputs within SPSS or as adjusted means derived from ANCOVA results.

Chapter 3: Results

3. Results

3.1. Effect of gestational DSS on pregnant dams

Analysis of fluid intake obtained at 24 h, 48 h, and 72 h after the initiation of DSS treatment in pregnant dams (19 DSS and 19 control) did not reveal any group difference [F<1] (**Fig 3.1A**). Both groups exhibited a monotonic increase in daily fluid intake over the three days. A 2 × 3 (Group × Time) ANOVA only yielded a significant effect of Time [$F_{(2,72)} = 8.62$, $p < 0.001$, $\eta_p^2 = 0.19$]. Based on fluid intake, the average amount of DSS consumed was 0.184 ± 0.005 g per DSS-treated dam per day.

Body weight changes in pregnant dams were assessed across three periods: GD5–9 (pre-DSS treatment), GD10–13 (DSS administration and 24 h post-treatment), and GD14–17 (48–120 h post-DSS treatment). Data up to GD13 included 19 DSS-treated and 19 control dams, while data from GD14 onward included 8 DSS-treated and 9 control dams. As illustrated in **Fig. 3.1B**, the body weights of DSS and control dams were highly comparable before DSS administration from GD5 to GD9. However, DSS-treated dams exhibited a transient increase in weight gain on GD11 and GD12 compared to controls, followed by a marked and persistent reduction in weight gain from GD13 onward. These impressions were supported by separate ANOVA over specific observation periods, analysing percent body weight (%BW) relative to GD0.

For GD5 to 9 (pre-DSS treatment), a 2 × 5 (Group × GDs) ANOVA revealed only a significant main effect of GDs [$F_{(4,144)} = 230.96$, $p < 0.001$, $\eta_p^2 = 0.87$], indicating comparable weight gain between groups. For GD10 to 13 (DSS administration and 24 hours post-treatment), a 2× 4 ANOVA of %BW revealed a significant main effect of GDs [$F_{(3,108)} = 446.41$, $p < 0.001$, $\eta_p^2 = 0.93$] and a Group × GDs interaction [$F_{(3,108)} = 18.98$, $p < 0.001$, $\eta_p^2 = 0.35$]. Post-hoc comparisons indicated the lack of a group difference 24 h after DSS treatment initiation on GD10 [$p = 0.45$], the higher %BW in DSS-treated dams on GD11 and GD12 [both p's < 0.001] followed a significant decrease on GD13 [$p < 0.001$]. From GD14–17 (48–120 hours post-DSS treatment), a 2 × 4 ANOVA yielded a highly significant main effect of Group [$F_{(1, 15)} = 19.07$, $p < 0.001$, $\eta_p^2 = 0.56$], GDs [$F_{(3,45)} = 21.76$, $p < 0.001$, $\eta_p^2 = 0.59$], as well as their interaction [$F_{(3,45)} = 8.86$, $p < 0.001$, $\eta_p^2 = 0.37$]. Post-hoc comparisons across successive days showed that DSS-treated dams did not exhibit a significant increase in %BW during

this period and remained significantly below control dams (all $p < 0.001$), who displayed a linear increase in weight.

A reduction in colonic length in DSS-treated dams compared to control dams was evident on both GD13 and GD17 (**Fig. 3.1C, 3.1D**). A 2 × 2 (Group × Harvest Day) randomized block ANOVA revealed a highly significant main effect of Group [$F_{(1,34)} = 23.23$, $p < 0.0001$, $\eta_p^2 = 0.42$] without other effects [F's < 1]. H&E staining (**Fig. 3.1G**) demonstrated the presence of colonic mucosal epithelial damage in DSS-treated dams (but not control dams) on GD17, with characteristic signs of inflammatory cell infiltration (✚), loss of crypt structure (➔), and oedema (★) (**Fig. 3.2A**). Alcian Blue staining **(Fig. 3.2B)** confirmed reduced colonic mucin secretion in DSS-treated dams by GD17.

Comparison of spleen weight expressed as percent body weight confirmed the presence of splenomegaly in DSS-treated dams, but this was primarily seen in DSS-treated dams harvested on GD13 (see examples in **Fig. 3.1E & F**). Splenomegaly was no longer evident on GD17 (**Fig. 3.1 G**). These impressions were confirmed by a 2 × 2 (Group × Harvest Day) ANOVA, which yielded a significant effect of Group [$F_{(1,34)} = 5.57$, $p < 0.05$, $\eta_p^2 = 0.14$], Harvest Day [$F_{(1,34)} = 191.71$, $p < 0.001$, $\eta_p^2 = 0.85$], and their interaction [$F_{(1,34)} = 10.23$, $p < 0.01$, $\eta_p^2 = 0.231$]. Post-hoc Fisher's LSD revealed that the interaction was mainly driven by the significant group difference on GD13 [$p < 0.001$], which was absent on GD17 [$p = 0.58$]. It can confirm that analysis of absolute spleen mass revealed a significant interaction term [$F_{(1,34)} = 13.23$, $p < 0.01$, $\eta_p^2 = 0.28$].

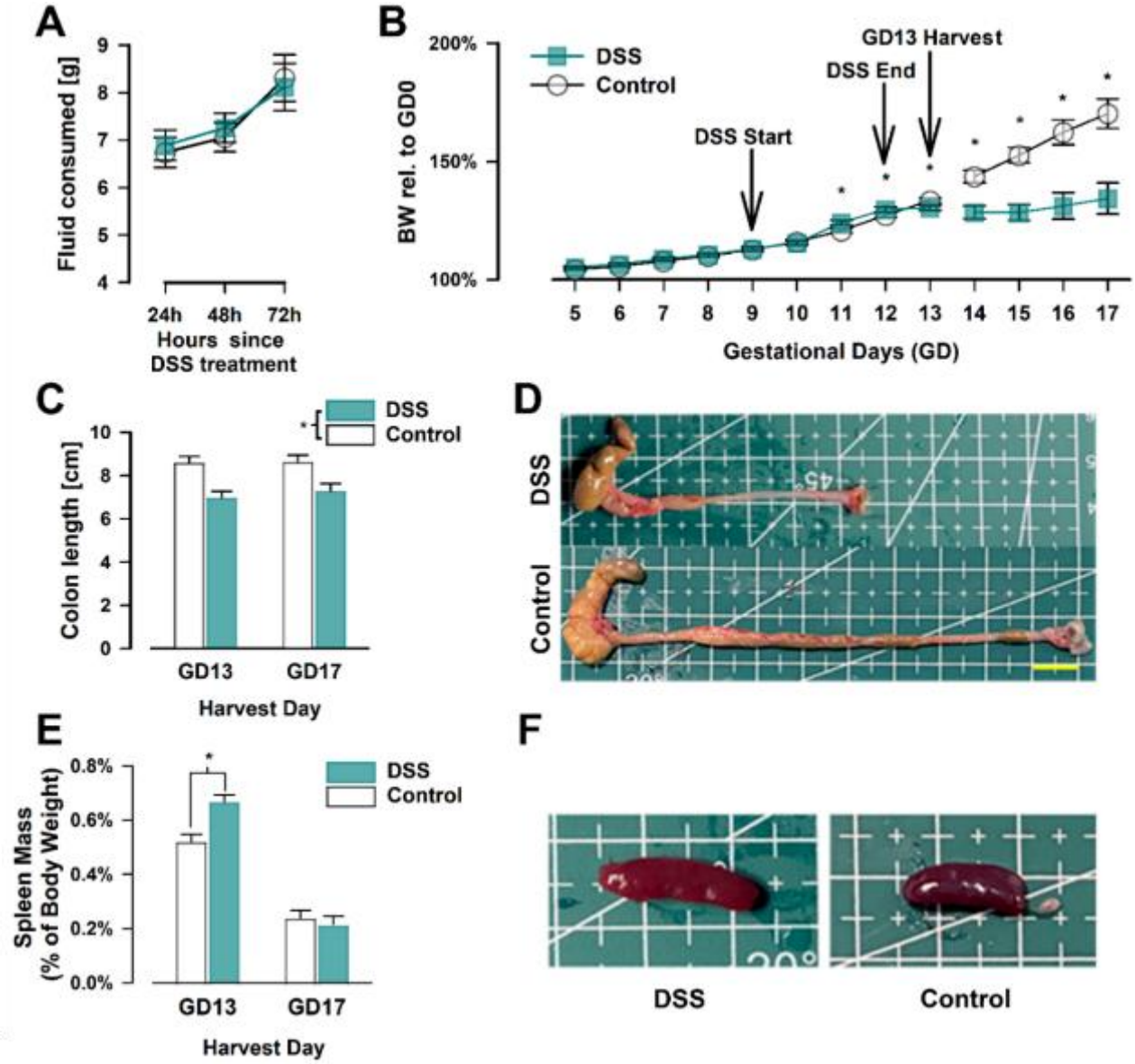

Figure 3.1. Maternal effects of DSS exposure during pregnancy.
(A) Fluid consumption was measured over 72 h (GD9 to GD12) in both DSS-treated (n = 19) and control (n = 19) groups. (**B**) Percentage change in body weight was tracked from GD5 to GD17, with GD0 serving as the baseline. During the pre-treatment period from GD5 to GD9, an increasing trend in body weight was observed. From GD10 (24 h post-DSS treatment initiation) to GD13 (one of the harvest days points), body weight continued to increase, with both DSS-treated and control groups following the closely aligned curves. From GD14 to GD17, a significant divergence emerged between groups. The first two arrows indicate the start and end of the 72-h DSS treatment, while the third arrow marks the harvest day on GD13. Data up to GD13 came from 19 DSS-treated and 19 control dams, while data were available from 8 DSS-treated and 9 control dams since GD14. **(C)** Maternal colon length measured at two harvest time points in DSS-treated and control dams and **(D)** the examples of the caecum, colon, rectum, and anus from DSS-treated (upper panel) and control (lower panel) groups harvested on GD13. Each grid on the cutting mat represents 10 mm (yellow scale). **(E)** Maternal spleen mass measured at two harvest time points in DSS-treated and control dams and **(F)** Representative images of maternal spleens from DSS-treated (left panel) and control (right panel) groups, harvested on GD13, are shown. Each grid on the cutting mat represents 10 mm. Data = mean ± SE, with "*" indicating $p < 0.05$

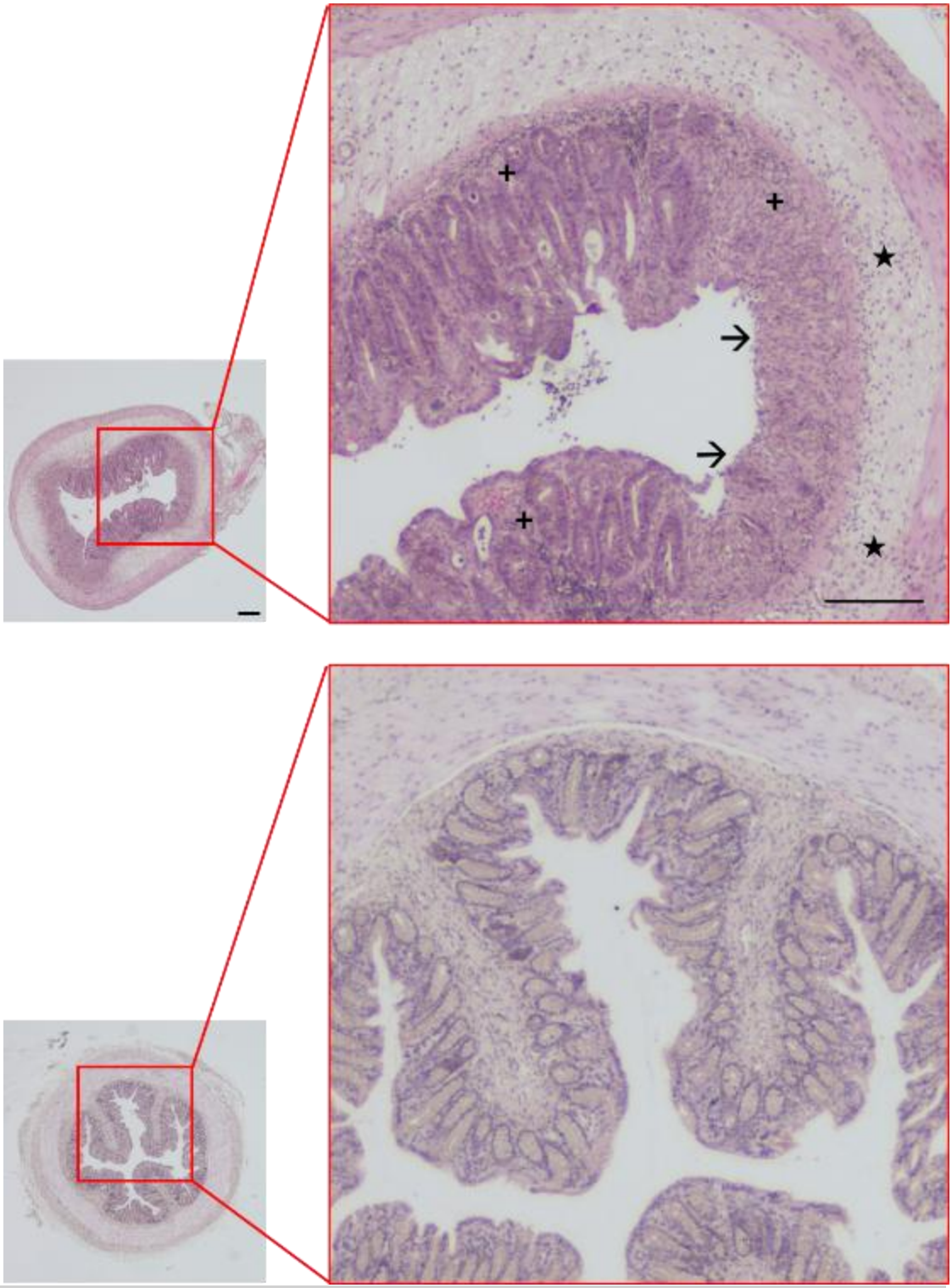

Figure 3.2. Histopathological Changes in H&E-Stained Colon Sections of DSS-Treated Dams.
Examples of H&E-stained colon sections from DSS-treated (upper panel) and control (lower panel) dams harvested on GD17 (120 h after DSS treatment cessation). Photomicrographs are shown at 4× magnification (left; scale bar = 250 µm) and 20× magnification (right; scale bar = 150 µm). with characteristic signs of inflammatory cell infiltration (✚), loss of crypt structure (➜), and oedema (★)

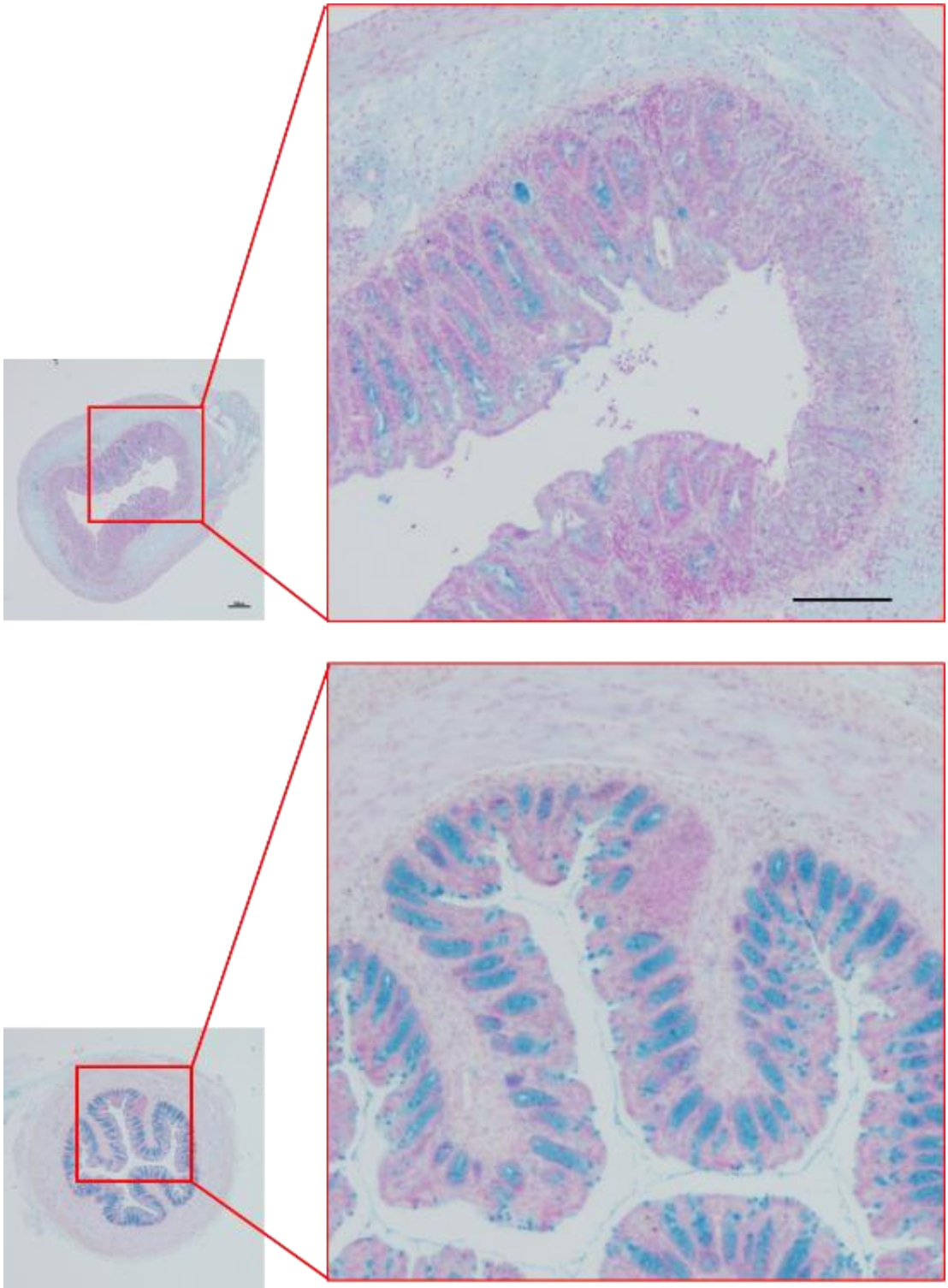

Figure 3.3. Reduced goblet cell mucin production in DSS-treated dams: alcian blue-stained colon section.
Alcian blue-stained colon sections (adjacent to those in **Fig.3.2**) from DSS-treated (upper panel) and control (lower panel) dams on GD17. Sections are shown at 4× magnification (left; scale bar = 250 µm) and 20× magnification (right; scale bar = 150 µm). Positive Alcian Blue staining, indicating goblet cell mucin production, was markedly reduced in DSS-treated dams compared to controls, reflecting goblet cell depletion.

The presence of local immune response in the colon of DSS-treated dams was evidenced by the upregulated RNA expression of selected immune cytokines (depicted in **Fig. 3.4A** as fold change relative to control expression level). Separate independent *t*-tests (of $_{\Delta\Delta}$Ct values) confirmed the significant increase in the gene expression of pro-inflammatory cytokines (IL-1β, IL-6, and TNF-α) and anti-inflammatory cytokine (IL-10) on GD13 [minimal $t_{4.92} = 3.07$, all p's < 0.05]. The effect size of increased expression was the highest for IL-1β [Cohen's $d = 3.68$], followed by IL-6 [Cohen's $d = 2.72$], IL-10 [Cohen's $d = 2.31$] and TNF-α [Cohen's $d = 1.94$]. On GD17, the elevation of IL-1β gene expression induced by DSS treatment remained the highest [Cohen's $d = 2.72$], followed by TNF-α [Cohen's $d = 2.12$] and IL-6 [Cohen's $d = 1.93$]. The upregulation of these pro-inflammatory cytokines all achieved statistical significance [minimal $t_{4.18} = 3.05$, all p's < 0.05], but the increased gene expression of IL-10 was only detected as a trend [$p = 0.09$, Cohen's $d = 1.21$].

The systemic immune response to DSS exposure was assessed by comparing maternal serum levels of IL-1β, IL-6 and TNF-α obtained by ELISA (**Fig. 3.4B**). Dams whose IL-1β and IL-6 level were below the detection limit had their values replaced by the lowest calibration standard (0.00435 pg/mL) for IL-1β and (15.625 pg/mL) for IL-6, respectively. These included all control dams. The comparison was performed using nonparametric Mann–Whitney U tests, which confirmed that serum IL-1β level in DSS-treated dams was significantly higher than control dams on GD13 [$U = 8$, $p < 0.05$, $r = 0.72$] and GD17 [$U = 4$, $p < 0.005$, $r = 0.81$]. And serum IL-6 level showed no significant difference between DSS-treated dams and the control on GD13 [$U = 15$, $p = 0.32$, $r = 0.29$] and GD17 [$U = 9$, $p = 0.06$, $r = 0.55$]. Independent t-tests on $\log_{10}$ transformation serum TNF-α levels revealed a significant increase induced by DSS treatment on GD13 [$p < 0.01$, Cohen's $d = 1.96$], but no significant difference on GD17 [$p = 0.94$, Cohen's $d = 0.05$].

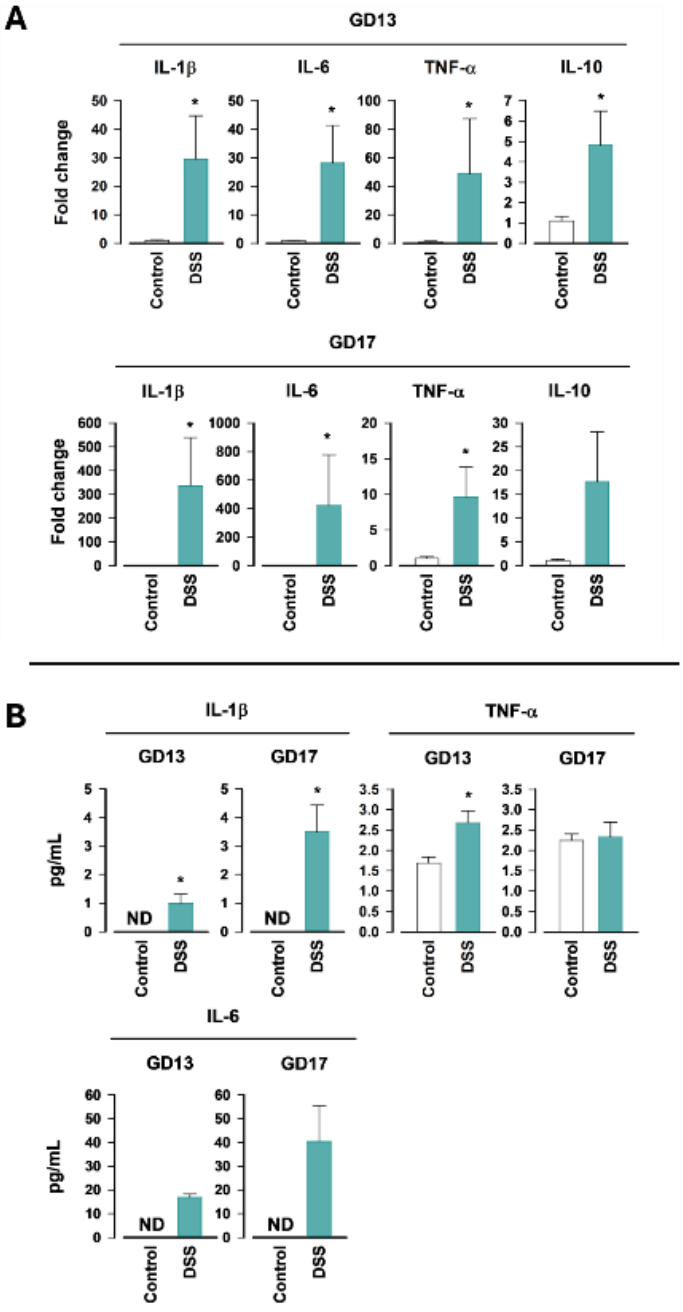

Figure 3.4. DSS modulates the maternal inflammatory response in pregnant dams. **(A)** Total RNA was extracted from the distal colon of DSS-treated and control pregnant dams, harvested on GD13 and GD17. Cytokine mRNA expression was quantified by real-time PCR, with data presented as relative fold changes normalised to ACTB (n = 5 dams per group). Gestational DSS upregulated pro-inflammatory cytokines on GD13 and 17 and upregulated anti-inflammatory cytokines on GD13, compared to controls. **(B)** Protein levels of TNF-α and IL-6 (n = 6 per group) and IL-1β (n = 8 per group) were measured in maternal serum (expressed in pg/mL) at GD13 and GD17. The IL-1β and IL-6 levels in the serum of the control group were below the detection limit **(ND)** at both time points. "*' indicates the significant group difference ($p < 0.05$).

3.2. Effect of gestational DSS on progeny *in utero*

Examination of the proportion of resorbed foetuses per dam identified in pregnancies terminated on GD13 and GD17 (**Fig. 3.5.A**) and the litter size per dam *in utero* (excluding instances of foetal resorption) did not differ substantially between the DSS-treated and control dams (**Fig. 3.5.B**). These was supported by the absence of any significant effects from the 2 × 2 (Group × Harvest Day) ANOVAs of both resorption rate and litter size per dam *in utero*. Next, the average mass of foetuses *in utero* per dam (excluding the resorbed foetuses) was submitted to a 2 × 2 (Group × Harvest Day) ANOVA. As expected, the main effect of Harvest Day achieved statistical significance [$F_{(134)} = 230.57$, $p < 0.001$, $\eta_p^2 = 0.87$], reflecting foetal growth from GD13 to GD17 (**Fig. 3.5.C**). Neither the main effect of Group nor its interaction with Harvest Day achieved statistical significance.

Parallel analysis of the average placental mass *in utero* per dam only yielded a significant main effect of Group [$F_{(134)} = 4.47$, $p < 0.05$, $\eta_p^2 = 0.12$], indicating the reduction of placental mass due to DSS treatment (**Fig. 3 .5. D).** The marginal reduction of placental mass from GD13 to GD17 approached significance [$F_{(1,34)} = 3.87$, $p = 0.06$, $\eta_p^2 = 0.10$], and its interaction with Group was far from significant [$F < 1$].

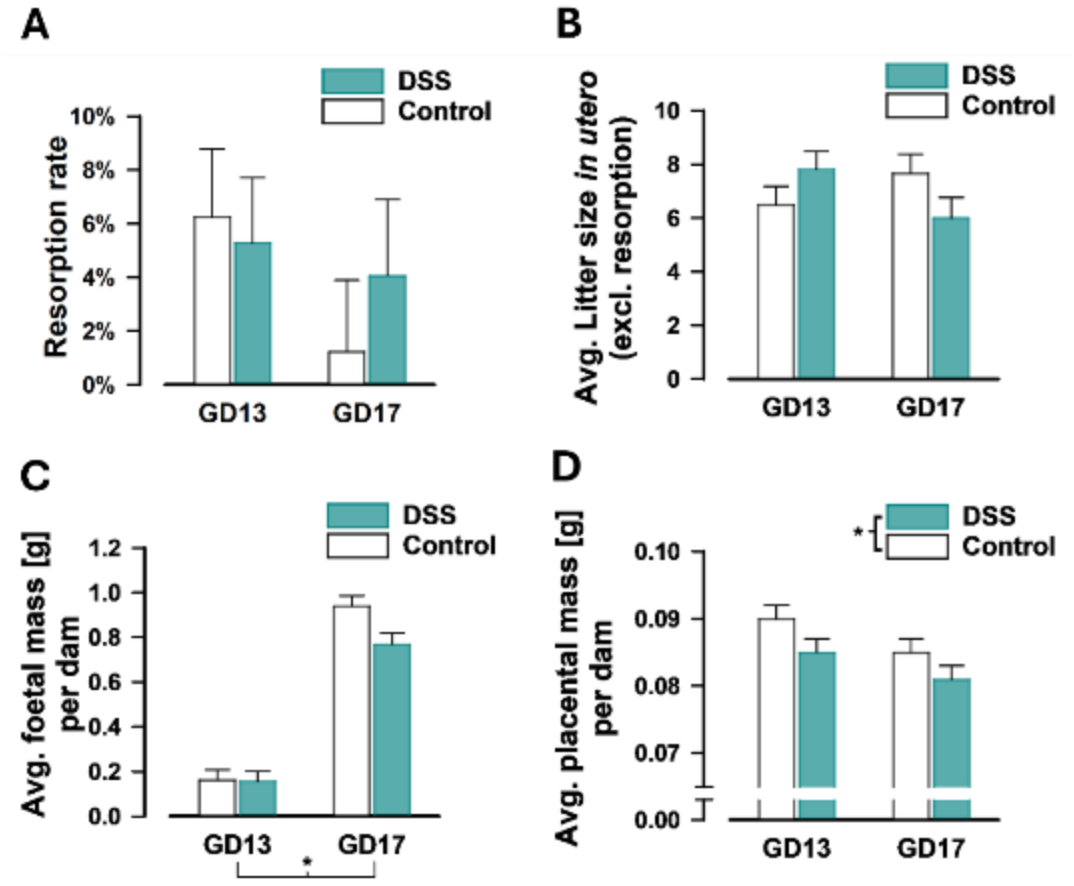

Figure 3.5. Gestational DSS impacts foetal and placental outcomes in pregnant dams at GD13 and GD17.

(A) Proportions of resorbed foetuses, **(B)** litter size, **(C)** average foetal mass, and **(D)** average placental mass per pregnant dam are presented for DSS-treated and control groups at two harvest time points. Resorbed foetuses were excluded from these measurements. For GD13, data were collected from 11 DSS-treated dams and 10 control dams. For GD17, data were from 8 DSS-treated dams and 9 control dams. Data are presented as mean ± SE. "*" indicates statistically significant main effect of either Group or Harvest Day ($p < 0.05$).

The neuroinflammatory response in the foetal brain of DSS-treated dams was evidenced by upregulated RNA expression of selected immune cytokines (depicted in **Fig. 3.6,** presented as fold change relative to control expression level). Independent *t*-tests of $_{\Delta\Delta}$Ct values confirmed that the expression of IL-1β was significantly elevated by gestational DSS on GD13 [$t_8 = 2.38$, $p < 0.05$, $d = 1.51$], but not on GD17 [$p = 0.11$, Cohen's d = 1.14]. TNF-α and IL-6 did not achieve statistical significance on GD13 and GD17. IL-10 expression was nondetectable (Ct > 35) in both groups on GD13 and GD17.

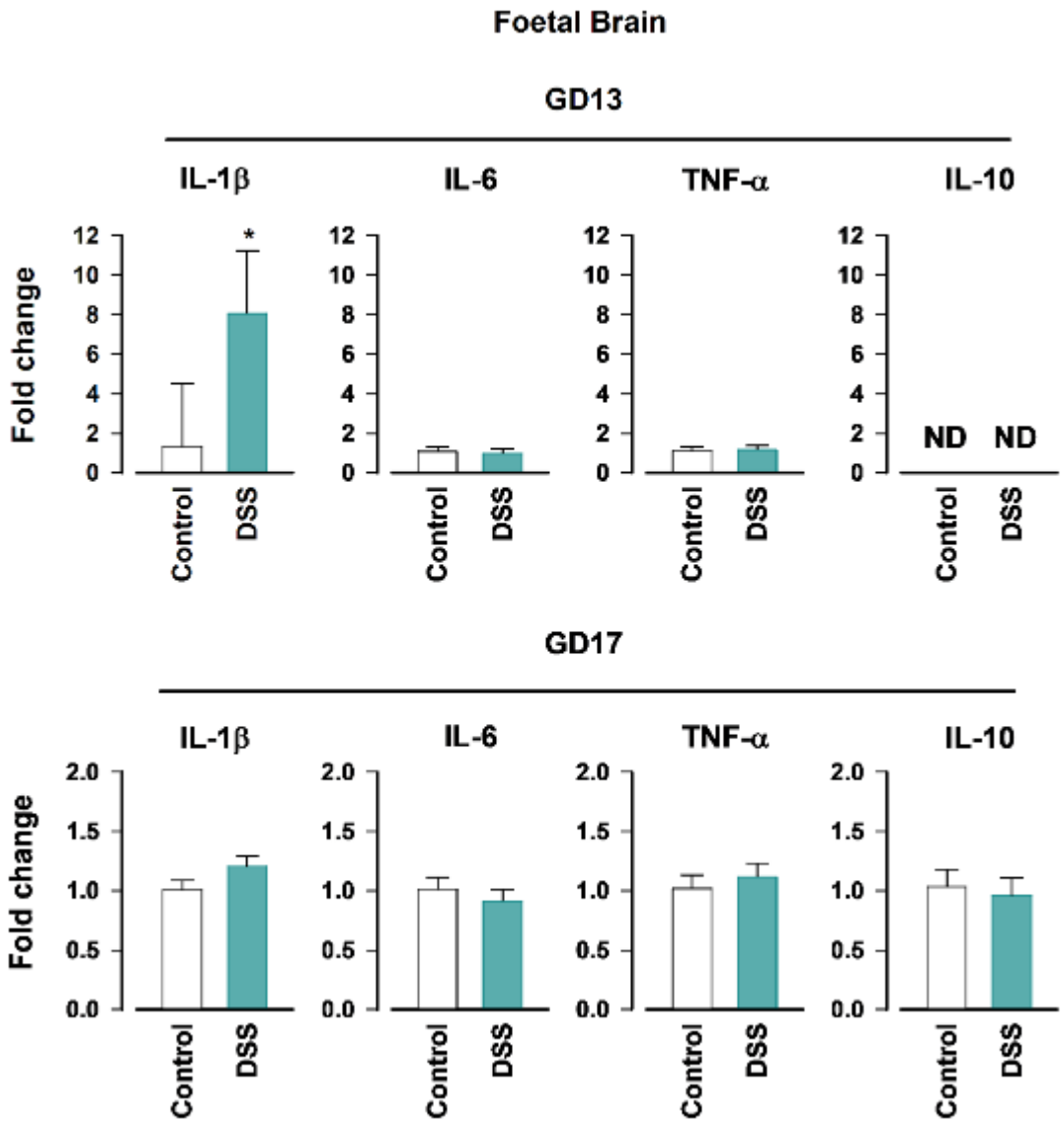

Figure 3.6. DSS modulates IL-1β expression in the foetal brain of pregnant dams at GD13.
Total RNA was extracted from the foetal brain of foetuses from DSS-treated and control pregnant dams, harvested on GD13 and GD17. IL-1β mRNA expression was quantified by real-time PCR, with data presented as relative fold changes normalised to GAPDH ($n = 5$ dams per group; mean ± SEM; $p < 0.05$ for significant changes). DSS treatment significantly upregulated IL-1β expression in the foetal brain on GD13, with no significant change observed on GD17, compared to controls. (ND) indicated below the detection limit.

In contrast, no significant immune response was detected in the placenta based on selected inflammatory cytokine markers (**Fig. 3.7,** expressed as fold change relative to controls). Independent *t*-tests of $_{\Delta\Delta}$Ct values confirmed that IL-1β and TNF-α did not achieve statistical significance on GD13 and GD17. IL-6 expression showed a non-significant trend toward upregulation on GD17 ($p = 0.07$, Cohen's d = 1.34), but not on GD13 ($p = 0.75$, Cohen's d = 0.21). IL-10 expression was nondetectable (Ct > 35) in both groups on GD13 and GD17.

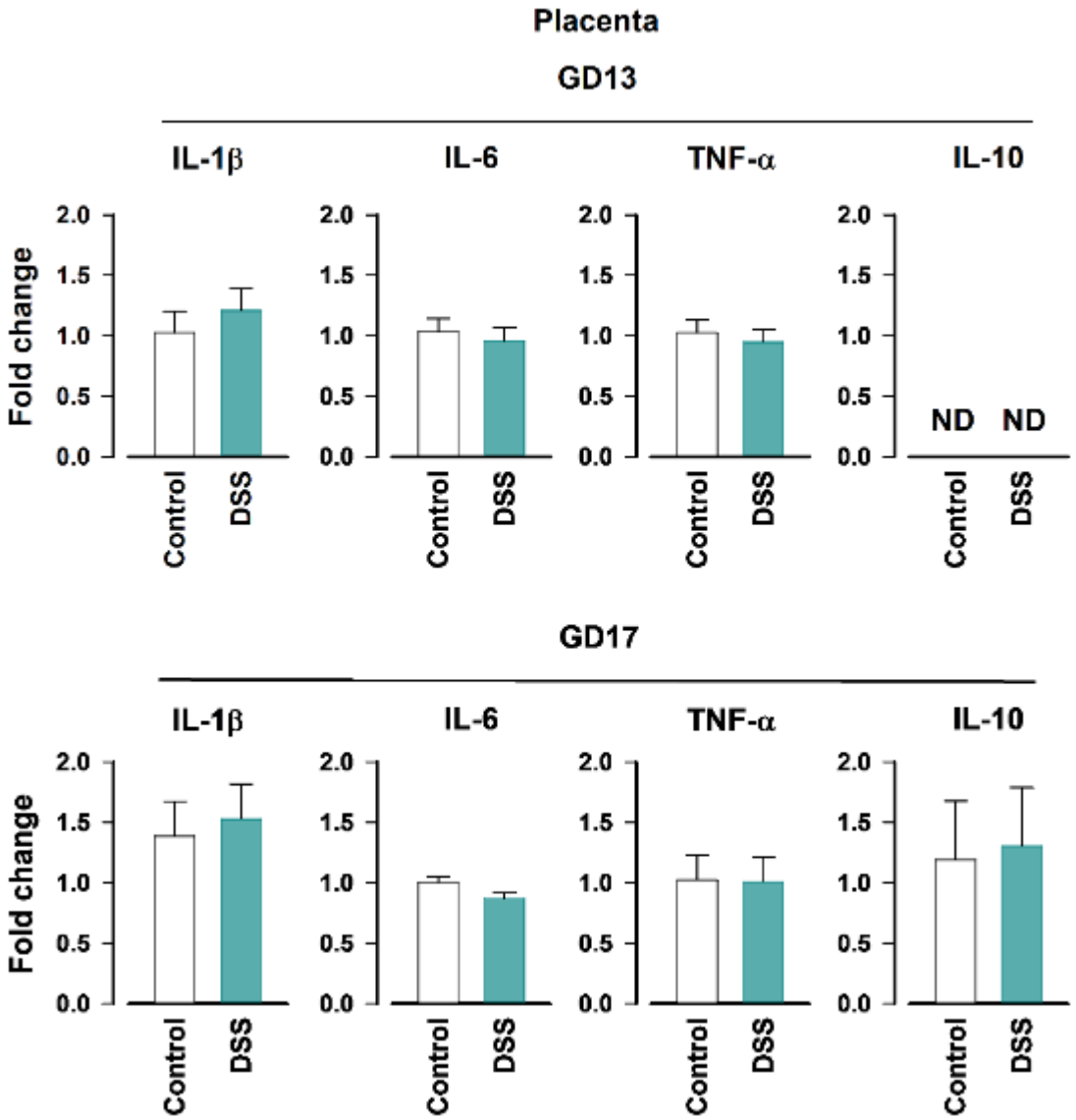

Figure 3.7. DSS does not alter cytokine expression in the placenta from pregnant dams at GD13 and GD17.
Total RNA was extracted from the placenta of DSS-treated and control pregnant dams, harvested on GD13 and GD17. Cytokine mRNA expression was quantified by real-time PCR, with data presented as relative fold changes normalised to GAPDH (n = 5 dams per group; mean ± SEM; $p > 0.05$). No significant changes in cytokine expression (e.g., IL-1β, TNF-α, IL-10) were observed between DSS-treated and control groups at either time point. IL-10 was below the detection limit (ND) in both groups.

3.3. Effects of gestational DSS treatment in the foetal brain.

Building on the observed activation of the maternal immune response and upregulation of IL-1β, this study revealed significant alterations in protein expression within the foetal brain following gestational DSS treatment. Protein expression levels of tight junction proteins, synaptic protein markers, and inflammasome protein markers were quantified in the foetal brain at two harvest time points, with relative protein concentrations normalised to the total protein loaded (see **Fig. 3.8.A**). Notably, gestational DSS treatment markedly upregulated the synaptic protein synaptophysin and the inflammasome protein apoptosis-associated speck-like protein containing a CARD (ASC) in the foetal brain, expressed as fold changes relative to control levels (see **Fig. 3.8. B & C**). Synaptophysin levels were significantly elevated by 9-fold, and ASC levels by 1.9-fold, in foetuses exposed to prenatal DSS treatment, highlighting a robust impact on synaptic and inflammasome pathways. A 2 × 2 (Group × Harvest Time Point) ANOVA on adjusted total protein levels of synaptophysin confirmed a significant main effect of Group, [$F_{(1,12)} = 11.70$, $p = 0.005$, $\eta_p^2 = 0.49$]. Similarly, a 2 × 2 ANOVA for ASC protein levels revealed a significant main effect of Group, [$F_{(1, 12)} = 5.98$, $p < 0.05$, $\eta_p^2 = 0.33$]. No significant interaction effects were observed for either protein. Additionally, while not statistically significant, protein levels of synaptotagmin-1, NOD-like receptor protein 3 (NLRP3), and cleaved IL-1β in foetuses with prenatal DSS exposure exhibited notable increasing trends of 3.9-fold, 2.7-fold, and 3.2-fold, respectively (see **Fig. 3.8.C**). In contrast, the tight junction protein zonula occludens-1 (ZO-1) and phosphorylated nuclear factor kappa B (pNFkB) showed non-significant decreasing trends of 0.53-fold and 0.52-fold, respectively (see **Fig. 3.8.C**). On the other hand, the synaptic protein markers, including shank 3, complexin 1/2 and synapsin 1 showed no significant difference between groups.

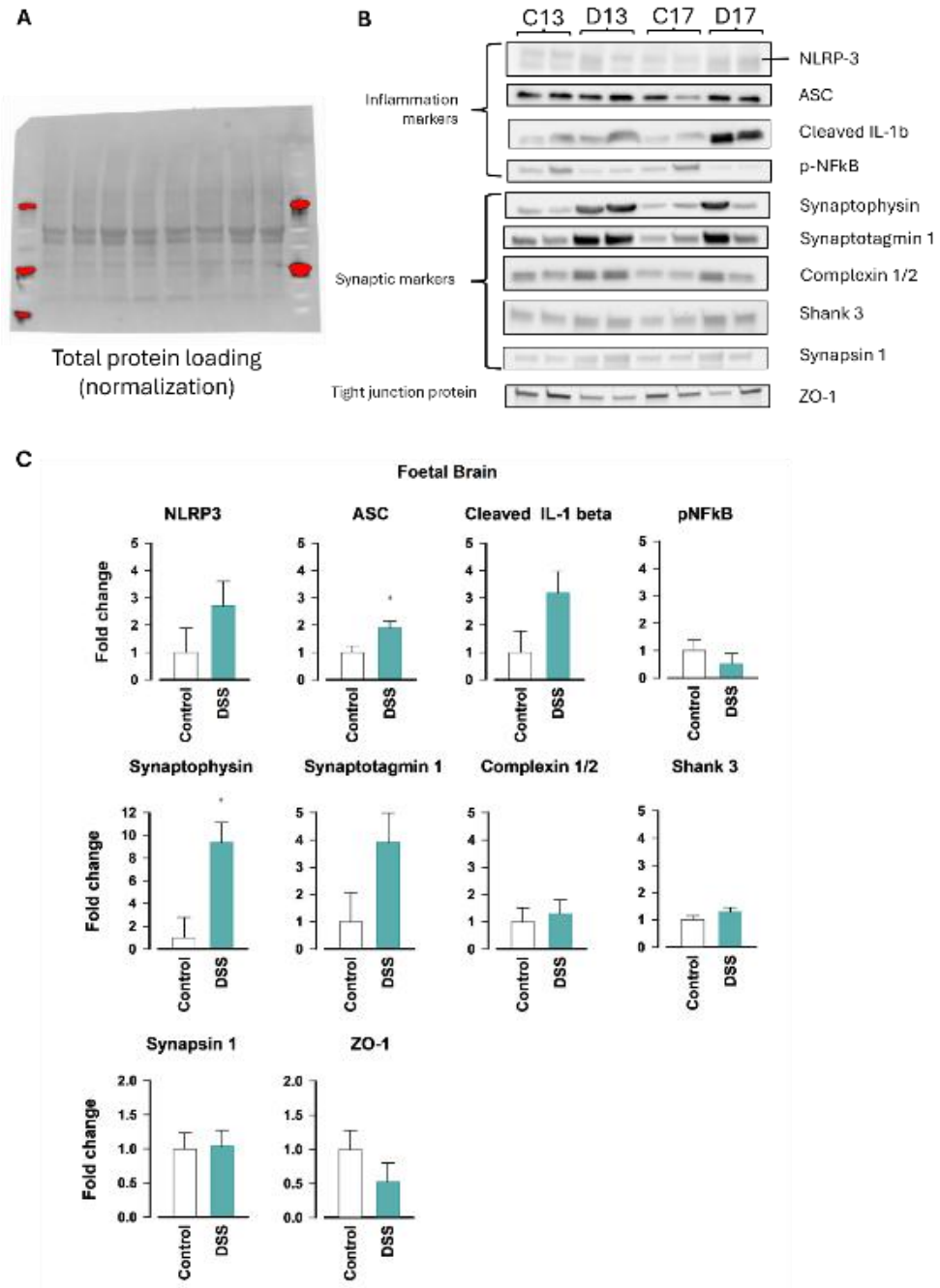

Figure 3.8. Elevated protein levels of ASC and synaptophysin in the foetal brain following gestational DSS treatment.

(A) Total protein loading on the membrane, assessed using a stain-free gel, was used for protein normalisation. **(B)** Immunoblot analysis of protein levels across three categories, including inflammasome, synaptic, and tight junction protein markers, was conducted to evaluate the impact of gestational DSS exposure on the foetal brain. Samples were obtained from gestational DSS-treated and control groups at two distinct harvest time points (GD13 and GD17). **(C)** Quantification of fold changes in the expression levels of ten protein markers. Graphs represent fold change data from n = 4 foetal brains, each derived from individual dams per group. Data are presented as mean ± SEM. Statistical significance between gestational DSS-treated and control groups is indicated by (*).

3.4. Effects of gestational DSS treatment on the offspring's body weights.

The long-term effects of gestational DSS on body weight were evaluated in the behavioural naïve offspring of Cohort C, (see **Fig 2.1**) because they were free from interference by multiple behavioural assays. They were only subjected to weekly weighing before their brains were harvested on either PND 40 or PND 110~113.

Analysis of body weight in the juvenile period (Weeks 3 to 5) included all mice in Cohort C (**Fig. 3.9.A**). The 2 × 2 × 3 (Group × Sex × Weeks) ANOVA of body weight confirmed the expected sex difference [$F_{(1,72)} = 41.34$, $p < 0.001$, $\eta_p^2 = 0.37$]. The sex difference became highly visible after the third week of age, which led to the significant Sex × Weeks interaction [$F_{(2,144)} = 40.74$, $p < 0.001$, $\eta_p^2 = 0.36$]. There was no statistical evidence for any group difference in this period.

The increment of body weight beyond Week 5 (i.e., weeks 6 to 15) was examined in the subset of mice in Cohort C sacrificed after Week 15. The sex difference persisted over this entire period (weeks 6 to 15), with the male mice exhibiting a higher growth rate regardless of gestational treatment (**Fig. 3.9.A**). These impressions were supported by the highly significant main effect of Sex [$F_{(134)} = 341.18$, $p < 0.001$, $\eta_p^2 = 0.91$] and the Sex × Weeks interaction [$F_{(9,306)} = 7.30$, $p < 0.001$, $\eta_p^2 = 0.17$] in the 2 × 2 × 10 (Group × Sex × Weeks) ANOVA of body weight. In addition, the ANOVA revealed a significant Group × Weeks interaction but its effect size was limited [$F_{(9,306)} = 2.67$, $p < 0.01$, $\eta_p^2 = 0.07$]. It stemmed from the marginally slower growth rate in the DSS offspring compared with control offspring (**Fig. 3.9.B**). Notably, the main effect of Group was far from statistical significance [$F < 1$]

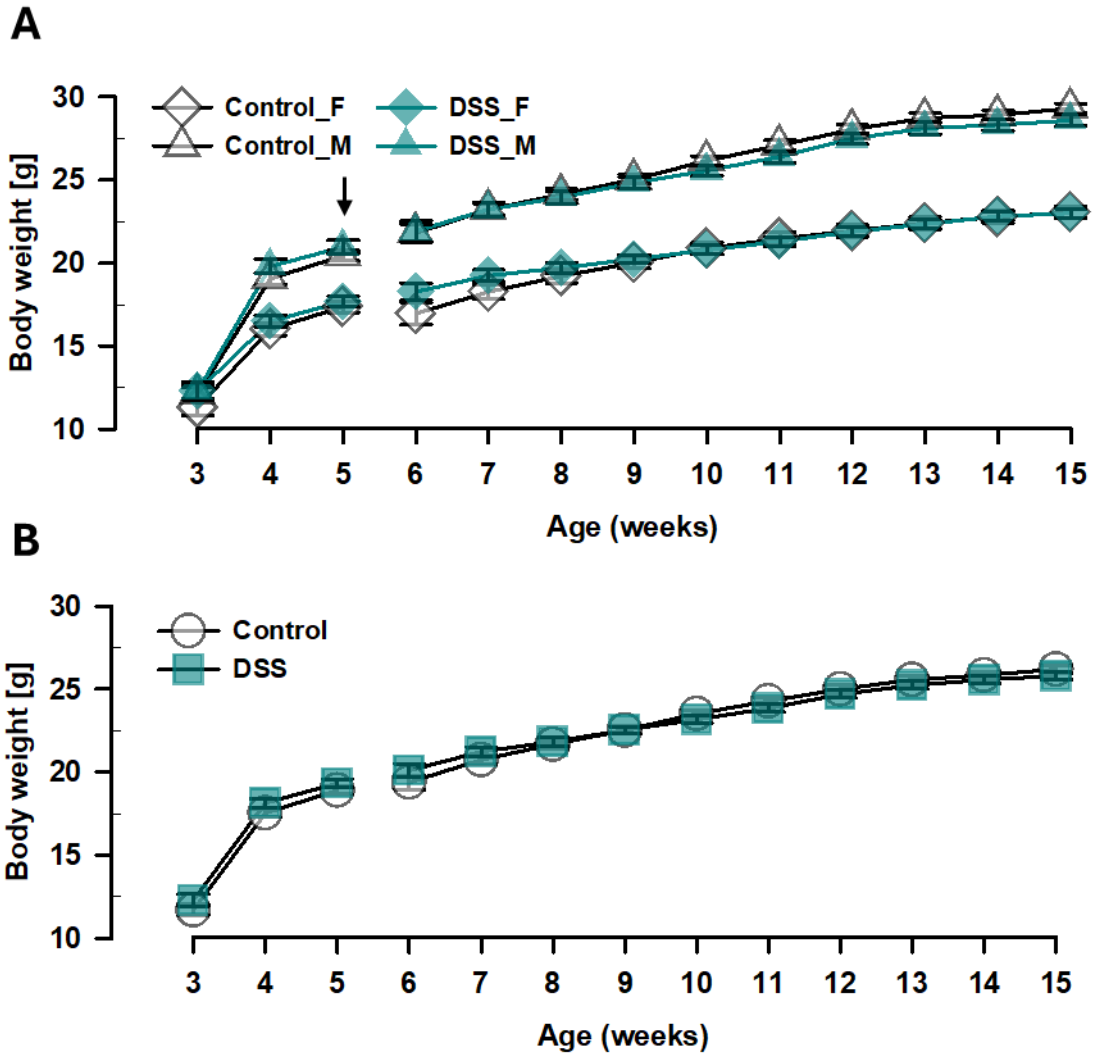

Figure 3.9. The effect of gestational DSS on the offspring's body weights
(A) Body weight (in g) is expressed as a function of Age (in weeks) for both male and female offspring from DSS-treated and control groups. The arrow indicates the planned harvest time point at PND 40 for juvenile mice. During the juvenile period (weeks 3–5), all mice in Cohort C were tracked, including 21 females and 14 males from DSS-treated pregnant dams and 18 females and 23 males from control dams. Following the planned sacrifice of the juvenile subset, the remaining mice were tracked during the adulthood period (weeks 6–15), comprising 12 females and 8 males from DSS-treated dams and 7 females and 11 males from control dams. The data were also collapsed across sex and presented in **(B)** to show the subtle reduction in the growth rate of DSS offspring relative to control offspring. Data are presented as mean ± standard error (SE) based on the relevant ANOVAs performed in SPSS.

3.5. Behavioural effects of gestational DSS treatment: juvenile vs adult age

The first four behavioural tests were conducted under identical conditions and sequence in two cohorts of mice (Cohorts A and B) that only differed in the age at the time of testing (see **Section 2.1** and **Fig. 2.1**). This permitted us to evaluate age-dependent DSS-induced phenotypes in these selected tests. Briefly, we obtained evidence for an age-dependent deficit in DSS offspring in the expression of prepulse inhibition (PPI) and a deficit in the Y-maze test of spatial familiarity judgement that was largely independent of the age of testing.

3.5.1. Anxiety-like behaviour in EPM was not affected by gestational DSS treatment

Gestational DSS did not modify the expression of anxiety-like behaviour in EPM when evaluated in the juvenile and adult age, and regardless of sex (**Fig. 3 .10. A**). A 2 × 2 × 2 (Group × Sex × Age) ANOVA of the percentage time in open arms relative to all arms did not reveal any significant main effect or interactions of group. Separate analysis of total distance moved in the maze surface (**Fig. 3 .10. B**) or percentage entries into open arms relative to all arms yielded similar interpretative statistics (data not shown). Yet, the ANOVAs identified a Sex × Age interaction in both the percentage of time spent in the open arms [$F_{(1,90)} = 5.23$, $p < 0.05$, $\eta_p^2 = 0.06$] and the distance moved in the maze [$F_{(1,90)} = 8.27$, $p < 0.01$, $\eta_p^2 = 0.08$]. It appeared that upon reaching maturity, female mice exhibited an increase in locomotor activity and exploration of the open arms, while an opposite pattern was observed in the males (data not shown).

3.5.2. Gestational DSS treatment led to reduced preference for spatial novelty in the Y-maze

The sample phase was uneventful. All mice explored the assigned familiar arm, with no significant difference in the average exploration time to the familiar arm between groups [DSS = 129.9 ± 5.6 s; control = 128.8 ± 4.8 s]. During the 3-min test phase, the gestational DSS treatment led to a reduction in the preference for the novel arm compared with control offspring (**Fig. 3 .10. C**). There was a visual tendency that

the impaired novelty preference was more pronounced in the juvenile mice. A 2 × 2 × 2 (Group × Sex × Age) ANOVA of the novelty preference index revealed a significant main effect of Group [$F_{(1,90)} = 4.61, p < 0.05, \eta_p^2 = 0.05$] but the Group × Age interaction did not achieve significance [$F_{(1,90)} = 1.44, p = 0.23, \eta_p^2 = 0.02$]. There was no evidence that the effect of gestational DSS treatment depended on sex (data not shown). Separate analysis of total distance moved in the maze surface during the test phase (**Fig. 3 .10. D**) did not reveal any significant main effect or interactions of group. Yet, the 2 × 2 × 2 (Group × Sex × Age) ANOVA only identified a Sex × Age interaction in total distance moved in the maze [$F_{(1,90)} = 12.354, p < 0.001, \eta_p^2 = 0.121$]. Neither the main effects of Group, interactions of Age × Group, nor Age × Group × Sex approached statistical significance [all F's < 1].

3.5.3. Preference for social stimulus and social novelty was unaffected by Gestational DSS treatment

Gestational DSS treatment did not modify social behaviour in the offspring evaluated either as juveniles or adults, and regardless of sex, in the three-chamber sociability test. The acclimatisation phase was uneventful: all mice readily explored all three chambers of the apparatus. In the social interaction test, a preference for the mouse (relative to the toy clone) was evident in both DSS and control mice tested as juveniles or adults (**Fig. 3 .10. E**). In the following phase, when a choice between a novel and a familiar mouse was presented, a novelty preference was also comparably observed in DSS and control offspring, regardless of their age at the time of testing or their sex (**Fig. 3 .10. F**). Separate 2 × 2 × 2 (Group × Age × Sex) ANOVAs of the preferencing index in both test phases (social preference test and social novelty test) yield no evidence of any group difference.

3.5.4. Gestational DSS treatment impaired prepulse inhibition (PPI) in adult but not juvenile offspring

Gestational DSS treatment did not significantly modify the startle reaction in pulse-alone trials (pulse intensity: 100, 110, 120 dB) in juvenile or adult offspring, regardless of sex (in Supplementary Material). A 2 × 2 × 2 × 3 (Group × Sex × Age × Pulse intensity) analysis of covariance (ANCOVA) of reactivity scores obtained on these pulse-only trials (with body weights on the day of PPI testing as covariate to

control for confounding influence mediated by the known effects of sex and age) did not reveal any group differences [all F's < 1]. Only a significant Sex × Age interaction [$F_{(2,89)} = 7.11$, $p < 0.01$, $\eta_p^2 = 0.07$] of limited effect size was identified, suggesting that the stronger reaction in the male over the female mice was primarily observed in the adult but not the juvenile age.

Against the lack of an effect of DSS treatment on startle response, a clear impairment of PPI expression in the DSS offspring compared with control offspring emerged in the adult age (**Fig. 3 .10. G**). This age-specific impairment in adult offspring in the DSS group was apparent across all prepulse intensities. By contrast, the expression of PPI in juvenile DSS offspring was highly comparable with juvenile control offspring. These impressions were supported by the presence of a significant Group × Age interaction [$F_{(1,89)} = 4.57$, $p < 0.05$, $\eta_p^2 = 0.05$] and Group × Age × Pulse intensity interaction [$F_{(2,178)} = 4.93$, $p < 0.01$, $\eta_p^2 = 0.05$] in the 2 × 2 × 2 × 3 × 3 (Group × Sex × Age × Pulse intensity × Prepulse intensity) ANCOVA of %PPI, with body weights as the covariate. Post hoc comparisons confirmed that gestational DSS treatment attenuated PPI expression in the adult offspring [$p < 0.05$] but not the juvenile offspring [$p = 0.68$] (**Fig. 3 .10. H**). The age-dependent DSS treatment effect on PPI expression was apparent between sexes without any statistical support for a sex dependency, Group × Age × Sex: [$F < 1$].

The ANCOVA also revealed that adult mice overall exhibited stronger PPI than juvenile mice by the presence of a highly significant Age effect [$F_{(1,89)} = 23.54$, $p < 0.001$, $\eta_p^2 = 0.21$]. This effect was more prominent with more intense prepulse, Age × Prepulse intensity: [$F_{(2,178)} = 7.28$, $p < 0.001$, $\eta_p^2 = 0.08$] (data not shown). The stronger expression of PPI in male than female mice was also more apparent in trials with prepulse of higher intensity Sex × Pulse intensity: [$F_{(2,178)} = 3.46$, $p < 0.05$, $\eta_p^2 = 0.04$] (data not shown).

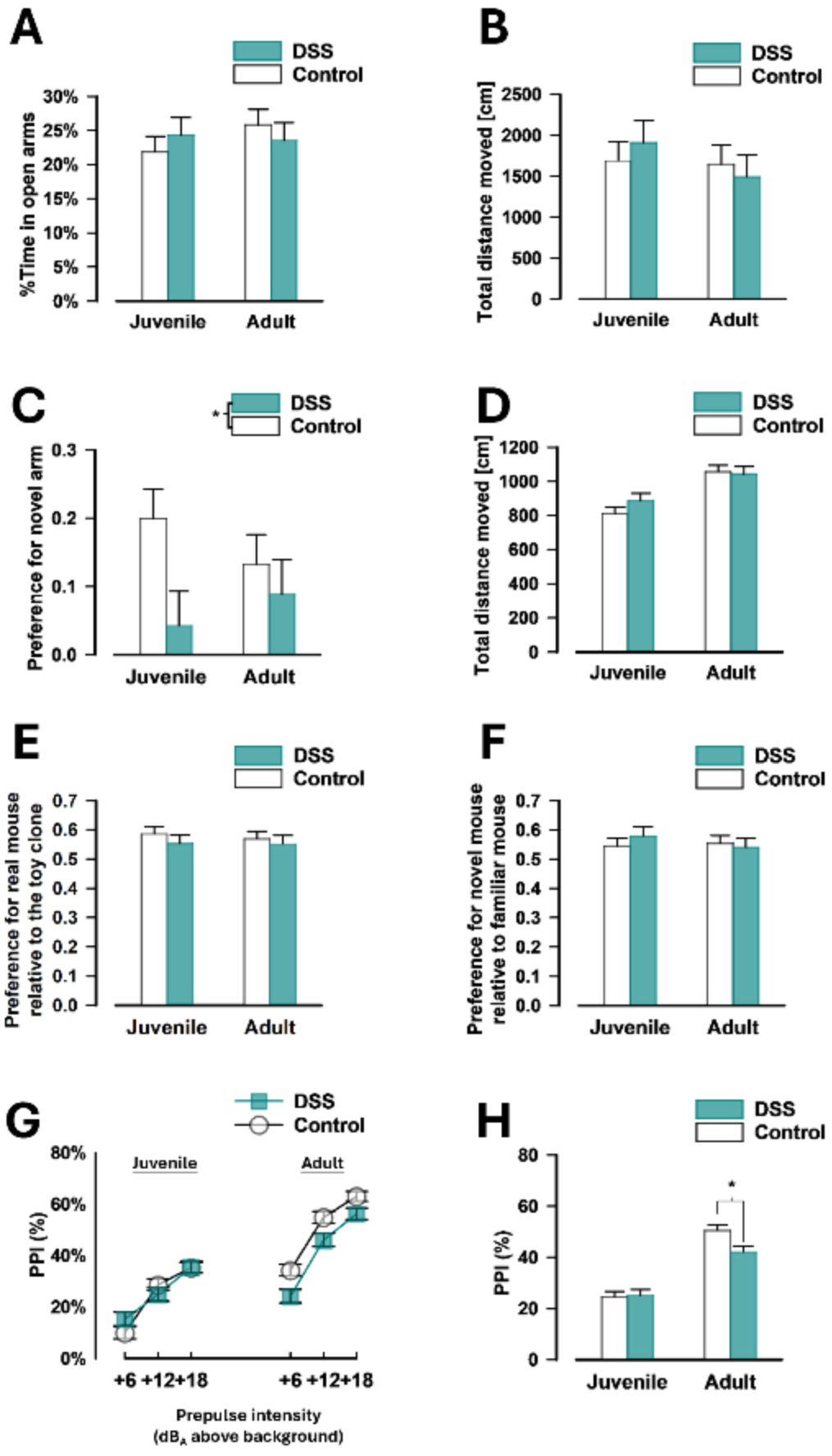
A
DSS
Control
%Time in open arms
30%
25%
20%
15%
10%
5%
0%
Juvenile
Adult
B
DSS
Control
Total distance moved [cm]
2500
2000
1500
1000
500
0
Juvenile
Adult
C
DSS
Control
*
Preference for novel arm
0.3
0.2
0.1
0.0
Juvenile
Adult
D
DSS
Control
Total distance moved [cm]
1200
1000
800
600
400
200
0
Juvenile
Adult
E
DSS
Control
Preference for real mouse relative to the toy clone
0.7
0.6
0.5
0.4
0.3
0.2
0.1
0.0
Juvenile
Adult
F
DSS
Control
Preference for novel mouse relative to familiar mouse
0.7
0.6
0.5
0.4
0.3
0.2
0.1
0.0
Juvenile
Adult
G
DSS
Control
Juvenile
Adult
PPI (%)
80%
60%
40%
20%
0%
+6 +12+18
+6 +12+18
Prepulse intensity
(dBA above background)
H
DSS
Control
*
PPI (%)
80
60
40
20
0
Juvenile
Adult

Figure 3.10. The results of the four behavioural tests were conducted in both juvenile and adult offspring.
(A) Anxiety-like behaviour was evaluated using the EPM. Performance was indexed by the percentage of total time spent in the open arms. (B) Total distance travelled in the EPM for 5 min. (C) Spatial familiarity judgment in the Y-maze test was measured by a preference ratio, where >0 indicate a novelty preference and = 0 indicates no preference. "*" indicates the significant group main effect ($p < 0.05$). (D) Total distance travelled in the Y-maze for 5 min in the test phase. Social preference was assessed in two phases, social interaction phase **(E)** and social novelty phase **(F).** They were all indexed by the preference ratio (> 0 indicates for the live mouse chamber in social interaction phase or novel mice chamber in social novelty phase; < 0 indicates preference for dummy toy chamber in the social interaction phase or familiar mouse chamber in social novelty phase; 0 = no preference) (**G**) Prepulse inhibition was indexed by %PPI, expressed as a function of increasing prepulse intensity. The data were also collapsed across prepulse intensities and shown in **(H)** with "*" indicates the significant group difference identified in adult age ($p < 0.05$). Data are presented as mean ± SE. Control/Juvenile, n = 28; Control Adult, n = 28; DSS/Juvenile, n = 21; DSS/Adult, n = 21.

3.6. Behavioural tests only evaluated in adult offspring

Five behavioural tests that were performed only in adult offspring (see **Fig. 2.1**). Amongst the five tests, the water maze spatial working memory test was conducted in Cohort A, whereas the two tests of depression-related behaviour (SPT and FST) were conducted in Cohort B. These were performed after they underwent the same common set of tests for comparison between juvenile and adult offspring as described in **Section 2.1** above. After completing the water maze spatial working memory test (Cohort A), or SPT and FST (Cohort B), both cohorts participated in the test of latent inhibition (LI) – a form of learned inattention, followed by the assessment of the locomotor response to an acute challenge to the psychostimulant drug, MK-801. Since Cohort A and Cohort B differed in terms of behavioural test history as well as housing conditions (Cohort B was maintained in individual housing since SPT), an additional factor of cohort was included in the analysis of data obtained in the LI and MK-801 tests, followed by separate analyses restricted to either cohort.

3.6.1. Working memory test in Morris water maze (Cohort A)

Pretraining with a visible escape platform was uneventful. All mice swam and effectively climbed onto the platform to escape from the water. Next, spatial working memory was assessed with the escape platform, adopting a new daily position over 11 days. A comparable reduction in escape latency was observed in both adult offspring in the DSS and control group (**Fig 3.11. A and B**). The 2 × 2 × 2 ×11 (Group × Sex × Trials × Days) ANOVA of escape latency revealed a significant main effect of Trials [$F_{(1,45)} = 6.66$, $p < 0.05$, $\eta_p^2 = 0.13$] with the Group × Trials being far from significance [$F<1$]. This suggested a gradual learning progression across testing sessions, as mice demonstrated a steady decline in escape latency over the 11-day period. An overall reduction of escape latency across days was also suggested by the presence of a significant effect of Days [$F_{(10,450)} = 2.23$, $p < 0.05$, $\eta_p^2 = 0.05$]. No other effects and interactions achieved statistical significance.

3.6.2. Tests of depression-related behaviour (Cohort B)

In the sucrose preference test (SPT), all mice exhibited a preference for the sucrose solution. This preference gradually weakened as sucrose concentration was reduced from 1%, 0.5%, 0.25% to 0.0625% (**Fig 3.11. C**). Throughout the course of the SPT,

the sucrose preference was comparable between DSS and control mice. A 2 × 2 × 4 (Treatment × Sex × Concentrations) ANOVA of the percentage sucrose preference only revealed the expected main effect of Concentrations [$F_{(3,135)} = 44.84$, $p < 0.001$, $\eta_p^2 = 0.50$] without any evidence for a group effect or its interaction [all F's < 1].

Performance in the forced swim test (FST) was also highly comparable between DSS and control mice (**Fig 3.11. D**). The emergence of floating behaviour as indexed by immobility time in the two groups closely approximated each other throughout the 10-min observation period. This conclusion was supported by a 2 × 2 × 10 (Group × Sex × Bins) ANOVA of immobility time over successive 1-min bins. Neither the main effect of Group nor its interactions approached statistical significance [all F's < 1].

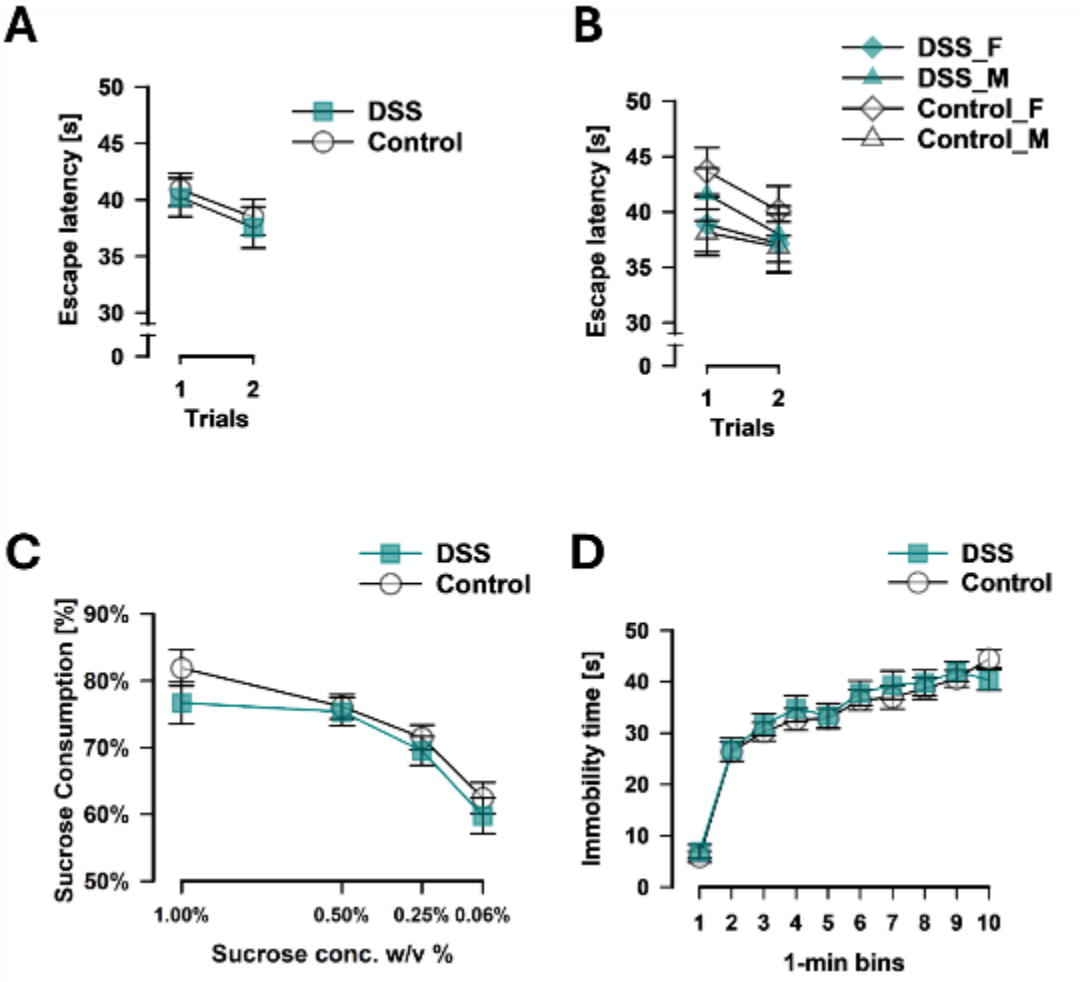

Figure 3.11. Behavioural performance on spatial memory, sucrose preference, and forced swim tests.
(**A**) Mean escape latency (in seconds) to locate the hidden platform across 11 days during the water maze task. The data were also split by sex and presented in (**B**). (**C**) Sucrose preference across four sequential dilutions (1%, 0.5%, 0.25%, and 0.0625%) was depicted. (**D**) Immobility time (in seconds) recorded in the forced swim test is plotted against the successive 1-minute time bins. Data presented are mean ± SE. Control, n = 28; DSS, n = 21.

3.6.3. Gestational DSS treatment potentiated the latent inhibition of the conditioned freezing (Cohorts A & B)

Weaker expression of the conditioned freezing response by mice in the pre-exposed (PE) condition relative to mice in the (non-pre-exposed) nPE condition constitutes the latent inhibition (LI) effect. LI was clearly evident in the tone-CS test on day 3, and its magnitude was potentiated in the DSS adult offspring (**Fig 3.12. A**). The modulation of LI expression by gestational DSS treatment to the maternal host was supported by the emergence of a Group × Pre-exposure interaction [$F_{(1,82)} = 4.16$, $p < 0.05$, $\eta_p^2 = 0.05$] in the 2 × 2 × 2 × 2 (Group × Pre-exposure × Sex × Cohort) ANOVA of the increment in freezing time over the first two minutes in the presence of the CS relative from the preceding 2-min pre-CS baseline period. The ANOVA also yielded a highly significant effect of Pre-exposure [$F_{(1,82)} = 86.98$, $p < 0.001$, $\eta_p^2 = 0.52$]. Neither the expression of LI nor its modulation by gestational DSS treatment was significantly influenced by sex.

However, there was a visual impression that the potentiation of LI expression by gestational DSS was more prominent in Cohort A when the magnitude of LI seen in control mice was relatively weak (see **Fig 3.12. A**). By contrast, the expression of LI appeared more comparable between DSS and control groups in Cohort B when LI was more strongly expressed in control mice. Although this impression did not yield a significant Group × Pre-exposure × Cohort interaction [$F < 1$], planned ANOVAs restricted to either cohort showed that the critical Group × Pre-exposure interaction remained significant in Cohort A [$F_{(1,41)} = 5.53$, $p < 0.05$, $\eta_p^2 = 0.12$] but was far from significance in Cohort B [$F < 1$]. In Cohort A, the visibly lower expression of conditioned freezing in DSS-PE mice than that in Control-PE mice approached statistical significance [LSD: $p = 0.08$] in keeping with the outcome of the overall AVOVA.

The above interpretation concerning the disparate findings between Cohorts A and B was further consolidated by examination of the development of CS-freezing over the three CS-US conditioning trials on day 1. Freezing recorded during the 30-s CS presentation in the second and third conditioning trials may be used to index the conditioned response developed after the first CS-US pairing. A 2 × 2 × 2 × 2 (Group × Pre-exposure × Sex × Cohort) ANOVA of the CS-freezing time obtained in the second

and third conditioning trials revealed a significant Group × Pre-exposure × Cohort interaction [$F_{(1,82)} = 4.15$, $p < 0.05$, $\eta_p^2 = 0.05$] despite the clear absence of the Group × Pre-exposure interaction [$F<1$]. As illustrated in (**Fig 3.12. B**), the significant 3-way interaction stemmed from the potentiation of the CS pre-exposure effect by gestational DSS treatment that was uniquely demonstrated in Cohort A. In agreement, a significant Group × Pre-exposure interaction [$F_{(1,41)} = 6.46$, $p < 0.05$, $\eta_p^2 = 0.14$] was obtained in the planned ANOVA restricted to Cohort A but not that restricted to Cohort B [$F < 1$].

Finally, although the animals showed low levels of immobility over the 8-min context test, a CS pre-exposure effect was detected. On average, mice in the PE condition exhibited more freezing than those in the nPE condition [7.62 ± 0.85 vs 5.15 ± 0.85 in %time freezing], yielding a significant main effect of Pre-exposure [$F_{(1,82)} = 4.20$, $p < 0.05$, $\eta_p^2 = 0.05$] in the 2 × 2 × 2 × 2 (Group × Pre-exposure × Sex × Cohort) ANOVA. This is in keeping with theories emphasizing the competition between the CS and context for associability with the shock US (Rescorla & Wagner, 1972). Female mice in general also displayed significantly more immobility during the context test than male mice [7.69 ± 0.86 vs 5.08 ± 0.84 in %time freezing; $F_{(1,82)} = 4.69$, $p < 0.05$, $\eta_p^2 = 0.05$], but the factor Sex did not significantly interact with Group or Pre-exposure [F's < 1].

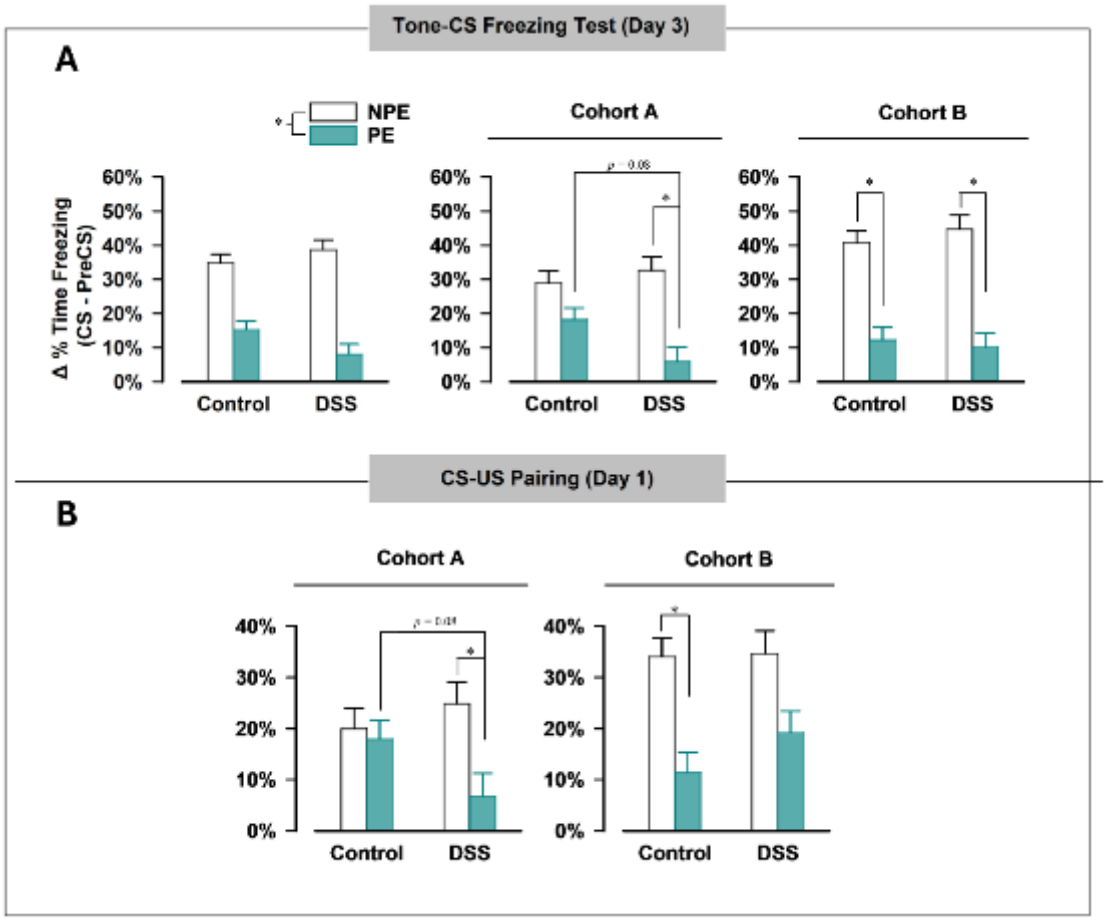

Figure 3.12. The modification of LI expression in mice born to pregnant dams exposed to DSS during gestation.
(A) The freezing response to the tone CS on Day 3 (first day of tone-CS test) was calculated as the percentage of time freezing during the first 2 minutes after CS onset minus the percentage of time freezing during the pre-CS baseline period. Latent inhibition is evidenced by a greater increase in the percentage of time freezing in the nPE group compared to the PE group. Data from Cohort A and Cohort B are shown in the panels on the right. **(B)** Developing CS-freezing response during CS (tone)-US (shock) pairing on Day 1 were expressed by the percentage of time freezing during the 30-s CS presentation in the 2nd and 3rd CS-US conditioning trials. The freezing level in PE group tended to be lower than in the nPE group, further constituting the latent inhibition effect. Data from Cohort A and B are presented separately in the panels on the right. In **Cohort A**, Control/nPE, n = 13; Control/PE, n = 15; DSS/nPE, n = 11; DSS/PE, n = 10. In **Cohort B**, Control/nPE, n = 15; Control/PE, n = 13; DSS/nPE, n = 10; DSS/PE, n = 11. All data are presented as mean ± SE; "*" denotes the presence of a significant main effect of Pre-exposure.

3.6.4. Gestational DSS treatment attenuated the stimulant response to acute NMDA receptor blockade by MK-801

As illustrated in **Fig 3.10**, rapid habituation was observed over the first 15 min of acclimatisation to the arenas as supported by the highly significant effect of time bins [$F_{(2,180)} = 97.29$, $p < 0.001$, $\eta_p^2 = 0.52$] in a 4-way (Group × Sex × Cohort × 5-min Bins) ANOVA. The Sex × Bins interaction also achieved statistical significance [$F_{(2,180)} = 8.55$, $p < 0.001$, $\eta_p^2 = 0.09$] due to the steeper habituation profile in the female mice (data not shown). Locomotor activity began to stabilise over the next 30 min following saline injection, and only the main effect of Bins achieved significance [$F_{(5,450)} = 4.28$, $p < 0.001$, $\eta_p^2 = 0.05$]. Next, the motor stimulant effect subsequent to the systemic challenge of MK-801 at 0.2 mg/kg (i.p.) was observed for two hours. Motor activation reached its peak at 30-35 min after the MK-801 injection. Afterwards, the motor stimulant effect of MK-801 subsided, and DSS and control offspring began to diverge, with DSS offspring consistently showing lower activity level than control offspring. The two groups eventually converged over the last 9-10 bins of the observation period. The attenuation of the motor stimulant effect of MK-801 in the DSS offspring was supported by the presence of a significant Group × Bins interaction [$F_{(23,2070)} = 1.89$, $p < 0.01$, $\eta_p^2 = 0.02$], and the near-significant main effect of Group [$F_{(1,90)} = 3.91$, $p = 0.05$, $\eta_p^2 = 0.04$] (**Fig. 3.13. A, Left panel**). The lower motor response to MK-801 in DSS offspring compared to control offspring during the 7th to 15th bins after MK-801 challenge was confirmed by post-hoc Fisher's LSD comparisons [p's < 0.01] (**Fig. 3.13. A, Right panel**). The attenuation of MK-801 motor stimulant response by gestational DSS treatment did not critically differ between Cohorts A and B (see separate depictions of the data in **Fig. 3.13. B**). Neither the main effect of Cohort nor its interaction terms approached statistical significance [F's < 1], and Cohort × Sex [$p = 0.75$].

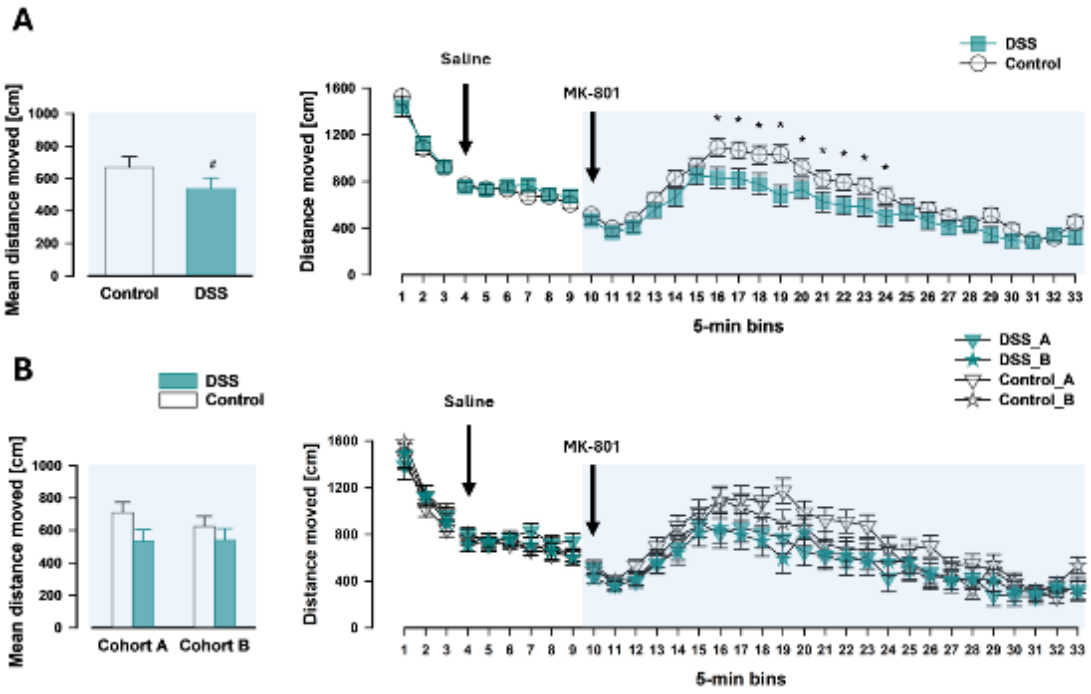

Figure 3.13. The motor stimulant response to acute NMDA receptor blockade by systemic MK-801

(A) Locomotor activity is expressed as a function of successive 5-min bins over the three consecutive phases (Habituation phase: Bin 1-3; Saline Phase: Bin 4-9; MK-801 phase: Bin 10-33). Time bins with a significant difference between DSS and Control offsprings at $p < 0.01$ based on Fisher's LSD are labelled with "*". The group comparison of averaged distance per bin across the 24 bins during the MK-801 phase was illustrated on the right. "#" indicates the just missed significant main effect of group of the motor stimulation by MK-801 ($p = 0.05$). The data from cohort A and cohort B were split and illustrated in **(B).** The observed attenuation of MK-801 response on locomotor activity by gestational DSS treatment was largely consistent between cohort A and cohort B. All values are presented as mean ± SE. In (**A**) Control, n = 56; DSS, n = 42. In (**B**), Control, n = 28; DSS, n = 21 for Cohort A and Cohort B, respectively.

3.7. Impacts of gestational DSS on the offspring's brain (Cohort C)

The behaviourally naïve cohort C offspring was prepared for the harvest of offspring brain tissues (**Fig. 2.1**). The hippocampus from the right hemisphere was processed for molecular analysis, including quantification of hippocampal BDNF protein level and RNA expression level of NMDA receptor subunits (*GRIN1*, *GRIN2A* and *GRIN2B*). The left hemisphere was fixed for histological evaluation, specifically to assess the density of DCX-immunoreactive cells in the dentate gyrus.

3.7.1. Elevated BDNF protein level in the hippocampus of offspring from dams with gestational DSS

Gestational DSS upregulated the levels of BDNF detected in the hippocampus (**Fig. 3.14**). A 2 × 2 × 2 (Group × Sex × Age) ANOVA of hippocampal BDNF expression levels yielded only a significant effect of Group [$F_{(1,32)} = 4.87$, $p < 0.05$, $\eta_p^2 = 0.13$]. Gestational DSS treatment upregulated hippocampal BDNF in adulthood only, but there was no statistical support for a significant Group × Age interaction [$p = 0.29$]. There was also no evidence that the effect of gestational DSS depended on sex (data not shown).

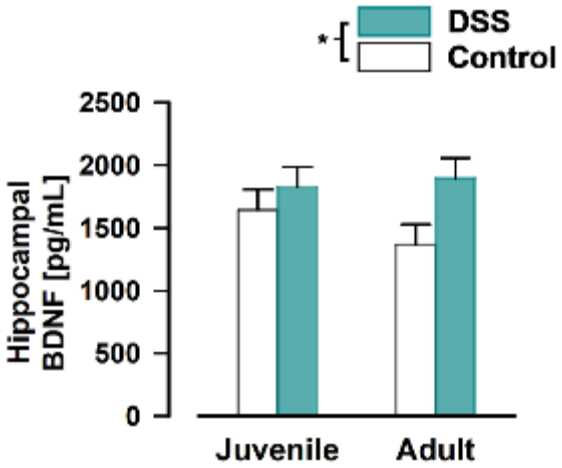

Figure 3.14. Elevated hippocampal brain-derived neurotrophic factor (BDNF) levels in offspring following gestational DSS.
BDNF in the hippocampus (pg/mL of protein) was evaluated in behavioural naïve offspring (harvested on PND40: juvenile and PND 110: Adult) from Cohort C. $N = 5$ per group per age per sex. "*" refers to the significant main effect of Group at $p < 0.05$, suggesting that gestational DSS treatment led to the upregulation of hippocampal BDNF expression. Data are expressed as mean ± SE.

3.7.2. Neural proliferation in the hippocampus by DCX immunohistochemistry

Gestational DSS treatment did not significantly alter the density of DCX-immunoreactive cells in the hippocampal dentate gyrus (**Fig. 3.15.A**). An independent t-test indicated no statistically significant difference (t_4 = -1.67, p = 0.88, Cohen's d = 0.136). Photomicrographs of DCx-ir cells in the dentate gyrus of sections obtained from the dorsal hippocampus of offspring born to gestational DSS-treated and control dams are shown in **Fig. 3.15.B & C**, respectively.

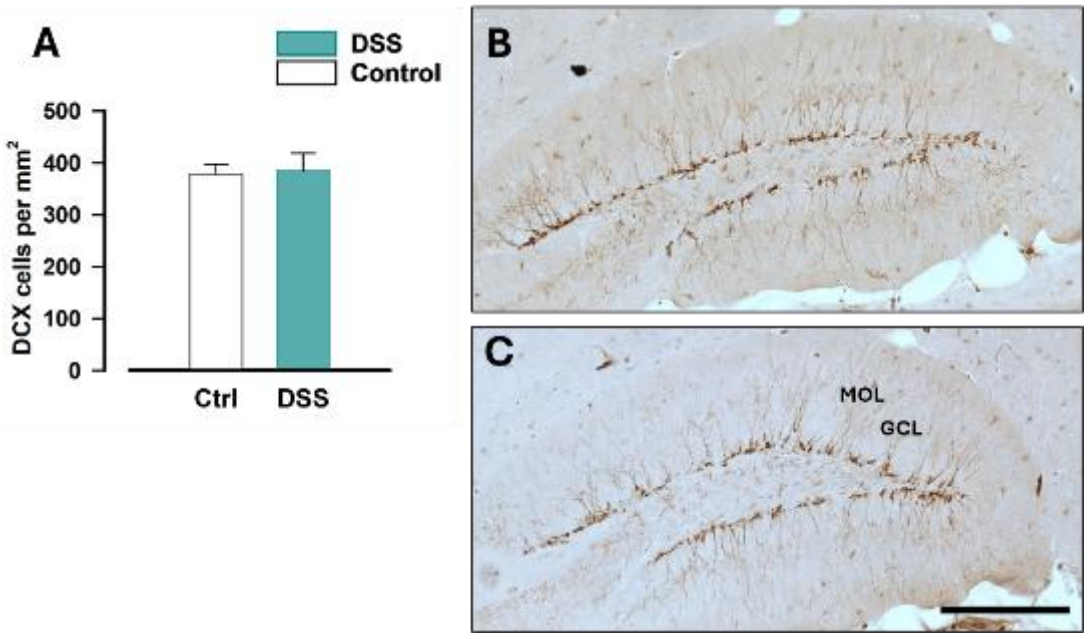

Figure 3.15. Mean density of DCX-immunoreactive cells in the dentate gyrus
(A) Mean density (cells/mm²) of DCX-immunoreactive (DCX-ir) cells in the dentate gyrus, averaged across dorsal sections. DCX-ir cells were quantified in behaviourally naïve adult offspring (at PND 110) from Cohort C (N = 3 per group). Data are presented as mean ± standard error (SE). Representative images from mice of the gestational DSS group **(B)** and control group **(C)** dams. DCX-ir cells were observed in the granule cell layer (GCL), with dendritic fibres extending towards the molecular layer (MOL) and away from the hilus. Scale bar = 250µm.

3.7.3. Total mRNA expression of NMDA receptor subunit in hippocampus

The mRNA expressions of three critical NMDA receptor subunit genes *(GRIN1*, *GRIN2A* and *GRIN2B*) in the hippocampus were at comparable levels between DSS and Control offspring. Fold change of mRNA expression in DSS group relative to control group was close to unity: *GRIN1* = 0.9 ± 0.6 fold change [$p = 0.39$, Cohen's $d = 0.57$], *GRIN2A* = 0.9 ± 0.9 fold change [$p = 0.39$, Cohen's $d = 0.58$], and *GRIN2B* = 0.9 ± 0.7 fold change [$p = 0.17$, Cohen's $d = 0.95$].

Chapter 4: Discussion and conclusion

4. Discussion and conclusion

Infectious MIA models, such as Poly I:C and LPS, have been widely used to investigate the impact of gestational acute systemic inflammation on neurodevelopment, with associations established between MIA and disorders such as ASD and schizophrenia (Kentner et al., 2019; Meyer, 2014). The MIA concept proposes that disruptions to the maternal immune status during pregnancy could negatively affect foetal brain development, potentially increasing the risk of neurodevelopmental disorders in the offspring (Meyer, 2019; Woods et al., 2021).

However, the relationship between maternal UC and offspring neurodevelopmental outcomes remains less well understood. Unlike infectious MIA models, which typically involve a systemic acute immune challenge (Bucknor et al., 2022), IBD is characterised by chronic inflammation (Binion & Rafiee, 2009). Epidemiological studies on maternal IBD and neurodevelopmental disorders have produced conflicting findings, some report no association with conditions such as ASD or schizophrenia (Andersen et al., 2014; Jolving et al., 2017; Prentice et al., 2024), whereas others suggest a heightened risk of neurodevelopmental disorders such as ASD and attention deficit hyperactivity disorder (ADHD) (Sadik et al., 2022).

By employing a gestational UC-like model, the present study provided an opportunity to clarify the association between maternal IBD and neuropsychiatric alteration. These findings may refine the conceptual framework of MIA, expanding its implications beyond acute immune challenges to encompass chronic and subchronic inflammatory conditions like UC, thereby offering a broader perspective on immune-mediated neurodevelopmental risk.

Building on the suggested link between maternal IBD and neurodevelopmental disorders, this study successfully established a DSS-induced UC model, a widely used and representative chemical-induced model, in pregnant C57BL/6J mice to investigate its impact on offspring neurodevelopment (Chassaing et al., 2014; Yang & Merlin, 2024). UC-like pathology was induced via DSS, 2.5% administered in drinking water between GD 9 and 12. The face validity of UC-like pathology became evident by mid-gestation (GD13) and persisted through late pregnancy (GD17) (**Fig. 3.1)**. The impact of gestational DSS on offspring psychological functioning from juvenile (PND 31–40)

to adulthood (PND 73–120) was investigated

Behavioural evaluations in offspring revealed both similarities (**Sections 4.1 and 4.2**) and notable discrepancies (**Sections 4.3 and 4.5**) compared to the infectious MIA models based on viral and bacterial immune stimulation (Aguilar-Valles & Luheshi, 2011; Meyer, 2014; Meyer et al., 2005; Smith et al., 2007; Zuckerman & Weiner, 2005). Post-mortem analysis revealed evidence of a distinct neurodevelopmental trajectory in gestational UC offspring, which will be discussed in **Section 4.6**.

These behavioural and molecular outcomes may provide new insight into the inconsistent epidemiological findings regarding the link between maternal IBD and neurodevelopmental disorders. Subsequent sections integrated these findings, compared them to infection-based MIA models and discussed their implications for schizophrenia and ASD-like phenotypes.

4.1. Impairment of PPI in the offspring in adulthood

Impaired prepulse inhibition (PPI) of the acoustic startle reflex is a hallmark phenotype associated with schizophrenia-like outcomes across numerous studies of MIA models, including Poly I:C, LPS, and TURP (Aguilar-Valles et al., 2020; Kentner et al., 2019; Meyer, 2014). The current study showed that offspring exposed to gestational DSS treatment exhibited PPI deficits in adulthood (See **Fig. 3 .10**), but not at juvenile age, irrespective of sex. This pattern aligns with most infectious MIA studies using Poly I:C, LPS or TURP (Aguilar-Valles & Luheshi, 2011; Kentner et al., 2019; Meyer, 2014; Meyer et al., 2005; Meyer, Murray, et al., 2008; Zuckerman & Weiner, 2005), except for a study employing staphylococcal enterotoxin A/B (Glass et al., 2019) and imiquimod (Missig et al., 2020), which reported no PPI impairment. Furthermore, the age-dependent PPI deficits in MIA models consistently manifest in adulthood (postnatal day 73 or later) rather than at juvenile stages (postnatal day 30-40) (Lipina et al., 2013; Scarborough et al., 2021). My results suggest that gestational DSS was capable of inducing offspring's developmentally delayed emergence of a schizophrenia related behavioural outcome as documented in infectious MIA models (Kentner et al., 2019). This age-dependent PPI impairment further reinforces the established link between *in utero* exposure to maternal immune activation and an increased risk of developing schizophrenia-related psychopathology in adulthood.

4.2. Weak memory deficits in the offspring from maternal DSS-treatment

Consistent with the suggestion that hippocampal dysfunction contributes to the psychopathology of schizophrenia and autism, my gestational DSS model also resulted in some impaired spatial memory in offspring (Banker et al., 2021; Lieberman et al., 2018; Rexrode et al., 2024). Gestational DSS exposure led to weak and inconsistent memory deficits across three behavioural tasks commonly used in MIA studies: the Y-maze, Morris's water maze (MWM), and social interaction test. These tests assessed distinct aspects of hippocampus-dependent cognitive function, including spatial recognition memory in the Y-maze (Bitanihirwe et al., 2010; Richetto et al., 2013), spatial working memory in MWM (Meyer et al., 2010; Meyer et al., 2005; Meyer, Nyffeler, et al., 2008), and social memory in the social interaction test (Mueller et al., 2021; Smith et al., 2007; Vuillermot et al., 2017).

In infectious MIA models, deficits are observed across all three tasks, with impairments in working memory in MWM, spatial recognition in the Y-maze, and social interaction deficits (Bitanihirwe et al., 2010; Meyer et al., 2005). However, in my study, memory impairment detectable at juvenile age and persisting into adulthood was only evident in the spatial familiarity discrimination test in the Y-maze (**Fig. 3.10**). By contrast, working memory in MWM (**Fig. 3.11**) and social interaction (**Fig. 3.10**) remained intact.

One possible explanation for this discrepancy was that the MWM had higher task demands and a shorter inter-trial delay compared to the Y-maze. The Morris Water Maze (MWM) is a cognitively demanding spatial working memory task designed to assess trial-dependent learning (Morris et al., 1986). Animals must locate a submerged platform using extra-maze spatial cues, such as visual markers (Vorhees & Williams,

2006). The motivation to escape the water reinforces spatial learning across multiple trials, while daily platform relocation increases retrieval difficulty, requiring mnemonic flexibility to suppress memory of the previous platform positions, which consolidates the new position. In infectious maternal immune activation (MIA) models, offspring exhibit normal working memory performance under minimal or no inter-trial interval (ITI) condition but demonstrated deficits when longer ITIs (60 seconds to 10 minutes) were employed (Meyer et al., 2010; Meyer et al., 2005; Meyer, Nyffeler, et al., 2008). Consistent with these findings, the current study observed no working memory impairment under minimal or no ITI conditions, although extended ITIs (60 seconds to 10 minutes) were not used. Under this interpretation, working memory remains intact under low-demand conditions but deteriorates when tasks impose greater mnemonic flexibility and temporal storage.

The longer inter-trial delay in the Y-maze task may also have contributed to the detection of cognitive deficits in DSS-treated offspring. Unlike the minimal delays employed in the MWM and social interaction test, the Y-maze utilised a 30-minute inter-trial delay, which significantly increased cognitive demand (Dudchenko, 2004). This extended delay likely contributed to the emergence of spatial memory deficits. Based on this reasoning, longer delays between trials in the MWM and social interaction test could have allowed for more effective detection of memory impairments.

Given these task-specific differences, the spatial recognition memory impairment observed in the Y-maze task offers a critical insight into the cognitive deficits induced by gestational DSS exposure in offspring. The preference for novelty in Y-maze memory, observed as a reduced duration spent in the novel arm, does not appear to result from impaired mobility. Total distance travelled in the Y-maze was comparable between DSS-treated and control offspring (**Fig. 3.10**), indicating intact

locomotor activity. Since time spent in the novel arm depended on both movement and memory, comparable total distances ruled out mobility as the cause of the reduced alternation, pointing to a specific deficit in spatial working memory. Furthermore, intact social memory performance in the three-chamber test suggests that the Y-maze deficit does not reflect a general memory impairment but rather specifically affects spatial recognition memory. This spatial memory impairment aligns with cognitive deficits observed in schizophrenia, further supporting the relevance of the gestational DSS model to schizophrenia-like phenotypes (Rizzo et al., 1996).

These findings indicated that gestational DSS exposure was sufficient to induce spatial recognition memory deficits in offspring, resembling schizophrenia-related behavioural outcome documented in infection-based MIA models (Howland et al., 2012; Richetto et al., 2013). However, short-term working memory and sociability remained intact, indicating a less pervasive impact compared to viral and bacterial infectious MIA models (Meyer et al., 2010; Meyer et al., 2005; Meyer, Nyffeler, et al., 2008). Another plausible explanation could be that immune activation in the gestational DSS model may be weaker or more localised than in infectious models (see **section 4.3**).

In infectious MIA models, it typically reduces DCX-positive cells and BDNF levels in the hippocampus of offspring exposed to prenatal inflammation (Golia et al., 2019; Meyer et al., 2010). These reductions are often associated with memory deficits. In contrast, no change in DCX-positive cells in the hippocampus and an abnormal elevation of hippocampal BDNF levels were observed in DSS-treated offspring (see **Fig 3.14 & 3.15**). Since DCX-positive cells label young neurons, the absence of change in these cells suggests that the spatial memory deficit observed in the Y-maze task may not be related to the alterations in newly generated neurons caused by gestational DSS

treatment (Vukovic et al., 2013). However, abnormally high hippocampal BDNF levels may disrupt synaptic plasticity (Cunha et al., 2009; Pietropaolo et al., 2007). Yet, this may suggest that both excessively high and excessively low hippocampal BDNF levels can impair spatial memory, resembling an inverted U-shaped relationship. Therefore, the abnormally elevated hippocampal BDNF induced by gestational DSS treatment may contribute to the spatial memory deficit observed in the Y-maze task. These opposite changes in BDNF and neurogenesis highlight that similar behavioural deficits may arise from opposite neurochemical directions, depending on the prenatal stimuli. **Section 4.3** further explores the differences between the DSS model and infectious MIA models by comparing their immune responses.

4.3. The difference in immune response between gestational DSS and Infectious MIA models

The gestational DSS model, validated through histological, gross pathological, and molecular evidence, consistently induced a mild and protracted maternal immune response, distinct from the robust inflammation observed in infectious MIA models. Administration of 2.5% DSS at GD9 in C57BL/6 mice induced colitis pathology, supporting the model's face validity for studying maternal inflammation during pregnancy **(Fig. 3.1&3.4)**. This validation is further substantiated by gross pathological changes, which confirm the model's alignment with established DSS-induced colitis characteristics. Gross pathological changes, consistent with non-pregnant DSS-induced colitis models (Chassaing et al., 2014; Yang & Merlin, 2024), were evident by GD13. DSS-treated mice exhibited significant colon shortening (**Fig. 3.1C&D**), indicative of inflammation-driven tissue remodelling. Additionally, splenomegaly, reflected by increased spleen weight (**Fig. 3.1E**) and size at GD13 (**Fig. 3.1F**), suggested a systemic immune response. These gross pathological findings were corroborated by histological evidence of colitis, including disrupted crypt architecture and immune cell infiltration (**Fig. 3.2**). These pathological features confirmed the validity of colitis-like pathology for examining the molecular mechanisms underlying the maternal immune response in this model.

Molecular analyses confirmed a sustained immune response in the maternal colon and systemic circulation following 2.5% DSS administration at GD9 in C57BL/6 mice. Upregulation of pro-inflammatory cytokines (IL-1β, IL-6, TNF-α) alongside anti-inflammatory IL-10 in the maternal colon (**Fig. 3.4**) aligned with the immunopathology of DSS-induced colitis in a non-pregnant model (Egger et al., 2000). Delayed increases in circulating IL-1β at GD17 and TNF-α at GD13 (**Fig. 3.4**) indicated protracted

immune activation persisting for at least five days post-DSS treatment, spanning early mid to late gestation. This protracted immune response mirrored the progression from acute to chronic inflammation observed in non-pregnant DSS models using 2.5–5% DSS, which manifests systemic symptoms (Chassaing et al., 2014). These molecular findings in the maternal system prompted further investigation into the inflammatory effects on the foetal brain, a critical aspect of neurodevelopmental outcomes.

Foetal brain inflammation was evidenced by elevated IL-1β expression at GD13 (**Fig. 3.6&3.8**) and increased ASC (central adaptor of inflammasome protein) at GD13 and GD17 (**Fig. 3.8**). Although the synthesized origin of IL-1β RNA and ASC protein observed in the foetal brain could not be identified, these inflammatory components may be synthesized in maternal tissue or in the placenta and subsequently influence foetal brain development (Hsiao & Patterson, 2011). These findings suggest that gestational DSS treatment induced an inflammatory environment in the foetal brain, potentially impacting neurodevelopmental trajectories (Kwon et al., 2022). Given these foetal brain changes (Kwon et al., 2022) and the maternal immune response, the immunological profile of the gestational model partially aligned with the infectious MIA models.

According to one hypothesis, the maternal cytokine response to infections may play a crucial role in the association between MIA and brain development (Gilmore & Jarskog, 1997). Studies of MIA models (e.g., Poly I:C, lipopolysaccharide (LPS), or turpentine (TURP)) have suggested that a single administration elicited an acute immune response (Bucknor et al., 2022), inducing activation of pro-inflammatory cytokines. These models triggered rapid and robust elevations of pro-inflammatory (IL-6, IL-1β, TNF-α) and anti-inflammatory (IL-10) cytokines in maternal serum within hours, accompanied by a febrile reaction that resolves within two days (Aguilar-Valles

& Luheshi, 2011; Kentner et al., 2019; Meyer, Nyffeler, et al., 2006; Ortega et al., 2011). These inflammatory cytokines can modulate neuronal differentiation, survival, and dendrite growth (Gilmore et al., 2004; Jarskog et al., 1997). Similarly, the altered cytokine profile in the current gestational DSS model, notably the upregulation of IL-1β in the foetal brain, suggests that chronic inflammation, as in IBD, can also induce cytokine-mediated neurodevelopmental effects.

In the current gestational DSS-induced model, limitations in cytokine profiling resulted from the sensitivity of the Bio-Plex assay and the limited availability of maternal serum following assay optimisation. Consequently, ELISA-based analysis of IL-1β, IL-6, and TNF-α was selected to compare the immunological profile of this model with viral and bacterial infectious MIA models (Ortega et al., 2011; Paraschivescu et al., 2020; Smith et al., 2007), as these cytokines are also associated with IBD (Yang & Merlin, 2024). The foetal brain IL-1β upregulation, consistent with MIA models (Ortega et al., 2011), indicates that maternal cytokines may cross the placenta, impacting foetal neurodevelopment. Surprisingly, the current model did not exhibit the expected elevation of circulating IL-6 in the maternal host (**Fig. 3.4**) and the upregulation of selective inflammatory cytokines in the placenta (**Fig. 3.7**), both of which are prominent features of infectious MIA models (Smith et al., 2007; Wu et al., 2017). Elevated circulating IL-6 is a prominent feature in the non-pregnant DSS-induced colitis model (Chassaing et al., 2014), but this was not observed in the current gestational DSS model. Direct comparison of the immune response between the gestational DSS model and infectious MIA models is challenging due to the different features of induced immunogens. However, immune stimuli rapidly and robustly elevate levels of pro-inflammatory cytokines (IL-1β, IL-6, TNF-α) in maternal serum (Aguilar-Valles & Luheshi, 2011; Paraschivescu et al., 2020), whereas the DSS model

showed no significant elevation of IL-6 in maternal serum. These findings suggest that the immune response in the DSS model is weaker than that observed in infectious MIA paradigms, potentially contributing to the distinct neurodevelopmental outcomes observed in offspring.

The milder and protracted immune response from gestational DSS likely contributed to the observed offspring outcomes: weak memory deficits, preserved affective behaviours (e.g., no anxiety or depression-like behaviours), and disrupted prepulse inhibition (PPI). Disrupted PPI, a behavioural hallmark of the Poly I:C MIA model (Kentner et al., 2019), suggested that, despite the DSS model being a milder variant of MIA models, the offspring still exhibited robust psychiatric changes in PPI. Typically, infectious MIA models with cytokine imbalances cause PPI disruption, latent inhibition (LI) disruption, and increased MK-801 hypersensitivity (See **Table 1.2**). However, the findings of enhanced LI and attenuated MK-801 hypersensitivity in the DSS model contrasted with those of infectious MIA models. These differences indicated that the distinct maternal immune response in the DSS model, beyond typical MIA pathways, may drive these unique neurodevelopmental outcomes.

4.4. Enhanced LI in offspring with gestational DSS treatment

Infectious MIA models reliably impair latent inhibition, a cognitive process where animals gradually turn down attention to irrelevant stimuli (e.g., a tone) based on prior non-reinforcement in the pre-exposure phase (Meyer et al., 2005; Meyer, Feldon, et al., 2006; Zuckerman & Weiner, 2003). A key finding in the current study was that adult offspring of both sexes from dams treated with gestational DSS exhibited enhanced LI in Cohort A when control offspring showed weak LI. In contrast, Cohort B offspring from both control and gestational DSS-treated dams displayed clear LI, with no significant group difference observed (**Fig. 3.12**). These findings indicated that the offspring from gestational DSS-treated dams failed to disrupt LI, unlike the disrupted LI observed in infectious MIA models.

Typically, infectious MIA studies, using immunogens like Poly I:C or LPS across various species and gestational days (GD6–17), consistently reported LI disruption, particularly with early-to-mid-gestation (GD6–12) immune challenges (Meyer et al., 2006). However, mid- to late-gestation (GD15–17) Poly I:C MIA models in mice have produced inconsistent outcomes. For instance, no changes in LI were observed when Poly I:C was administered on GD15 or GD17 (Meyer, Feldon, et al., 2006; Vorhees et al., 2012). In contrast, enhanced LI was reported in male offspring when Poly I:C was administered on GD17, using a two-way avoidance paradigm where control animals exhibited no LI (Bitanihirwe et al., 2010). The current gestational DSS model aligns with this finding, failing to disrupt LI (Cohort B, similar to (Meyer, Feldon, et al., 2006; Vorhees et al., 2012)) or enhancing LI (Cohort A, similar to (Bitanihirwe et al., 2010)), depending on the presence of LI in control offspring. Thus, gestational DSS treatment does not disrupt LI but may enhance or preserve it, suggesting a distinct neurocognitive profile compared to infectious MIA models.

A plausible explanation for the observed persistent LI involves the onset timing and duration of the maternal immune response in the DSS model. Unlike early-to-mid-gestation (GD9–12) MIA models that disrupt LI, the gestational DSS model, despite administration at GD9, induced a protracted inflammatory response persisting into late gestation (GD17; see **Section 4.3)**. This protracted inflammation, induced by gestational DSS in mid- to late-gestation, may align my DSS model with late-gestation MIA models, which often show no LI change or abnormal enhanced LI (Bitanihirwe et al., 2010; Meyer, Feldon, et al., 2006). To my knowledge, few studies report both persistent LI and no LI change within the same MIA model, making the current findings a novel extension of prior rodent models of gestational viral and bacterial infections. Thus, the current DSS model suggests that late prenatal immune activation may solely promote abnormally enhanced LI without evidence of disrupting LI in offspring, relative to control offspring.

Infectious MIA models have frequently linked LI disruption to impaired attentional filtering, a hallmark of schizophrenia's positive symptoms (Meyer, Feldon, et al., 2006; Smith et al., 2007; Weiner, 2003; Zuckerman & Weiner, 2005). In contrast, the current DSS model suggests persistent or enhanced LI, indicative of cognitive rigidity. According to Weiner (2003), the two-headed LI model, disrupted LI reflects excessive attentional switching (positive symptoms), while abnormally enhanced LI reflects retarded switching (negative/cognitive symptoms). This framework emphasised dysfunctional attentional switching to explain how cognitive deficits manifest in schizophrenia. Bitanihirwe et al. (2010) suggested that prenatally immune-challenged offspring exhibited preservation of LI linked to hypoglutamatergic states in the medial prefrontal cortex and dorsal hippocampus. Converging evidence derived from studies in human and translational animal models suggested that impaired

glutamatergic signalling induced by MK-801 can induce similar abnormal enhanced LI in rats and mice states (Gaisler-Salomon et al., 2008; Gaisler-Salomon & Weiner, 2003). Hence, I went on to investigate the psychostimulant response to the NMDA receptor antagonist, MK-801, and subsequently the synthesis of NMDA receptor subunits, *GRIN1*, *GRIN2A*, and *GRIN2B* (discussed in **Section 4.5**) in the hippocampus of the offspring. These findings may suggest a potential glutamatergic basis for the observed abnormally enhanced LI, but the direction of the abnormal glutamatergic status is opposite to expectations for abnormally enhanced LI.

4.5. Attenuated MK-801 hypersensitivity in the offspring with gestational DSS treatment

The current study revealed a striking attenuation of the locomotor response to a low dose of MK-801 (0.2 mg/kg), a non-competitive NMDA receptor antagonist, in adult offspring exposed to maternal DSS treatment *in utero*. Typically, MK-801 induces locomotor hyperactivity at lower doses (e.g., 0.15–0.2 mg/kg), whereas higher doses (e.g., 0.5 mg/kg) elicit ataxia-like symptoms, such as head weaving or body rolling, which can reduce locomotor activity (Liljequist et al., 1991). In contrast to infectious MIA models, where offspring typically exhibit hypersensitivity to MK-801's locomotor effects at low doses (Basta-Kaim et al., 2011; Meyer et al., 2005; Zuckerman & Weiner, 2005), the attenuated response in DSS-exposed offspring suggests an opposite alteration in NMDA receptor function. This disagrees with the NMDA receptor hypofunction commonly associated with schizophrenia-like phenotypes in infectious MIA models and may suggest a unique neurodevelopmental trajectory following prenatal DSS exposure.

Only some rat studies using lower doses of Poly I:C during mid-to-late gestation (GD15–18) have reported similarly attenuated MK-801-induced locomotor responses (Bronson et al., 2011; Missault et al., 2014; Vorhees et al., 2012, 2015). Bronson et al. (2011) proposed that maternal body weight loss might mediate this attenuation, a hypothesis consistent with the significant maternal body weight reduction observed in the current gestational DSS model (**Fig. 3.1**). However, this interpretation is complicated by reports of heightened MK-801 sensitivity in other MIA models despite maternal weight loss, suggesting that body weight alone does not fully account for the observed effects. Additionally, the absence of systemic immune activation data in these rat studies (Bronson et al., 2011; Missault et al., 2014; Vorhees et al., 2012, 2015) limits

direct comparisons to the maternal immune response in the current study. In the current model, maternal immune activation during mid-to-late gestation (similar to the studies in rats), potentially combined with localised gut inflammation, may create a prenatal immune challenge in the foetal brain (**Fig. 3.6 & 3.8**). This environment could regulate the expression of synaptic proteins, such as synaptophysin (**Fig. 3.8**), which may modulate glutamatergic pathways in adult offspring. Increased synaptophysin expression might enhance glutamate release, potentially reducing the availability of NMDA receptors for MK-801 binding, thereby attenuating the MK-801-induced locomotor response. The precise mechanisms underlying this attenuated MK-801 response, however, remain unclear in the current study.

The adult offspring subjected to the LI test and the lower dose of MK-801 exhibited neurobehavioural effects that diverged from those typically observed in infectious MIA models. Building on the outcomes from the LI test, the offspring exposed to gestational DSS treatment suggested hypofunction of NMDA receptors. Yet, their psychostimulant response to MK-801 was significantly attenuated (**Fig. 3.13**) and suggested enhanced NMDA systems, presenting an apparent contradiction between the LI and locomotor activity findings. This unique combination of neurobehavioral effects mirrors observations in forebrain neurons of selective glycine transporter 1 (GlyT1) knockout mice (Yee et al., 2006), suggesting a potential role of NMDA receptor dysfunction. These findings highlight the need to further investigate NMDA receptor and glycine transporter involvement to clarify these neurodevelopmental alterations.

One potential explanation for this discrepancy lies in altered NMDA receptor function in critical brain regions, such as the hippocampus. For example, increased NMDA receptor density or sensitivity could counteract the antagonistic effects of MK-801, as supported by prior research (Xi et al., 2009). In the current study, gene

expression of NMDA receptor subunits (*GRIN1*, *GRIN2a*, *GRIN2b*) in the hippocampus revealed no differences compared to controls. However, to determine whether NMDA receptor protein levels are altered despite unchanged mRNA expression, IHC staining for the NR1 subunit (encoded by *GRIN1*) will be performed on hippocampal sections from both control offspring and offspring of DSS-treated dams. Since the NR1 subunit is an obligatory component of all functional NMDA receptors (Laube et al., 1998), quantitative analysis of NR1 immunoreactivity (optical density) in the CA1, CA3, and dentate gyrus subregions will be conducted. Elevated NR1 protein expression would suggest an increase in NMDA receptor density, potentially underlying the observed attenuation in MK-801-induced hyperlocomotion. Elevated NR1 levels could indicate increased NMDA receptor numbers, potentially explaining the reduced MK-801 sensitivity.

Overall, these findings indicated that the attenuated MK-801 response in DSS-exposed offspring is not due to alteration of NMDA receptor RNA expression in the hippocampus. However, changes in synaptic protein levels or NMDA receptors' function cannot be excluded as contributing factors. Consistent with the latent inhibition findings, the gestational DSS model exhibits neurobehavioural effects directly opposing those observed in most viral or bacterial MIA models, typically showing an increasing motor-stimulant response to MK-801. These findings highlight fundamental differences in the neurodevelopmental consequences of distinct maternal immune challenges, underscoring the need to further dissect their underlying mechanisms.

4.6. Divergence from the infectious MIA models

The behavioural and molecular findings of the offspring in the current study suggested that gestational IBD is neurodevelopmentally impactful (see **Table 4.1**). However, infectious MIA models often report abnormal behaviour associated with broad psychiatric disorders, including schizophrenia and autism spectrum disorder (ASD), as well as anxiety and depression-like behaviour in offspring exposed to prenatal immune challenges (Haddad et al., 2020; Meyer, 2019). Notably, the current gestational DSS model did not exhibit anxiety or depression like behaviours, marking a key divergence.

Age-dependent PPI disruption in adulthood was well documented in schizophrenia (Swerdlow et al., 1994; Swerdlow & Geyer, 1998). This disruption was also observed, indicating impaired sensory filtering, a characteristic commonly shared across schizophrenia, ASD, and ADHD (Castellanos et al., 1996; Geyer, 2006; Perry et al., 2007). Additionally, spatial recognition impairment was observed in the Y-maze, a core component of schizophrenia-related cognitive impairment (Gray et al., 1991; Swerdlow et al., 1994) and potentially related ASD (Edgin & Pennington, 2005). An abnormally enhanced latent inhibition (LI) may indicate negative symptoms of schizophrenia, according to Weiner (2003). These findings collectively underscore the link between maternal IBD during pregnancy and neurodevelopmental implications in offspring, especially concerning cognitive impairments.

However, the depression and anxiety-like behaviour were not detected in the current model, as well as asociality, which is the core ASD-associated feature (**Fig. 3.10**) (Tiede & Walton, 2021). Offspring exposed to gestational DSS showed no significant differences in the elevated plus maze (EPM) test across juvenile and adult ages (**Fig. 3.10**), indicating an absence of anxiety-like behaviours, a feature also observed in

schizophrenia (Hall, 2017) and ASD (Burnette et al., 2005). Similarly, open field test (OFT) analysis did not detect anxiety-like behaviour, increased exploration, or increased average distance from the wall during the 15-minute habituation phase before MK-801 administration (data not shown), further confirming the absence of anxiogenic effects in the EPM and OFT. In contrast, infectious MIA models using immunogens such as Poly I:C or imiquimod typically exhibit reduced OFT exploration and anxiogenic effects (Meyer et al., 2005; Missig et al., 2020). Therefore, the gestational DSS model produces the opposite behavioural profile for these schizophrenia and autism relevant domains.

Likewise, assessments of anhedonia via the sucrose preference test, as well as the behavioural despair via the Porsolt forced swimming test (**Fig. 3.11**), failed to detect depression-like behaviour. In contrast, infectious MIA models typically exhibit pronounced social deficits and depression-like behaviour following prenatal immune challenge (Depino, 2015), further distinguishing the gestational DSS model from MIA paradigms. These findings highlight a key divergence from existing infectious MIA models.

Notably, some behavioural phenotypes in the gestational DSS model, such as PPI deficits and recognition memory impairment, closely align with those observed in infectious MIA models. Similarly, sex differences in schizophrenia-like behaviours within the DSS model align with findings in infectious MIA models in mice (Meyer et al., 2005) and rats (Zuckerman & Weiner, 2005). However, behavioural phenotypes without sex difference contrast with clinical observations, where male schizophrenia patients typically exhibit an earlier onset and more severe clinical profile, particularly in positive symptoms and cognitive deficits of schizophrenia (Angermeyer & Kuhn, 1988; Eranti et al., 2013; Faraone et al., 1994; Roy et al., 2001).

In contrast to infectious MIA models, the gestational DSS model showed an upregulation of synaptic proteins in the foetal brain and an increase in hippocampal BDNF levels during the juvenile and adult stages. In MIA models, hippocampal BDNF disruption is commonly reported, potentially contributing to the loss of synaptic connectivity in schizophrenia due to dysregulation of the developmental pruning process (McGlashan & Hoffman, 2000; Woo & Crowell, 2005). In contrast, the gestational DSS model exhibited an upregulation of synaptic proteins, which may suggest a dysregulated compensatory mechanism in response to maternal UC. Specifically, increased levels of synaptophysin and a trend toward increased synaptotagmin 1 in the foetal brain were observed, alongside elevations in hippocampal BDNF (Fig. 3.8 and 3.14) in offspring at juvenile and adult stages. These findings suggest that, rather than impairing synaptic connectivity, maternal DSS exposure may drive abnormal synaptic pruning, which could potentially lead to aberrant synaptic maturation. Aberrant synaptic pruning has been linked to neurodevelopmental disorders, including ASD and a subtype of schizophrenia (Glausier & Lewis, 2013). In ASD, insufficient synaptic pruning is associated with hyperconnectivity and contributes to impairments in cognitive processing (Rapoport et al., 2009; Sakai, 2020). Conversely, excessive synaptic pruning in a subtype of schizophrenia, like childhood-onset schizophrenia, is linked to progressive cognitive decline (Rapoport et al., 2009). This distinct synaptic adaptation suggests a divergent neurodevelopmental trajectory from the foetal stage to adulthood compared to traditional maternal immune activation models. However, the precise interplay between neuroimmune interaction and synaptic connectivity remains to be elucidated.

The presence of schizophrenia-like behaviours irrespective of sex in the DSS model, alongside unique synaptic and behavioural adaptations, may reinforce the

generalisability of prior rodent models of gestational viral and bacterial infections. This further supports the hypothesis that *in utero* exposure to maternal immune activation increases the risk of developing schizophrenia-related psychopathology.

Therefore, the present study suggested that gestational IBD is neurodevelopmentally impactful in the rodent model. It may help clarify the inconclusive epidemiological findings (see **Section 4.7**).

4.7. Epidemiological consideration and implication

The association between maternal IBD and ASD risk in offspring remains inconclusive. While some studies have found no increased risk (Andersen et al., 2014; Prentice et al., 2024), others suggest an elevated ASD risk specifically linked to UC (Sadik et al., 2022). The gestational DSS model used in this study may help clarify these discrepancies, which may arise due to the lack of classification of subpopulations and IBD subtypes. Additionally, some pregnant IBD patients have chronic IBD, having been diagnosed before pregnancy, which could influence the maternal immune response.

Recently, the pregnancy-onset IBD (POIBD) subpopulation has been classified, identifying patients who develop IBD during the first trimester of pregnancy (Koslowsky et al., 2018; Yu et al., 2021). This study employed a DSS-induced UC-like pathology face validity model at GD9 to evaluate behavioural outcome in offspring. The timing of model induction during pregnancy may provide insights into the POIBD subpopulation in humans (Koslowsky et al., 2018; Yu et al., 2021).

In summary, the gestational DSS model supports epidemiological findings, suggesting that maternal UC is not strongly associated with ASD in offspring but may instead be linked to schizophrenia risk. While previous studies on maternal IBD and neurodevelopmental disorders (Jolving et al., 2017) found no increased risk of schizophrenia, they often aggregated UC and Crohn's disease under the broad IBD category, without isolating UC or POIBD cases. Additionally, these studies typically overlook the focus on early life tracking rather than long-term follow-up, schizophrenia onset in young adulthood (Nielsen et al., 2014; Prentice et al., 2024).

The present findings suggest that pregnancy-onset UC-like pathology may influence the offspring's behaviour by altering early neurodevelopmental trajectories. This hypothesis underscores the clinical and epidemiological significance of long-term

psychiatric outcome studies, particularly those focusing on POIBD subpopulations (Koslowsky et al., 2018; Yu et al., 2021). Extended follow-up studies tracking offspring from adolescence into early adulthood are essential, given that schizophrenia typically manifests between late adolescence and early adulthood (Kahn et al., 2015).

4.8. Limitations and future investigations

There are several important caveats to consider for the current study. First, the translatability of the current gestational DSS model. It evaluated neurodevelopmental outcomes from DSS administration linked to a specific gestational window (GD9–12), corresponding to the first and second trimesters in humans (Clancy et al., 2001; Clancy et al., 2007). This model reflects pregnancy-onset IBD, which models a subpopulation with disease onset during pregnancy, rather than chronic or pre-existing conditions.

Second, the offspring's behavioural outcomes may have been influenced by unexamined confounding factors, such as DSS to the maternal host (directly) and microbiota change (indirectly). Postpartum maternal care and microbiota dysregulation (Chassaing et al., 2014; Hakansson et al., 2015; Li et al., 2018) in the maternal host are key areas for future exploration. Existing literature suggests that maternal microbiota can influence the maternal brain via the gut-brain axis (Morais et al., 2021) and may indirectly affect offspring brain development through postpartum maternal care (Jasarevic, Howerton, et al., 2015; Schwendener et al., 2009). Furthermore, some epidemiological studies indicate that women with IBD who experienced symptoms during pregnancy have an increased risk of new-onset psychiatric disorders in postpartum (Vigod et al., 2019). To investigate the link between maternal UC and offspring behaviour, future studies should examine postpartum maternal care and maternal brain alterations in the gestational DSS model, alongside postpartum maternal behaviour (DeRosa et al., 2022). To distinguish between prenatal and postnatal maternal influences, future research should incorporate the gestational DSS manipulation using a cross-fostering design (Richetto et al., 2013; Scarborough et al., 2024). Also, DSS-induced UC-like pathology is a widely used chemical model for IBD. Other UC-like models can be used to replicate a similar experimental design, potentially reducing the

confounding effect of the DSS model on the offspring's behavioural outcome.

A key limitation of this study was the inability to assess the response to amphetamine, a non-selective indirect agonist that enhances dopamine release, due to a year-long logistical delay in its delivery from a US supplier. Given the established behavioural deficits observed in offspring from DSS-treated dams, future studies should incorporate amphetamine challenges to investigate dopaminergic involvement in abnormal enhanced LI, PPI disruption, and other phenotypes associated with dopamine dysregulation (Swerdlow & Geyer, 1998; Weiner, 2003). By addressing these limitations and exploring the outlined future directions, further research can provide deeper insights into the neurodevelopmental consequences of maternal UC and strengthen the link between maternal immune activation and neurodevelopmental outcomes.

4.9. Conclusion:

This study successfully established a gestational UC model in mice, demonstrating its distinct neurodevelopmental impact on offspring and providing a novel framework for understanding maternal IBD-related neurodevelopmental changes beyond infectious MIA models. By revealing both consistencies and divergences, these findings qualify the interpretation of infectious MIA models, underscoring the variability in immune signalling and its long-term consequences for offspring brain function.

Gestational UC induced by DSS exposure in drinking water can produce synaptic and behavioural adaptations distinct from viral and bacterial infectious MIA models, highlighting the need to broaden the scope of immune-driven psychiatric risk models in early life **(Fig. 4.1)**. The absence of sociality impairment, along with the opposing effects observed in latent inhibition and NMDA sensitivity, further underscores the specific impact of UC as a maternal immune condition. Future studies should refine the mechanistic links between gestational UC and neurodevelopmental alterations to delineate its influence better.

Ultimately, this research underscores the importance of considering diverse maternal inflammatory conditions in neurodevelopmental studies, advancing the understanding of immune-mediated psychopathology.

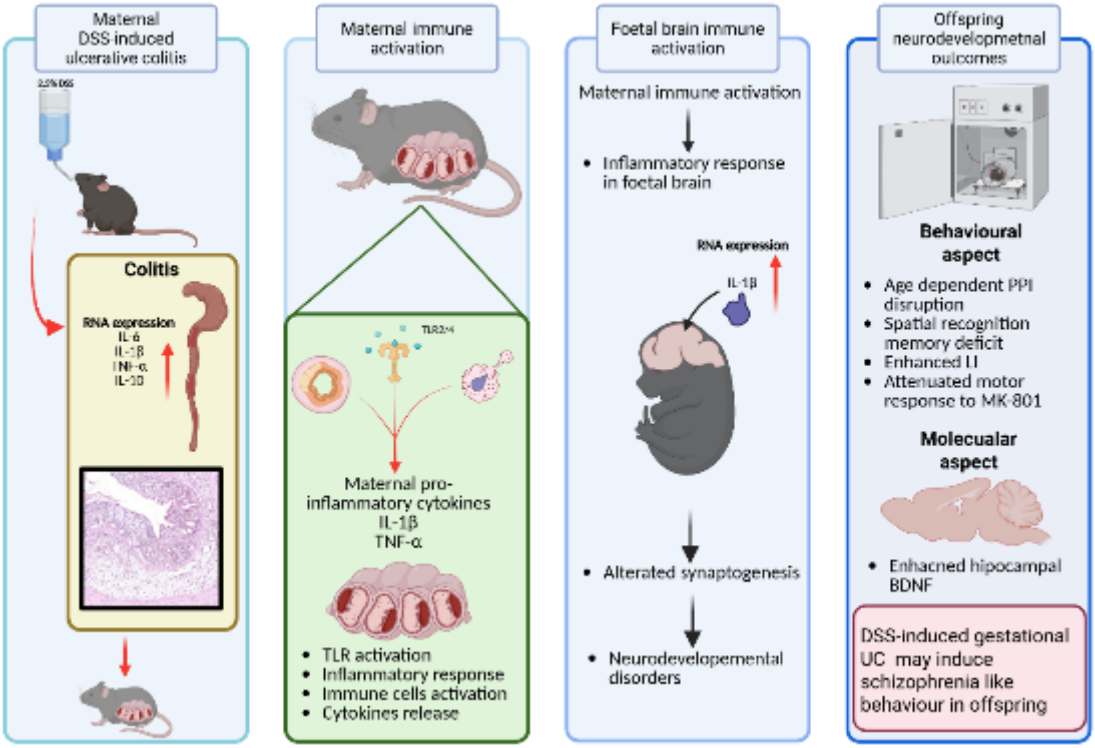

Figure 3.16. Schematic overview of maternal, foetal, and offspring outcomes in a DSS-induced ulcerative colitis-like pathology mouse model.
The diagram includes three sections: (1) Model validation, illustrating DSS-induced ulcerative colitis in pregnant C57BL/6J mice and associated maternal immune activation and gut alterations; (2) Foetal brain changes, highlighting immune activation and upregulated synaptic plasticity-related proteins; and (3) Neurodevelopmental outcomes in offspring, showcasing behavioural deficits. Key findings are illustrated to depict the pathway from maternal UC to offspring neurodevelopment.

	EPM	Y-maze	SI	PPI	MWM	FST	SPT	LI	MK-801	Reference
Gestational DSS	=	↓ [i]	=	↓ [d]	=	=	=	↑/=	↓	
PolyI:C (early-mid)	↑/=	↓	↓	↓ [d]	↓ [g]	↑	=	↓	↑	Vuillermot et al., (2017); Meyer et al., (2010), Smith et al., (2007), Meyer et al., (2006)
PolyI:C (late)	=	↓	↓	↓	↓ [f]		↓	↑/=	↑/↓	Meyer et al., (2007); Bitanihirwe et al., (2010), Nakamura et al., (2021)
LPS	↑		↓/= [e]	↓		↑		↓	↑	Basta-Kaim et al., (2011); Abu-Ata et al., (2023), Depino, (2015), Fernandez de Cossio et al., (2017), Waterhouse et al., (2016, 2017), Imai et al., (2018)
Cytokines				↓				↓		Smith et al., (2007)
TURP			↓	↓ [b]						Aguilar-Valles et al., (2011)
SEA	↑		↓	=	↓ [a]					Glass et al., (2019)
SEB	↑		=	=	=					Glass et al., (2019)
Imiquimod	=		↑	=						Missig et al., (2020)
STAg	↑ [g]		↓							Spini et al., (2020)

Table 3.1. Overview of experimental paradigms for investigating behavioural and neurochemical abnormalities in infectious MIA models and the current study

Appendix:

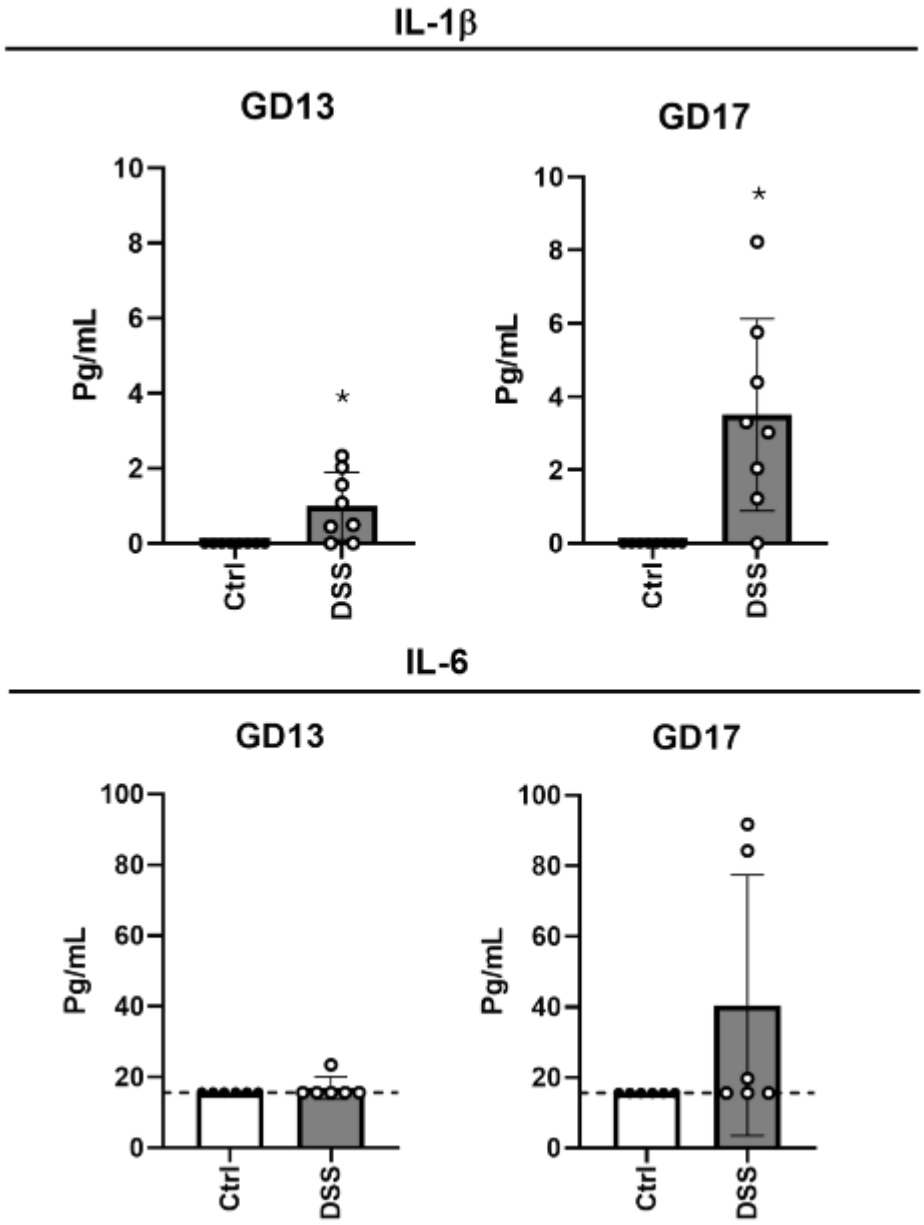

Appendix Figure 1. Effect of gestational DSS treatment on circulating IL-1β levels. Maternal serum levels of IL-6 (n = 6 per group) and IL-1β (n = 8 per group), expressed in pg/mL, were measured at gestational days (GD) 13 and 17. Circulating IL-1β was significantly elevated in the gestational DSS-treated group at both time points. The dotted line in the corresponding graph represents the minimum detection limit for IL-6. (*) indicate statistically significant differences between groups ($p < 0.05$).

References

Abhyankar, A., Ham, M., & Moss, A. C. (2013). Meta-analysis: the impact of disease activity at conception on disease activity during pregnancy in patients with inflammatory bowel disease. *Aliment Pharmacol Ther*, *38*(5), 460-466. https://doi.org/10.1111/apt.12417

Abraham, C., & Cho, J. (2009). Interleukin-23/Th17 pathways and inflammatory bowel disease. *Inflamm Bowel Dis*, *15*(7), 1090-1100. https://doi.org/10.1002/ibd.20894

Abu-Ata, S., Shukha, O. N., Awad-Igbaria, Y., Ginat, K., Palzur, E., Golani, I., & Shamir, A. (2023). Blocking the ErbB pathway during adolescence affects the induction of anxiety-like behavior in young adult maternal immune activation offspring. *Pharmacol Biochem Behav*, *222*, 173497. https://doi.org/10.1016/j.pbb.2022.173497

Aguilar-Valles, A., & Luheshi, G. N. (2011). Alterations in cognitive function and behavioral response to amphetamine induced by prenatal inflammation are dependent on the stage of pregnancy. *Psychoneuroendocrinology*, *36*, 634-648. https://doi.org/10.1016/j.psyneuen.2010.09.006

Aguilar-Valles, A., Poole, S., Mistry, Y., Williams, S., & Luheshi, G. N. (2007). Attenuated fever in rats during late pregnancy is linked to suppressed interleukin-6 production after localized inflammation with turpentine. *Journal of Physiology*, *583*, 391-403. https://doi.org/10.1113/jphysiol.2007.132829

Aguilar-Valles, A., Rodrigue, B., & Matta-Camacho, E. (2020). Maternal Immune Activation and the Development of Dopaminergic Neurotransmission of the Offspring: Relevance for Schizophrenia and Other Psychoses. In *Frontiers in Psychiatry* (Vol. 11): Frontiers Media S.A.

Al-Haddad, B. J. S., Jacobsson, B., Chabra, S., Modzelewska, D., Olson, E. M., Bernier, R., Enquobahrie, D. A., Hagberg, H., Östling, S., Rajagopal, L., Adams Waldorf, K. M., & Sengpiel, V. (2019). Long-term risk of neuropsychiatric disease after exposure to infection in utero. *JAMA Psychiatry*, *76*, 594-602. https://doi.org/10.1001/jamapsychiatry.2019.0029

Aleman, A., Kahn, R. S., & Selten, J. P. (2003). Sex differences in the risk of schizophrenia: evidence from meta-analysis. *Arch Gen Psychiatry*, *60*(6), 565-571. https://doi.org/10.1001/archpsyc.60.6.565

Ananthakrishnan, A. N. (2016). Vitamin D and Inflammatory Bowel Disease. *Gastroenterol Hepatol (N Y)*, *12*(8), 513-515. https://www.ncbi.nlm.nih.gov/pubmed/27917088

Andersen, A. B. T., Ehrenstein, V., Erichsen, R., Frøslev, T., & Sørensen, H. T. (2014).

Autism spectrum disorders in children of parents with inflammatory bowel disease - a nationwide cohort study in Denmark. *Clinical and experimental gastroenterology*, *7*, 105-110. https://doi.org/10.2147/CEG.S59360

Andersen, C. L., Jensen, J. L., & Orntoft, T. F. (2004). Normalization of real-time quantitative reverse transcription-PCR data: A model-based variance estimation approach to identify genes suited for normalization, applied to bladder and colon cancer data sets. *Cancer Research*, *64*(15), 5245-5250. https://doi.org/Doi 10.1158/0008-5472.Can-04-0496

Angermeyer, M. C., & Kuhn, L. (1988). Gender differences in age at onset of schizophrenia. An overview. *Eur Arch Psychiatry Neurol Sci*, *237*(6), 351-364. https://doi.org/10.1007/BF00380979

Antoniou, E., Margonis, G. A., Angelou, A., Pikouli, A., Argiri, P., Karavokyros, I., Papalois, A., & Pikoulis, E. (2016). The TNBS-induced colitis animal model: An overview. *Annals of medicine and surgery (2012)*, *11*, 9-15. https://doi.org/10.1016/j.amsu.2016.07.019

Arsenault, D., St-Amour, I., Cisbani, G., Rousseau, L. S., & Cicchetti, F. (2014). The different effects of LPS and poly I: C prenatal immune challenges on the behavior, development and inflammatory responses in pregnant mice and their offspring. *Brain, Behavior, and Immunity*, *38*, 77-90. https://doi.org/10.1016/j.bbi.2013.12.016

Baddeley, A. (1992). Working memory. *Science*, *255*(5044), 556-559. https://doi.org/10.1126/science.1736359

Baddeley, A. (2003). Working memory: looking back and looking forward. *Nat Rev Neurosci*, *4*(10), 829-839. https://doi.org/10.1038/nrn1201

Baddeley, A. D., & Hitch, G. (1974). Working Memory. In G. H. Bower (Ed.), *Psychology of Learning and Motivation* (Vol. 8, pp. 47-89). Academic Press. https://doi.org/https://doi.org/10.1016/S0079-7421(08)60452-1

Balding, J., Livingstone, W. J., Conroy, J., Mynett-Johnson, L., Weir, D. G., Mahmud, N., & Smith, O. P. (2004). Inflammatory bowel disease: the role of inflammatory cytokine gene polymorphisms. *Mediators Inflamm*, *13*(3), 181-187. https://doi.org/10.1080/09511920410001713529

Banker, S. M., Gu, X., Schiller, D., & Foss-Feig, J. H. (2021). Hippocampal contributions to social and cognitive deficits in autism spectrum disorder. *Trends Neurosci*, *44*(10), 793-807. https://doi.org/10.1016/j.tins.2021.08.005

Baruch, I., Hemsley, D. R., & Gray, J. A. (1988). Differential performance of acute and chronic schizophrenics in a latent inhibition task. *J Nerv Ment Dis*, *176*(10), 598-606. https://doi.org/10.1097/00005053-198810000-00004

Basta-Kaim, A., Fijal, K., Budziszewska, B., Regulska, M., Leskiewicz, M., Kubera, M., Golembiowska, K., Lason, W., & Wedzony, K. (2011). Prenatal lipopolysaccharide treatment enhances MK-801-induced psychotomimetic effects in rats. *Pharmacol Biochem Behav*, *98*(2), 241-249. https://doi.org/10.1016/j.pbb.2010.12.026

Benjamin, D., Lal, H., & Meyerson, L. R. (1990). The effects of 5-HT1B characterizing agents in the mouse elevated plus-maze. *Life Sci*, *47*(3), 195-203. https://doi.org/10.1016/0024-3205(90)90320-q

Binion, D. G., & Rafiee, P. (2009). Is inflammatory bowel disease a vascular disease? Targeting angiogenesis improves chronic inflammation in inflammatory bowel disease. *Gastroenterology*, *136*(2), 400-403. https://doi.org/10.1053/j.gastro.2008.12.029

Bitanihirwe, B. K., Peleg-Raibstein, D., Mouttet, F., Feldon, J., & Meyer, U. (2010). Late prenatal immune activation in mice leads to behavioral and neurochemical abnormalities relevant to the negative symptoms of schizophrenia. *Neuropsychopharmacology*, *35*, 2462-2478. https://doi.org/10.1038/npp.2010.129

Bitanihirwe, B. K., & Woo, T. U. (2011). Oxidative stress in schizophrenia: an integrated approach. *Neurosci Biobehav Rev*, *35*(3), 878-893. https://doi.org/10.1016/j.neubiorev.2010.10.008

Block, M. L., & Calderón-Garcidueñas, L. (2009). Air pollution: mechanisms of neuroinflammation and CNS disease. In *Trends in Neurosciences* (Vol. 32, pp. 506-516).

Boksa, P. (2010). Effects of prenatal infection on brain development and behavior: A review of findings from animal models. In *Brain, Behavior, and Immunity* (Vol. 24, pp. 881-897).

Bouton, M. E. (1993). Context, time, and memory retrieval in the interference paradigms of Pavlovian learning. *Psychol Bull*, *114*(1), 80-99. https://doi.org/10.1037/0033-2909.114.1.80

Braff, D. L., & Geyer, M. A. (1990). Sensorimotor gating and schizophrenia. Human and animal model studies. *Arch Gen Psychiatry*, *47*(2), 181-188. https://doi.org/10.1001/archpsyc.1990.01810140081011

Braff, D. L., Geyer, M. A., Light, G. A., Sprock, J., Perry, W., Cadenhead, K. S., & Swerdlow, N. R. (2001). Impact of prepulse characteristics on the detection of sensorimotor gating deficits in schizophrenia. *Schizophr Res*, *49*(1-2), 171-178. https://doi.org/10.1016/s0920-9964(00)00139-0

Braff, D. L., Geyer, M. A., & Swerdlow, N. R. (2001). Human studies of prepulse

inhibition of startle: normal subjects, patient groups, and pharmacological studies. *Psychopharmacology (Berl)*, *156*(2-3), 234-258. https://doi.org/10.1007/s002130100810

Braff, D. L., Grillon, C., & Geyer, M. A. (1992). Gating and habituation of the startle reflex in schizophrenic patients. *Arch Gen Psychiatry*, *49*(3), 206-215. https://doi.org/10.1001/archpsyc.1992.01820030038005

Bronson, S. L., Ahlbrand, R., Horn, P. S., Kern, J. R., & Richtand, N. M. (2011). Individual differences in maternal response to immune challenge predict offspring behavior: Contribution of environmental factors. *Behavioural Brain Research*, *220*, 55-64. https://doi.org/10.1016/j.bbr.2010.12.040

Bronson, S. L., & Bale, T. L. (2014). Prenatal stress-induced increases in placental inflammation and offspring hyperactivity are male-specific and ameliorated by maternal antiinflammatory treatment. *Endocrinology*, *155*, 2635-2646. https://doi.org/10.1210/en.2014-1040

Brown, A. S., & Meyer, U. (2018). Maternal immune activation and neuropsychiatric illness: A translational research perspective. In *American Journal of Psychiatry* (Vol. 175, pp. 1073-1083): American Psychiatric Association.

Bucknor, M. C., Gururajan, A., Dale, R. C., & Hofer, M. J. (2022). A comprehensive approach to modeling maternal immune activation in rodents. *Front Neurosci*, *16*, 1071976. https://doi.org/10.3389/fnins.2022.1071976

Burnette, C. P., Mundy, P. C., Meyer, J. A., Sutton, S. K., Vaughan, A. E., & Charak, D. (2005). Weak central coherence and its relations to theory of mind and anxiety in autism. *J Autism Dev Disord*, *35*(1), 63-73. https://doi.org/10.1007/s10803-004-1035-5

Cario, E. (2010). Toll-like receptors in inflammatory bowel diseases: a decade later. *Inflamm Bowel Dis*, *16*(9), 1583-1597. https://doi.org/10.1002/ibd.21282

Castellanos, F. X., Fine, E. J., Kaysen, D., Marsh, W. L., Rapoport, J. L., & Hallett, M. (1996). Sensorimotor gating in boys with Tourette's syndrome and ADHD: Preliminary results. *Biological Psychiatry*, *39*, 33-41. https://doi.org/10.1016/0006-3223(95)00101-8

Chassaing, B., Aitken, J. D., Malleshappa, M., & Vijay-Kumar, M. (2014). Dextran sulfate sodium (DSS)-induced colitis in mice. *Curr Protoc Immunol*, *104*, 15 25 11-15 25 14. https://doi.org/10.1002/0471142735.im1525s104

Chen, W. J., Maier, S. E., Parnell, S. E., & West, J. R. (2003). Alcohol and the developing brain: neuroanatomical studies. *Alcohol Res Health*, *27*(2), 174-180. https://www.ncbi.nlm.nih.gov/pubmed/15303628

Chen, X., Xiang, X., Xia, W., Li, X., Wang, S., Ye, S., Tian, L., Zhao, L., Ai, F., Shen,

Z., Nie, K., Deng, M., & Wang, X. (2023). Evolving Trends and Burden of Inflammatory Bowel Disease in Asia, 1990-2019: A Comprehensive Analysis Based on the Global Burden of Disease Study. *J Epidemiol Glob Health*, *13*(4), 725-739. https://doi.org/10.1007/s44197-023-00145-w

Cheung, K. K., Yeung, S. S., Au, S. W., Lam, L. S., Dai, Z. Q., Li, Y. H., & Yeung, E. W. (2011). Expression and association of TRPC1 with TRPC3 during skeletal myogenesis. *Muscle Nerve*, *44*(3), 358-365. https://doi.org/10.1002/mus.22060

Clancy, B., Darlington, R. B., & Finlay, B. L. (2001). Translating developmental time across mammalian species. *Neuroscience*, *105*, 7-17. https://doi.org/10.1016/S0306-4522(01)00171-3

Clancy, B., Finlay, B. L., Darlington, R. B., & Anand, K. J. S. (2007). Extrapolating brain development from experimental species to humans. *NeuroToxicology*, *28*, 931-937. https://doi.org/10.1016/j.neuro.2007.01.014

Coccia, M., Harrison, O. J., Schiering, C., Asquith, M. J., Becher, B., Powrie, F., & Maloy, K. J. (2012). IL-1beta mediates chronic intestinal inflammation by promoting the accumulation of IL-17A secreting innate lymphoid cells and CD4(+) Th17 cells. *J Exp Med*, *209*(9), 1595-1609. https://doi.org/10.1084/jem.20111453

Coleman, M. J., Cook, S., Matthysse, S., Barnard, J., Lo, Y., Levy, D. L., Rubin, D. B., & Holzman, P. S. (2002). Spatial and object working memory impairments in schizophrenia patients: a Bayesian item-response theory analysis. *J Abnorm Psychol*, *111*(3), 425-435. https://doi.org/10.1037//0021-843x.111.3.425

Cooper, H. S., Murthy, S. N., Shah, R. S., & Sedergran, D. J. (1993). Clinicopathologic study of dextran sulfate sodium experimental murine colitis. *Lab Invest*, *69*(2), 238-249. https://www.ncbi.nlm.nih.gov/pubmed/8350599

Cornish, J., Tan, E., Teare, J., Teoh, T. G., Rai, R., Clark, S. K., & Tekkis, P. P. (2007). A meta-analysis on the influence of inflammatory bowel disease on pregnancy. *Gut*, *56*(6), 830-837. https://doi.org/10.1136/gut.2006.108324

Coyle, P., Cowley, C., & Rofe, A. (2011). 15. Zinc in Pregnancy. In *Zinc in human health* (pp. 305-324). IOS Press.

Crespi, B., & Badcock, C. (2008). Psychosis and autism as diametrical disorders of the social brain. *Behav Brain Sci*, *31*(3), 241-261; discussion 261-320. https://doi.org/10.1017/S0140525X08004214

Cunha, C., Angelucci, A., D'Antoni, A., Dobrossy, M. D., Dunnett, S. B., Berardi, N., & Brambilla, R. (2009). Brain-derived neurotrophic factor (BDNF) overexpression in the forebrain results in learning and memory impairments. *Neurobiology of Disease*, *33*, 358-368.

https://doi.org/10.1016/j.nbd.2008.11.004

Cunningham, C., Campion, S., Teeling, J., Felton, L., & Perry, V. H. (2007). The sickness behaviour and CNS inflammatory mediator profile induced by systemic challenge of mice with synthetic double-stranded RNA (poly I:C). *Brain, Behavior, and Immunity*, *21*, 490-502. https://doi.org/10.1016/j.bbi.2006.12.007

Dai, H., & Carey, R. J. (1994). The NMDA antagonist MK-801 can impair attention to exteroceptive stimuli. *Behav Brain Res*, *62*(2), 149-156. https://doi.org/10.1016/0166-4328(94)90022-1

Depino, A. M. (2015). Early prenatal exposure to LPS results in anxiety- and depression-related behaviors in adulthood. *Neuroscience*, *299*, 56-65. https://doi.org/10.1016/j.neuroscience.2015.04.065

Der-Avakian, A., & Markou, A. (2012). The neurobiology of anhedonia and other reward-related deficits. *Trends Neurosci*, *35*(1), 68-77. https://doi.org/10.1016/j.tins.2011.11.005

DeRosa, H., Caradonna, S. G., Tran, H., Marrocco, J., & Kentner, A. C. (2022). Got milk? Maternal immune activation during the mid-lactational period affects nutritional milk quality and adolescent offspring sensory processing in male and female rats. *Mol Psychiatry*, *27*(12), 4829-4842. https://doi.org/10.1038/s41380-022-01744-y

Deverman, B. E., & Patterson, P. H. (2009). Cytokines and CNS development. *Neuron*, *64*(1), 61-78. https://doi.org/10.1016/j.neuron.2009.09.002

Dieleman, L. A., Elson, C. O., Tennyson, G. S., & Beagley, K. W. (1996). Kinetics of cytokine expression during healing of acute colitis in mice. *American Journal of Physiology - Gastrointestinal and Liver Physiology*, *271*. https://doi.org/10.1152/ajpgi.1996.271.1.g130

Dotan, I., Alper, A., Rachmilewitz, D., Israeli, E., Odes, S., Chermesh, I., Naftali, T., Fraser, G., Shitrit, A. B., Peles, V., & Reif, S. (2013). Maternal inflammatory bowel disease has short and long-term effects on the health of their offspring: a multicenter study in Israel. *J Crohns Colitis*, *7*(7), 542-550. https://doi.org/10.1016/j.crohns.2012.08.012

Dudchenko, P. A. (2004). An overview of the tasks used to test working memory in rodents. Neuroscience and Biobehavioral Reviews,

Edgin, J. O., & Pennington, B. F. (2005). Spatial cognition in autism spectrum disorders: superior, impaired, or just intact? *J Autism Dev Disord*, *35*(6), 729-745. https://doi.org/10.1007/s10803-005-0020-y

Egger, B., Bajaj-Elliott, M., Macdonald, T. T., Inglin, R., Eysselein, V. E., & Büchler,

M. W. (2000). Characterisation of acute murine dextran sodium sulphate colitis: Cytokine profile and dose dependency. *Digestion*, *62*, 240-248. https://doi.org/10.1159/000007822

Eichele, D. D., & Kharbanda, K. K. (2017). Dextran sodium sulfate colitis murine model: An indispensable tool for advancing our understanding of inflammatory bowel diseases pathogenesis. *World J Gastroenterol*, *23*(33), 6016-6029. https://doi.org/10.3748/wjg.v23.i33.6016

Ennaceur, A., & Delacour, J. (1988). A new one-trial test for neurobiological studies of memory in rats. 1: Behavioral data. *Behav Brain Res*, *31*(1), 47-59. https://doi.org/10.1016/0166-4328(88)90157-x

Eranti, S. V., MacCabe, J. H., Bundy, H., & Murray, R. M. (2013). Gender difference in age at onset of schizophrenia: a meta-analysis. *Psychol Med*, *43*(1), 155-167. https://doi.org/10.1017/S003329171200089X

Escobar, M., Oberling, P., & Miller, R. R. (2002). Associative deficit accounts of disrupted latent inhibition and blocking in schizophrenia. *Neurosci Biobehav Rev*, *26*(2), 203-216. https://doi.org/10.1016/s0149-7634(01)00067-7

Estes, M. L., & McAllister, A. K. (2015). Immune mediators in the brain and peripheral tissues in autism spectrum disorder. *Nat Rev Neurosci*, *16*(8), 469-486. https://doi.org/10.1038/nrn3978

Estes, M. L., & McAllister, A. K. (2016). Maternal immune activation: Implications for neuropsychiatric disorders. In *Science* (Vol. 353, pp. 772-777): American Association for the Advancement of Science.

Falter, U., Gower, A. J., & Gobert, J. (1992). Resistance of baseline activity in the elevated plus-maze to exogenous influences. *Behav Pharmacol*, *3*(2), 123-128. https://www.ncbi.nlm.nih.gov/pubmed/11224109

Fankhauser, C., Friedlander, R. M., & Gagliardini, V. (2000). Prevention of nuclear localization of activated caspases correlates with inhibition of apoptosis. *Apoptosis*, *5*(2), 117-132. https://doi.org/10.1023/a:1009672411058

Faraone, S. V., Chen, W. J., Goldstein, J. M., & Tsuang, M. T. (1994). Gender differences in age at onset of schizophrenia. *Br J Psychiatry*, *164*(5), 625-629. https://doi.org/10.1192/bjp.164.5.625

Fernandez de Cossio, L., Guzman, A., van der Veldt, S., & Luheshi, G. N. (2017). Prenatal infection leads to ASD-like behavior and altered synaptic pruning in the mouse offspring. *Brain Behav Immun*, *63*, 88-98. https://doi.org/10.1016/j.bbi.2016.09.028

File, S. E., & Hyde, J. R. (1978). Can social interaction be used to measure anxiety? *Br J Pharmacol*, *62*(1), 19-24. https://doi.org/10.1111/j.1476-5381.1978.tb07001.x

Fineberg, A. M., Ellman, L. M., Schaefer, C. A., Maxwell, S. D., Shen, L., Chaudhury, N. H., Cook, A. L., Bresnahan, M. A., Susser, E. S., & Brown, A. S. (2016). Fetal exposure to maternal stress and risk for schizophrenia spectrum disorders among offspring: Differential influences of fetal sex. *Psychiatry Research*, *236*, 91-97. https://doi.org/10.1016/j.psychres.2015.12.026

Franklin, K. B. J., & Paxinos, G. (2008). *The mouse brain in stereotaxic coordinates* (3rd compact ed.). London : Elsevier/Academic Press. http://bvbr.bib-bvb.de:8991/F?func=service&doc_library=BVB01&doc_number=016372855&line_number=0001&func_code=DB_RECORDS&service_type=MEDIA

Fuss, I. J., Heller, F., Boirivant, M., Leon, F., Yoshida, M., Fichtner-Feigl, S., Yang, Z., Exley, M., Kitani, A., Blumberg, R. S., Mannon, P., & Strober, W. (2004). Nonclassical CD1d-restricted NK T cells that produce IL-13 characterize an atypical Th2 response in ulcerative colitis. *Journal of Clinical Investigation*, *113*, 1490-1497. https://doi.org/10.1172/JCI19836

Gabrovska, V. S., Laws, K. R., Sinclair, J., & McKenna, P. J. (2003). Visual object processing in schizophrenia: evidence for an associative agnosic deficit. *Schizophr Res*, *59*(2-3), 277-286. https://doi.org/10.1016/s0920-9964(02)00168-8

Gaisler-Salomon, I., Diamant, L., Rubin, C., & Weiner, I. (2008). Abnormally persistent latent inhibition induced by MK801 is reversed by risperidone and by positive modulators of NMDA receptor function: differential efficacy depending on the stage of the task at which they are administered. *Psychopharmacology (Berl)*, *196*(2), 255-267. https://doi.org/10.1007/s00213-007-0960-3

Gaisler-Salomon, I., & Weiner, I. (2003). Systemic administration of MK-801 produces an abnormally persistent latent inhibition which is reversed by clozapine but not haloperidol. *Psychopharmacology (Berl)*, *166*(4), 333-342. https://doi.org/10.1007/s00213-002-1311-z

Gayle, D. A., Beloosesky, R., Desai, M., Amidi, F., Nuñez, S. E., & Ross, M. G. (2004). Maternal LPS induces cytokines in the amniotic fluid and corticotropin releasing hormone in the fetal rat brain. *American Journal of Physiology - Regulatory Integrative and Comparative Physiology*, *286*. https://doi.org/10.1152/ajpregu.00664.2003

Geyer, M. A. (2006). Are cross-species measures of sensorimotor gating useful for the discovery of procognitive cotreatments for schizophrenia? *Dialogues in Clinical Neuroscience*, *8*, 9-16. https://doi.org/10.31887/dcns.2006.8.1/mgeyer

Geyer, M. A., & Swerdlow, N. R. (2001). Measurement of startle response, prepulse inhibition, and habituation. *Curr Protoc Neurosci*, *Chapter 8*, Unit 8 7.

https://doi.org/10.1002/0471142301.ns0807s03

Gibson, D. L., Montero, M., Ropeleski, M. J., Bergstrom, K. S., Ma, C., Ghosh, S., Merkens, H., Huang, J., Mansson, L. E., Sham, H. P., McNagny, K. M., & Vallance, B. A. (2010). Interleukin-11 reduces TLR4-induced colitis in TLR2-deficient mice and restores intestinal STAT3 signaling. *Gastroenterology*, *139*(4), 1277-1288. https://doi.org/10.1053/j.gastro.2010.06.057

Gilmore, J. H., Fredrik Jarskog, L., Vadlamudi, S., & Lauder, J. M. (2004). Prenatal infection and risk for schizophrenia: IL-1beta, IL-6, and TNFalpha inhibit cortical neuron dendrite development. *Neuropsychopharmacology*, *29*(7), 1221-1229. https://doi.org/10.1038/sj.npp.1300446

Gilmore, J. H., & Jarskog, L. F. (1997). Exposure to infection and brain development: cytokines in the pathogenesis of schizophrenia. *Schizophr Res*, *24*(3), 365-367. https://doi.org/10.1016/s0920-9964(96)00123-5

Giovanoli, S., Notter, T., Richetto, J., Labouesse, M. A., Vuillermot, S., Riva, M. A., & Meyer, U. (2015). Late prenatal immune activation causes hippocampal deficits in the absence of persistent inflammation across aging. *J Neuroinflammation*, *12*, 221. https://doi.org/10.1186/s12974-015-0437-y

Glass, R., Norton, S., Fox, N., & Kusnecov, A. W. (2019). Maternal immune activation with staphylococcal enterotoxin A produces unique behavioral changes in C57BL/6 mouse offspring. *Brain, Behavior, and Immunity*, *75*, 12-25. https://doi.org/10.1016/j.bbi.2018.05.005

Glausier, J. R., & Lewis, D. A. (2013). Dendritic spine pathology in schizophrenia. *Neuroscience*, *251*, 90-107. https://doi.org/10.1016/j.neuroscience.2012.04.044

Goldstein, J. M., Cherkerzian, S., Tsuang, M. T., & Petryshen, T. L. (2013). Sex differences in the genetic risk for schizophrenia: history of the evidence for sex-specific and sex-dependent effects. *Am J Med Genet B Neuropsychiatr Genet*, *162B*(7), 698-710. https://doi.org/10.1002/ajmg.b.32159

Golia, M. T., Poggini, S., Alboni, S., Garofalo, S., Ciano Albanese, N., Viglione, A., Ajmone-Cat, M. A., St-Pierre, A., Brunello, N., Limatola, C., Branchi, I., & Maggi, L. (2019). Interplay between inflammation and neural plasticity: Both immune activation and suppression impair LTP and BDNF expression. *Brain Behav Immun*, *81*, 484-494. https://doi.org/10.1016/j.bbi.2019.07.003

Gottesman, II, & Gould, T. D. (2003). The endophenotype concept in psychiatry: etymology and strategic intentions. *Am J Psychiatry*, *160*(4), 636-645. https://doi.org/10.1176/appi.ajp.160.4.636

Goyal, N., Rana, A., Ahlawat, A., Bijjem, K. R. V., & Kumar, P. (2014). Animal models of inflammatory bowel disease: A review. In *Inflammopharmacology* (Vol. 22,

pp. 219-233): Birkhauser Verlag AG.

Graham, F. K. (1975). Presidential Address, 1974. The more or less startling effects of weak prestimulation. *Psychophysiology*, *12*(3), 238-248. https://doi.org/10.1111/j.1469-8986.1975.tb01284.x

Grahame, N. J., Barnet, R. C., Gunther, L. M., & Miller, R. R. (1994). *Latent inhibition as a performance deficit resulting from CS-context associations* [doi:10.3758/BF03209159].

Gray, J. A., Feldon, J., Rawlins, J. N. P., Hemsley, D. R., & Smith, A. D. (1991). The neuropsychology of schizophrenia. *Behavioral and Brain Sciences*, *14*, 1-20. https://doi.org/10.1017/s0140525x00065055

Gray, J. A., Joseph, M. H., Hemsley, D. R., Young, A. M. J., Clea Warburton, E., Boulenguez, P., Grigoryan, G. A., Peters, S. L., Rawlins, J. N. P., Taib, C. T., Yee, B. K., Cassaday, H., Weiner, I., Gal, G., Gusak, O., Joel, D., Shadach, E., Shalev, U., Tarrasch, R., & Feldon, J. (1995). The role of mesolimbic dopaminergic and retrohippocampal afferents to the nucleus accumbens in latent inhibition: implications for schizophrenia. *Behavioural Brain Research*, *71*. https://doi.org/10.1016/0166-4328(95)00154-9

Gray, N. (1992). Abolition of latent inhibition in acute, but not chronic, schizophrenics. *Neurology, Psychiatry and Brain Research*, *1*.

Gray, N. S., Pickering, A. D., Hemsley, D. R., Dawling, S., & Gray, J. A. (1992). Abolition of latent inhibition by a single 5 mg dose of d-amphetamine in man. *Psychopharmacology*, *107*, 425-430. https://doi.org/10.1007/BF02245170

Grayson, B., Idris, N. F., & Neill, J. C. (2007). Atypical antipsychotics attenuate a sub-chronic PCP-induced cognitive deficit in the novel object recognition task in the rat. *Behav Brain Res*, *184*(1), 31-38. https://doi.org/10.1016/j.bbr.2007.06.012

Griebel, G., Moreau, J. L., Jenck, F., Martin, J. R., & Misslin, R. (1993). Some critical determinants of the behaviour of rats in the elevated plus-maze. *Behav Processes*, *29*(1-2), 37-47. https://doi.org/10.1016/0376-6357(93)90026-N

Grillon, C., Morgan, C. A., Southwick, S. M., Davis, M., & Charney, D. S. (1996). Baseline startle amplitude and prepulse inhibition in Vietnam veterans with posttraumatic stress disorder. *Psychiatry Res*, *64*(3), 169-178. https://doi.org/10.1016/s0165-1781(96)02942-3

Guerri, C., Bazinet, A., & Riley, E. P. (2009). Foetal alcohol spectrum disorders and alterations in brain and behaviour. In *Alcohol and Alcoholism* (Vol. 44, pp. 108-114).

Haddad, F. L., Patel, S. V., & Schmid, S. (2020). Maternal Immune Activation by Poly

I:C as a preclinical Model for Neurodevelopmental Disorders: A focus on Autism and Schizophrenia. *Neurosci Biobehav Rev*, *113*, 546-567. https://doi.org/10.1016/j.neubiorev.2020.04.012

Hagenbuch, N., Feldon, J., & Yee, B. K. (2006). Use of the elevated plus-maze test with opaque or transparent walls in the detection of mouse strain differences and the anxiolytic effects of diazepam. *Behav Pharmacol*, *17*(1), 31-41. https://doi.org/10.1097/01.fbp.0000189811.77049.3e

Hakansson, A., Tormo-Badia, N., Baridi, A., Xu, J., Molin, G., Hagslatt, M. L., Karlsson, C., Jeppsson, B., Cilio, C. M., & Ahrne, S. (2015). Immunological alteration and changes of gut microbiota after dextran sulfate sodium (DSS) administration in mice. *Clin Exp Med*, *15*(1), 107-120. https://doi.org/10.1007/s10238-013-0270-5

Hall, J. (2017). Schizophrenia - an anxiety disorder? *Br J Psychiatry*, *211*(5), 262-263. https://doi.org/10.1192/bjp.bp.116.195370

Handley, S. L., & Mithani, S. (1984). Effects of alpha-adrenoceptor agonists and antagonists in a maze-exploration model of 'fear'-motivated behaviour. *Naunyn Schmiedebergs Arch Pharmacol*, *327*(1), 1-5. https://doi.org/10.1007/BF00504983

Hashash, J. G., & Kane, S. (2015). Pregnancy and Inflammatory Bowel Disease. *Gastroenterol Hepatol (N Y)*, *11*(2), 96-102. https://www.ncbi.nlm.nih.gov/pubmed/27099578

Hawes, J. E., Tesic, D., Whitehouse, A. J., Zosky, G. R., Smith, J. T., & Wyrwoll, C. S. (2015). Maternal vitamin D deficiency alters fetal brain development in the BALB/c mouse. *Behavioural Brain Research*, *286*, 192-200. https://doi.org/10.1016/j.bbr.2015.03.008

Heller, F., Fuss, I. J., Nieuwenhuis, E. E., Blumberg, R. S., & Strober, W. (2002). Oxazolone colitis, a Th2 colitis model resembling ulcerative colitis, is mediated by IL-13-producing NK-T cells. *Immunity*, *17*, 629-638. https://doi.org/10.1016/S1074-7613(02)00453-3

Hodges, H., Sowinski, P., Fleming, P., Kershaw, T. R., Sinden, J. D., Meldrum, B. S., & Gray, J. A. (1996). Contrasting effects of fetal CA1 and CA3 hippocampal grafts on deficits in spatial learning and working memory induced by global cerebral ischaemia in rats. *Neuroscience*, *72*(4), 959-988. https://doi.org/10.1016/0306-4522(96)00004-8

Hoffman, H. S., & Searle, J. L. (1965). Acoustic Variables in the Modification of Startle Reaction in the Rat. *J Comp Physiol Psychol*, *60*, 53-58. https://doi.org/10.1037/h0022325

Horan, W. P., Kring, A. M., & Blanchard, J. J. (2006). Anhedonia in schizophrenia: a review of assessment strategies. *Schizophr Bull*, *32*(2), 259-273. https://doi.org/10.1093/schbul/sbj009

Howland, J. G., Cazakoff, B. N., & Zhang, Y. (2012). Altered object-in-place recognition memory, prepulse inhibition, and locomotor activity in the offspring of rats exposed to a viral mimetic during pregnancy. *Neuroscience*, *201*, 184-198. https://doi.org/10.1016/j.neuroscience.2011.11.011

Hsiao, E. Y., & Patterson, P. H. (2011). Activation of the maternal immune system induces endocrine changes in the placenta via IL-6. *Brain Behav Immun*, *25*(4), 604-615. https://doi.org/10.1016/j.bbi.2010.12.017

Imai, K., Kotani, T., Tsuda, H., Nakano, T., Ushida, T., Iwase, A., Nagai, T., Toyokuni, S., Suzumura, A., & Kikkawa, F. (2018). Administration of molecular hydrogen during pregnancy improves behavioral abnormalities of offspring in a maternal immune activation model. *Sci Rep*, *8*(1), 9221. https://doi.org/10.1038/s41598-018-27626-4

Inoue, K. I., Takano, H., Yanagisawa, R., Hirano, S., Kobayashi, T., Ichinose, T., & Yoshikawa, T. (2006). Effects of organic chemicals derived from ambient particulate matter on lung inflammation related to lipopolysaccharide. *Archives of Toxicology*, *80*, 833-838. https://doi.org/10.1007/s00204-006-0105-1

Jarskog, L. F., Xiao, H., Wilkie, M. B., Lauder, J. M., & Gilmore, J. H. (1997). Cytokine regulation of embryonic rat dopamine and serotonin neuronal survival in vitro. *Int J Dev Neurosci*, *15*(6), 711-716. https://doi.org/10.1016/s0736-5748(97)00029-4

Jasarevic, E., Howerton, C. L., Howard, C. D., & Bale, T. L. (2015). Alterations in the Vaginal Microbiome by Maternal Stress Are Associated With Metabolic Reprogramming of the Offspring Gut and Brain. *Endocrinology*, *156*(9), 3265-3276. https://doi.org/10.1210/en.2015-1177

Jasarevic, E., Rodgers, A. B., & Bale, T. L. (2015). A novel role for maternal stress and microbial transmission in early life programming and neurodevelopment. *Neurobiol Stress*, *1*, 81-88. https://doi.org/10.1016/j.ynstr.2014.10.005

Jolving, L. R., Nielsen, J., Beck-Nielsen, S. S., Nielsen, R. G., Friedman, S., Kesmodel, U. S., & Norgard, B. M. (2017). The Association Between Maternal Chronic Inflammatory Bowel Disease and Long-term Health Outcomes in Children-A Nationwide Cohort Study. *Inflamm Bowel Dis*, *23*(8), 1440-1446. https://doi.org/10.1097/MIB.0000000000001146

Kahn, R., van der Doef, T., & van Berckel, B. (2015). Inflammation in the Brain of Early Onset Schizophrenia: An in-Vivo Study. *Schizophrenia Bulletin*, *41*,

S259-S259. <Go to ISI>://WOS:000353548200683

Kappelman, M. D., Moore, K. R., Allen, J. K., & Cook, S. F. (2013). Recent trends in the prevalence of Crohn's disease and ulcerative colitis in a commercially insured US population. *Dig Dis Sci*, *58*(2), 519-525. https://doi.org/10.1007/s10620-012-2371-5

Karasawa, J., Hashimoto, K., & Chaki, S. (2008). D-Serine and a glycine transporter inhibitor improve MK-801-induced cognitive deficits in a novel object recognition test in rats. *Behav Brain Res*, *186*(1), 78-83. https://doi.org/10.1016/j.bbr.2007.07.033

Kentner, A. C., Bilbo, S. D., Brown, A. S., Hsiao, E. Y., McAllister, A. K., Meyer, U., Pearce, B. D., Pletnikov, M. V., Yolken, R. H., & Bauman, M. D. (2019). Maternal immune activation: reporting guidelines to improve the rigor, reproducibility, and transparency of the model. In *Neuropsychopharmacology* (Vol. 44, pp. 245-258): Nature Publishing Group.

Khan, D., Fernando, P., Cicvaric, A., Berger, A., Pollak, A., Monje, F. J., & Pollak, D. D. (2014). Long-term effects of maternal immune activation on depression-like behavior in the mouse. *Transl Psychiatry*, *4*(2), e363. https://doi.org/10.1038/tp.2013.132

Khatri, V., & Kalyanasundaram, R. (2021). Therapeutic implications of inflammasome in inflammatory bowel disease. In *FASEB Journal* (Vol. 35): John Wiley and Sons Inc.

Kiesler, P., Fuss, I. J., & Strober, W. (2015). Experimental Models of Inflammatory Bowel Diseases. *Cell Mol Gastroenterol Hepatol*, *1*(2), 154-170. https://doi.org/10.1016/j.jcmgh.2015.01.006

Kim, M. A., Kim, Y. H., Chun, J., Lee, H. S., Park, S. J., Cheon, J. H., Kim, T. I., Kim, W. H., & Park, J. J. (2021). The Influence of Disease Activity on Pregnancy Outcomes in Women With Inflammatory Bowel Disease: A Systematic Review and Meta-Analysis. *J Crohns Colitis*, *15*(5), 719-732. https://doi.org/10.1093/ecco-jcc/jjaa225

Kitajima, S., Takuma, S., & Morimoto, M. (1999). Tissue Distribution of Dextran Sulfate Sodium (DSS) in the Acute Phase of Murine DSS-Induced Colitis. *Journal of Veterinary Medical Science*, *61*, 67-70. https://doi.org/10.1292/jvms.61.67

Kong, L., Chen, X., Gissler, M., & Lavebratt, C. (2020). Relationship of prenatal maternal obesity and diabetes to offspring neurodevelopmental and psychiatric disorders: a narrative review. *Int J Obes (Lond)*, *44*(10), 1981-2000. https://doi.org/10.1038/s41366-020-0609-4

Koslowsky, B., Grisaru-Granovsky, S., Livovsky, D. M., Milgrom, Y., Goldin, E., & Bar-Gil Shitrit, A. (2018). Pregnancy-Onset Inflammatory Bowel Disease: A Subtle Diagnosis. *Inflamm Bowel Dis*, *24*(8), 1826-1832. https://doi.org/10.1093/ibd/izy081

Kovacs, C. S. (2013). Maternal vitamin D deficiency: Fetal and neonatal implications. *Semin Fetal Neonatal Med*, *18*(3), 129-135. https://doi.org/10.1016/j.siny.2013.01.005

Kraemer, P. J., & Spear, N. E. (1992). The effect of nonreinforced stimulus exposure on the strength of a conditioned taste aversion as a function of retention interval: Do latent inhibition and extinction involve a shared process? *Animal Learning & Behavior*, *20*(1), 1-7. https://doi.org/10.3758/BF03199940

Krystal, J. H., D'Souza, D. C., Mathalon, D., Perry, E., Belger, A., & Hoffman, R. (2003). NMDA receptor antagonist effects, cortical glutamatergic function, and schizophrenia: toward a paradigm shift in medication development. *Psychopharmacology (Berl)*, *169*(3-4), 215-233. https://doi.org/10.1007/s00213-003-1582-z

Kwon, H. K., Choi, G. B., & Huh, J. R. (2022). Maternal inflammation and its ramifications on fetal neurodevelopment. *Trends Immunol*, *43*(3), 230-244. https://doi.org/10.1016/j.it.2022.01.007

Lalonde, R. (2002). The neurobiological basis of spontaneous alternation. *Neurosci Biobehav Rev*, *26*(1), 91-104. https://doi.org/10.1016/s0149-7634(01)00041-0

Lante, F., Meunier, J., Guiramand, J., Maurice, T., Cavalier, M., de Jesus Ferreira, M. C., Aimar, R., Cohen-Solal, C., Vignes, M., & Barbanel, G. (2007). Neurodevelopmental damage after prenatal infection: role of oxidative stress in the fetal brain. *Free Radic Biol Med*, *42*(8), 1231-1245. https://doi.org/10.1016/j.freeradbiomed.2007.01.027

Laube, B., Kuhse, J., & Betz, H. (1998). Evidence for a tetrameric structure of recombinant NMDA receptors. *The Journal of neuroscience : the official journal of the Society for Neuroscience*, *18*(8), 2954–2961. https://doi.org/10.1523/JNEUROSCI.18-08-02954.1998

Lee, C. H., Koh, S. J., Radi, Z. A., & Habtezion, A. (2023). Animal models of inflammatory bowel disease: novel experiments for revealing pathogenesis of colitis, fibrosis, and colitis-associated colon cancer. In *Intestinal Research* (Vol. 21, pp. 295-305): Korean Association for the Study of Intestinal Diseases.

Levin, A., & Shibolet, O. (2008). Toll-like receptors in inflammatory bowel disease-stepping into uncharted territory. *World J Gastroenterol*, *14*(33), 5149-5153. https://doi.org/10.3748/wjg.14.5149

Li, M., Wu, Y., Hu, Y., Zhao, L., & Zhang, C. (2018). Initial gut microbiota structure affects sensitivity to DSS-induced colitis in a mouse model. *Sci China Life Sci*, *61*(7), 762-769. https://doi.org/10.1007/s11427-017-9097-0

Lieberman, J. A., Girgis, R. R., Brucato, G., Moore, H., Provenzano, F., Kegeles, L., Javitt, D., Kantrowitz, J., Wall, M. M., Corcoran, C. M., Schobel, S. A., & Small, S. A. (2018). Hippocampal dysfunction in the pathophysiology of schizophrenia: a selective review and hypothesis for early detection and intervention. *Molecular Psychiatry*, *23*(8), 1764-1772. https://doi.org/10.1038/mp.2017.249

Liljequist, S., Ossowska, K., Grabowska-Anden, M., & Anden, N. E. (1991). Effect of the NMDA receptor antagonist, MK-801, on locomotor activity and on the metabolism of dopamine in various brain areas of mice. *Eur J Pharmacol*, *195*(1), 55-61. https://doi.org/10.1016/0014-2999(91)90381-y

Lipina, T. V., Zai, C., Hlousek, D., Roder, J. C., & Wong, A. H. C. (2013). Maternal immune activation during gestation interacts with Disc1 point mutation to exacerbate schizophrenia-related behaviors in mice. *Journal of Neuroscience*, *33*, 7654-7666. https://doi.org/10.1523/JNEUROSCI.0091-13.2013

Lister, R. G. (1987). The use of a plus-maze to measure anxiety in the mouse. *Psychopharmacology (Berl)*, *92*(2), 180-185. https://doi.org/10.1007/BF00177912

Liu, D., Saikam, V., Skrada, K. A., Merlin, D., & Iyer, S. S. (2022). Inflammatory bowel disease biomarkers. *Med Res Rev*, *42*(5), 1856-1887. https://doi.org/10.1002/med.21893

Livak, K. J., & Schmittgen, T. D. (2001). Analysis of relative gene expression data using real-time quantitative PCR and the 2(-Delta Delta C(T)) Method. *Methods*, *25*(4), 402-408. https://doi.org/10.1006/meth.2001.1262

Lu, Y., Li, X., Liu, S., Zhang, Y., & Zhang, D. (2018). Toll-like receptors and inflammatory bowel disease. In *Frontiers in Immunology* (Vol. 9): Frontiers Media S.A.

Lubow, R. E., & Gewirtz, J. C. (1995). Latent inhibition in humans: data, theory, and implications for schizophrenia. *Psychol Bull*, *117*(1), 87-103. https://doi.org/10.1037/0033-2909.117.1.87

Lubow, R. E., & Moore, A. U. (1959). Latent inhibition: the effect of nonreinforced pre-exposure to the conditional stimulus. *J Comp Physiol Psychol*, *52*, 415-419. https://doi.org/10.1037/h0046700

Lubow, R. E., Weiner, I., & Schnur, P. (1981). Conditioned Attention Theory11The preparation of this chapter was supported, in part, by a grant from the Israel National Academy of Sciences to the first author. In G. H. Bower (Ed.),

Psychology of Learning and Motivation (Vol. 15, pp. 1-49). Academic Press. https://doi.org/https://doi.org/10.1016/S0079-7421(08)60171-1

Ma, W., Miao, Z., & Novotny, M. V. (1998). Role of the adrenal gland and adrenal-mediated chemosignals in suppression of estrus in the house mouse: the lee-boot effect revisited. *Biol Reprod*, *59*(6), 1317-1320. https://doi.org/10.1095/biolreprod59.6.1317

Mackintosh, N. J. (1973). Stimulus selection: Learning to ignore stimuli that predict no change in reinforcement. Academic press,

Mackintosh, N. J. (1975). *A theory of attention: Variations in the associability of stimuli with reinforcement* [doi:10.1037/h0076778]. American Psychological Association.

Maeda, M., Watanabe, N., Neda, H., Yamauchi, N., Okamoto, T., Sasaki, H., Tsuji, Y., Akiyama, S., Tsuji, N., & Niitsu, Y. (1992). Serum tumor necrosis factor activity in inflammatory bowel disease. *Immunopharmacol Immunotoxicol*, *14*(3), 451-461. https://doi.org/10.3109/08923979209005404

Maelfait, J., Vercammen, E., Janssens, S., Schotte, P., Haegman, M., Magez, S., & Beyaert, R. (2008). Stimulation of Toll-like receptor 3 and 4 induces interleukin-1β maturation by caspase-8. *Journal of Experimental Medicine*, *205*, 1967-1973. https://doi.org/10.1084/jem.20071632

Marcus, R., & Watt, J. (1969). Seaweeds and ulcerative colitis in laboratory animals. *Lancet*, *294*, 489-490. https://doi.org/10.1016/s0140-6736(69)90187-1

Matsuura, M. (2013). Structural Modifications of Bacterial Lipopolysaccharide that Facilitate Gram-Negative Bacteria Evasion of Host Innate Immunity. *Front Immunol*, *4*, 109. https://doi.org/10.3389/fimmu.2013.00109

McAfoose, J., Koerner, H., & Baune, B. T. (2009). The effects of TNF deficiency on age-related cognitive performance. *Psychoneuroendocrinology*, *34*(4), 615-619. https://doi.org/10.1016/j.psyneuen.2008.10.006

McGlashan, T. H., & Hoffman, R. E. (2000). Schizophrenia as a disorder of developmentally reduced synaptic connectivity. *Arch Gen Psychiatry*, *57*(7), 637-648. https://doi.org/10.1001/archpsyc.57.7.637

McGrath, J. J., Eyles, D. W., Pedersen, C. B., Anderson, C., Ko, P., Burne, T. H., Norgaard-Pedersen, B., Hougaard, D. M., & Mortensen, P. B. (2010). Neonatal vitamin D status and risk of schizophrenia: a population-based case-control study. *Arch Gen Psychiatry*, *67*(9), 889-894. https://doi.org/10.1001/archgenpsychiatry.2010.110

McLaren, I. P. L., & Mackintosh, N. J. (2000). *An elemental model of associative learning: I. Latent inhibition and perceptual learning*

[doi:10.3758/BF03200258]. Psychonomic Society.

Mednick, S. A., Machon, R. A., Huttunen, M. O., & Bonett, D. (1988). Adult Schizophrenia Following Prenatal Exposure to an Influenza Epidemic. *Archives of General Psychiatry*, *45*, 189-192. https://doi.org/10.1001/archpsyc.1988.01800260109013

Meyer, Knuesel, I., Nyffeler, M., & Feldon, J. (2010). Chronic clozapine treatment improves prenatal infection-induced working memory deficits without influencing adult hippocampal neurogenesis. *Psychopharmacology*, *208*, 531-543. https://doi.org/10.1007/s00213-009-1754-6

Meyer, U. (2014). Prenatal poly(i:C) exposure and other developmental immune activation models in rodent systems. *Biol Psychiatry*, *75*(4), 307-315. https://doi.org/10.1016/j.biopsych.2013.07.011

Meyer, U. (2019). Neurodevelopmental Resilience and Susceptibility to Maternal Immune Activation. *Trends Neurosci*, *42*(11), 793-806. https://doi.org/10.1016/j.tins.2019.08.001

Meyer, U., Feldon, J., Schedlowski, M., & Yee, B. K. (2005). Towards an immuno-precipitated neurodevelopmental animal model of schizophrenia. *Neuroscience & Biobehavioral Reviews*, *29*(6), 913-947. https://doi.org/10.1016/j.neubiorev.2004.10.012

Meyer, U., Feldon, J., Schedlowski, M., & Yee, B. K. (2006). Immunological stress at the maternal-foetal interface: a link between neurodevelopment and adult psychopathology. *Brain Behav Immun*, *20*(4), 378-388. https://doi.org/10.1016/j.bbi.2005.11.003

Meyer, U., Feldon, J., & Yee, B. K. (2009). A review of the fetal brain cytokine imbalance hypothesis of schizophrenia. *Schizophr Bull*, *35*(5), 959-972. https://doi.org/10.1093/schbul/sbn022

Meyer, U., Murray, P. J., Urwyler, A., Yee, B. K., Schedlowski, M., & Feldon, J. (2008). Adult behavioral and pharmacological dysfunctions following disruption of the fetal brain balance between pro-inflammatory and IL-10-mediated anti-inflammatory signaling. *Molecular Psychiatry*, *13*, 208-221. https://doi.org/10.1038/sj.mp.4002042

Meyer, U., Nyffeler, M., Engler, A., Urwyler, A., Schedlowski, M., Knuesel, I., Yee, B. K., & Feldon, J. (2006). The time of prenatal immune challenge determines the specificity of inflammation-mediated brain and behavioral pathology. *J Neurosci*, *26*(18), 4752-4762. https://doi.org/10.1523/JNEUROSCI.0099-06.2006

Meyer, U., Nyffeler, M., Yee, B. K., Knuesel, I., & Feldon, J. (2008). Adult brain and

behavioral pathological markers of prenatal immune challenge during early/middle and late fetal development in mice. *Brain Behav Immun*, *22*(4), 469-486. https://doi.org/10.1016/j.bbi.2007.09.012

Miller, R. R., & Matzel, L. D. (1988). The Comparator Hypothesis: A Response Rule for The Expression of Associations. In G. H. Bower (Ed.), *Psychology of Learning and Motivation* (Vol. 22, pp. 51-92). Academic Press. https://doi.org/https://doi.org/10.1016/S0079-7421(08)60038-9

Missault, S., Van den Eynde, K., Vanden Berghe, W., Fransen, E., Weeren, A., Timmermans, J. P., Kumar-Singh, S., & Dedeurwaerdere, S. (2014). The risk for behavioural deficits is determined by the maternal immune response to prenatal immune challenge in a neurodevelopmental model. *Brain Behav Immun*, *42*, 138-146. https://doi.org/10.1016/j.bbi.2014.06.013

Missig, G., Robbins, J. O., Mokler, E. L., McCullough, K. M., Bilbo, S. D., McDougle, C. J., & Carlezon, W. A. (2020). Sex-dependent neurobiological features of prenatal immune activation via TLR7. *Molecular Psychiatry*, *25*, 2330-2341. https://doi.org/10.1038/s41380-018-0346-4

Mizoguchi, A. (2012). Animal models of inflammatory bowel disease. In *Progress in Molecular Biology and Translational Science* (Vol. 105, pp. 263-320). Elsevier B.V. https://doi.org/10.1016/B978-0-12-394596-9.00009-3

Montgomery, K. C. (1955). The relation between fear induced by novel stimulation and exploratory behavior. *J Comp Physiol Psychol*, *48*(4), 254-260. https://doi.org/10.1037/h0043788

Morais, L. H., Schreiber, H. L. t., & Mazmanian, S. K. (2021). The gut microbiota-brain axis in behaviour and brain disorders. *Nat Rev Microbiol*, *19*(4), 241-255. https://doi.org/10.1038/s41579-020-00460-0

Morato, S., & Castrechini, P. (1989). Effects of floor surface and environmental illumination on exploratory activity in the elevated plus-maze. *Braz J Med Biol Res*, *22*(6), 707-710. https://www.ncbi.nlm.nih.gov/pubmed/2620180

Morris, R. G., Hagan, J. J., & Rawlins, J. N. (1986). Allocentric spatial learning by hippocampectomised rats: a further test of the "spatial mapping" and "working memory" theories of hippocampal function. *Q J Exp Psychol B*, *38*(4), 365-395. https://www.ncbi.nlm.nih.gov/pubmed/3809580

Morris, R. G. M. (1981). Spatial localization does not require the presence of local cues. *Learning and Motivation*, *12*, 239-260. https://doi.org/10.1016/0023-9690(81)90020-5

Mueller, F. S., Scarborough, J., Schalbetter, S. M., Richetto, J., Kim, E., Couch, A., Yee, Y., Lerch, J. P., Vernon, A. C., Weber-Stadlbauer, U., & Meyer, U. (2021).

Behavioral, neuroanatomical, and molecular correlates of resilience and susceptibility to maternal immune activation. *Molecular Psychiatry*, *26*, 396-410. https://doi.org/10.1038/s41380-020-00952-8

Murch, S. H., Lamkin, V. A., Savage, M. O., Walker-Smith, J. A., & MacDonald, T. T. (1991). Serum concentrations of tumour necrosis factor alpha in childhood chronic inflammatory bowel disease. *Gut*, *32*(8), 913-917. https://doi.org/10.1136/gut.32.8.913

Nadler, J. J., Moy, S. S., Dold, G., Trang, D., Simmons, N., Perez, A., Young, N. B., Barbaro, R. P., Piven, J., Magnuson, T. R., & Crawley, J. N. (2004). Automated apparatus for quantitation of social approach behaviors in mice. *Genes, Brain and Behavior*, *3*, 303-314. https://doi.org/10.1111/j.1601-183X.2004.00071.x

Nakamura, J. P., Gillespie, B., Gibbons, A., Jaehne, E. J., Du, X., Chan, A., Schroeder, A., van den Buuse, M., Sundram, S., & Hill, R. A. (2021). Maternal immune activation targeted to a window of parvalbumin interneuron development improves spatial working memory: Implications for autism. *Brain Behav Immun*, *91*, 339-349. https://doi.org/10.1016/j.bbi.2020.10.012

Nielsen, O. H., Loftus, E. V., Jr., & Jess, T. (2013). Safety of TNF-alpha inhibitors during IBD pregnancy: a systematic review. *BMC Med*, *11*, 174. https://doi.org/10.1186/1741-7015-11-174

Nielsen, P. R., Benros, M. E., & Mortensen, P. B. (2014). Hospital contacts with infection and risk of schizophrenia: a population-based cohort study with linkage of Danish national registers. *Schizophr Bull*, *40*(6), 1526-1532. https://doi.org/10.1093/schbul/sbt200

Norgard, B. M., Jolving, L. R., Larsen, M. D., & Friedman, S. (2019). Parental IBD and Long-term Health Outcomes in the Offspring. *Inflamm Bowel Dis*, *25*(8), 1339-1348. https://doi.org/10.1093/ibd/izy396

Noworyta-Sokolowska, K., Gorska, A., & Golembiowska, K. (2013). LPS-induced oxidative stress and inflammatory reaction in the rat striatum. *Pharmacol Rep*, *65*(4), 863-869. https://doi.org/10.1016/s1734-1140(13)71067-3

O'Reilly, J. R., & Reynolds, R. M. (2013). The risk of maternal obesity to the long-term health of the offspring. In *Clinical Endocrinology* (Vol. 78, pp. 9-16).

Ohkusa, T. (1985). Production of Experimental Ulcerative Colitis in Hamsters by Dextran Sulfate Sodium and Change in Intestinal Microflora. *Nippon Shokakibyo Gakkai Zasshi*, *82*, 1327-1336. https://doi.org/10.11405/nisshoshi1964.82.1327

Okayasu, I., Hatakeyama, S., Yamada, M., Ohkusa, T., Inagaki, Y., & Nakaya, R. (1990). A novel method in the induction of reliable experimental acute and chronic

ulcerative colitis in mice. *Gastroenterology*, *98*, 694-702. https://doi.org/10.1016/0016-5085(90)90290-H

Olton, D. S., & Samuelson, R. J. (1976). Remembrance of places passed: Spatial memory in rats. *Journal of Experimental Psychology: Animal Behavior Processes*, *2*(2), 97-116. https://doi.org/10.1037/0097-7403.2.2.97

Ortega, A., Jadeja, V., & Zhou, H. (2011). Postnatal development of lipopolysaccharide-induced inflammatory response in the brain. *Inflamm Res*, *60*(2), 175-185. https://doi.org/10.1007/s00011-010-0252-y

Pal-Ghosh, S., Tadvalkar, G., Jurjus, R. A., Zieske, J. D., & Stepp, M. A. (2008). BALB/c and C57BL6 mouse strains vary in their ability to heal corneal epithelial debridement wounds. *Experimental Eye Research*, *87*, 478-486. https://doi.org/10.1016/j.exer.2008.08.013

Papp, M., Willner, P., & Muscat, R. (1991). An animal model of anhedonia: attenuation of sucrose consumption and place preference conditioning by chronic unpredictable mild stress. *Psychopharmacology (Berl)*, *104*(2), 255-259. https://doi.org/10.1007/BF02244188

Paraschivescu, C., Barbosa, S., Lorivel, T., Glaichenhaus, N., & Davidovic, L. (2020). Cytokine changes associated with the maternal immune activation (MIA) model of autism: A penalized regression approach. *PLoS ONE*, *15*(8), e0231609. https://doi.org/10.1371/journal.pone.0231609

Park, B. S., & Lee, J. O. (2013). Recognition of lipopolysaccharide pattern by TLR4 complexes. *Exp Mol Med*, *45*(12), e66. https://doi.org/10.1038/emm.2013.97

Patterson, P. H. (2009). Immune involvement in schizophrenia and autism: Etiology, pathology and animal models. *Behavioural Brain Research*, *204*, 313-321. https://doi.org/10.1016/j.bbr.2008.12.016

Pavlov, I. P. (1927). *Conditioned reflexes: an investigation of the physiological activity of the cerebral cortex*. Oxford Univ. Press.

Pedersen, N., Bortoli, A., Duricova, D., R, D. I., Panelli, M. R., Gisbert, J. P., Zoli, G., Lopez-Sanroman, A., Castiglione, F., Riegler, G., Annese, V., Gionchetti, P., Prada, A., Pont, E. D., Timmer, A., Felley, C., Shuhaibar, M., Tsianos, E. V., Dejaco, C.,…European Crohn-Colitis Organisation, E.-S. G. o. E. C.-E. (2013). The course of inflammatory bowel disease during pregnancy and postpartum: a prospective European ECCO-EpiCom Study of 209 pregnant women. *Aliment Pharmacol Ther*, *38*(5), 501-512. https://doi.org/10.1111/apt.12412

Pellow, S., Chopin, P., File, S. E., & Briley, M. (1985). Validation of open:closed arm entries in an elevated plus-maze as a measure of anxiety in the rat. *J Neurosci Methods*, *14*(3), 149-167. https://doi.org/10.1016/0165-0270(85)90031-7

Perry, W., Minassian, A., Feifel, D., & Braff, D. L. (2001). Sensorimotor gating deficits in bipolar disorder patients with acute psychotic mania. *Biol Psychiatry*, *50*(6), 418-424. https://doi.org/10.1016/s0006-3223(01)01184-2

Perry, W., Minassian, A., Lopez, B., Maron, L., & Lincoln, A. (2007). Sensorimotor gating deficits in adults with autism. *Biol Psychiatry*, *61*(4), 482-486. https://doi.org/10.1016/j.biopsych.2005.09.025

Pierik, M., Joossens, S., Van Steen, K., Van Schuerbeek, N., Vlietinck, R., Rutgeerts, P., & Vermeire, S. (2006). Toll-like receptor-1,-2, and-6 polymorphisms influence disease extension in inflammatory bowel diseases. *Inflammatory Bowel Diseases*, *12*(1), 1-8. https://doi.org/DOI 10.1097/01.MIB.0000195389.11645.ab

Pietropaolo, S., Paterna, J. C., Büeler, H., Feldon, J., & Yee, B. K. (2007). Bidirectional changes in water-maze learning following recombinant adenovirus-associated viral vector (rAAV)-mediated brain-derived neurotrophic factor expression in the rat hippocampus. *Behavioural Pharmacology*, *18*, 533-547. https://doi.org/10.1097/FBP.0b013e3282da0bf6

Porsolt, R. D., Anton, G., Blavet, N., & Jalfre, M. (1978). Behavioural despair in rats: A new model sensitive to antidepressant treatments. *European Journal of Pharmacology*, *47*(4), 379-391. https://doi.org/https://doi.org/10.1016/0014-2999(78)90118-8

Porsolt, R. D., Le Pichon, M., & Jalfre, M. (1977). Depression: a new animal model sensitive to antidepressant treatments. *Nature*, *266*(5604), 730-732. https://doi.org/10.1038/266730a0

Pothuizen, H. H. J., Neumann, K. R., Feldon, J., & Yee, B. K. (2006). Selective nucleus accumbens core lesions enhance dizocilpine-induced but not apomorphine-induced disruption of prepulse inhibition in rats. *Behavioural Pharmacology*, *17*, 107-117. https://doi.org/10.1097/01.fbp.0000190683.00232.ec

Prentice, R. E., Hunt, R. W., Spittle, A. J., Ditchfield, M., Chen, J., Burns, M., Flanagan, E. K., Wright, E., Ross, A. L., Goldberg, R., & Bell, S. J. (2024). Well controlled maternal inflammatory bowel disease does not increase the risk of abnormal neurocognitive outcome screening in offspring. *Brain, Behavior, and Immunity - Health*, *40*. https://doi.org/10.1016/j.bbih.2024.100827

Rakoff-Nahoum, S., Paglino, J., Eslami-Varzaneh, F., Edberg, S., & Medzhitov, R. (2004). Recognition of commensal microflora by toll-like receptors is required for intestinal homeostasis. *Cell*, *118*(2), 229-241. https://doi.org/10.1016/j.cell.2004.07.002

Randhawa, P. K., Singh, K., Singh, N., & Jaggi, A. S. (2014). A review on chemical-

induced inflammatory bowel disease models in rodents. *Korean J Physiol Pharmacol*, *18*(4), 279-288. https://doi.org/10.4196/kjpp.2014.18.4.279

Rapoport, J., Chavez, A., Greenstein, D., Addington, A., & Gogtay, N. (2009). Autism spectrum disorders and childhood-onset schizophrenia: clinical and biological contributions to a relation revisited. *J Am Acad Child Adolesc Psychiatry*, *48*(1), 10-18. https://doi.org/10.1097/CHI.0b013e31818b1c63

Rath, P. C., & Aggarwal, B. B. (1999). TNF-induced signaling in apoptosis. *J Clin Immunol*, *19*(6), 350-364. https://doi.org/10.1023/a:1020546615229

Rescorla, R. A., & Wagner, A. R. (1972). A theory of Pavlovian conditioning: Variations in the effectiveness of reinforcement and non-reinforcement. In *Classical conditioning, Current research and theory* (Vol. 2, pp. 64-69). Appleton-Century-Crofts.

Rexrode, L. E., Hartley, J., Showmaker, K. C., Challagundla, L., Vandewege, M. W., Martin, B. E., Blair, E., Bollavarapu, R., Antonyraj, R. B., Hilton, K., Gardiner, A., Valeri, J., Gisabella, B., Garrett, M. R., Theoharides, T. C., & Pantazopoulos, H. (2024). Molecular profiling of the hippocampus of children with autism spectrum disorder. *Molecular Psychiatry*, *29*(7), 1968-1979. https://doi.org/10.1038/s41380-024-02441-8

Richetto, J., Calabrese, F., Meyer, U., & Riva, M. A. (2013). Prenatal versus postnatal maternal factors in the development of infection-induced working memory impairments in mice. *Brain Behav Immun*, *33*, 190-200. https://doi.org/10.1016/j.bbi.2013.07.006

Rizzo, L., Danion, J. M., VanderLinden, M., Grange, D., & Rohmer, J. G. (1996). Impairment of memory for spatial context in schizophrenia. *Neuropsychology*, *10*(3), 376-384. https://doi.org/Doi 10.1037/0894-4105.10.3.376

Rogler, G., & Andus, T. (1998). Cytokines in inflammatory bowel disease. *World J Surg*, *22*(4), 382-389. https://doi.org/10.1007/s002689900401

Roy, M. A., Maziade, M., Labbe, A., & Merette, C. (2001). Male gender is associated with deficit schizophrenia: a meta-analysis. *Schizophr Res*, *47*(2-3), 141-147. https://doi.org/10.1016/s0920-9964(99)00231-5

Rung, J. P., Carlsson, A., Ryden Markinhuhta, K., & Carlsson, M. L. (2005). (+)-MK-801 induced social withdrawal in rats; a model for negative symptoms of schizophrenia. *Prog Neuropsychopharmacol Biol Psychiatry*, *29*(5), 827-832. https://doi.org/10.1016/j.pnpbp.2005.03.004

Sadik, A., Dardani, C., Pagoni, P., Havdahl, A., Stergiakouli, E., i, P. A. S. D. W. G., Khandaker, G. M., Sullivan, S. A., Zammit, S., Jones, H. J., Davey Smith, G., Dalman, C., Karlsson, H., Gardner, R. M., & Rai, D. (2022). Parental

inflammatory bowel disease and autism in children. *Nat Med*, *28*(7), 1406-1411. https://doi.org/10.1038/s41591-022-01845-9

Sakai, J. (2020). Core Concept: How synaptic pruning shapes neural wiring during development and, possibly, in disease. *Proc Natl Acad Sci U S A*, *117*(28), 16096-16099. https://doi.org/10.1073/pnas.2010281117

Sanderson, D. J., Gray, A., Simon, A., Taylor, A. M., Deacon, R. M., Seeburg, P. H., Sprengel, R., Good, M. A., Rawlins, J. N., & Bannerman, D. M. (2007). Deletion of glutamate receptor-A (GluR-A) AMPA receptor subunits impairs one-trial spatial memory. *Behav Neurosci*, *121*(3), 559-569. https://doi.org/10.1037/0735-7044.121.3.559

Sanderson, D. J., Pearce, J. M., Kyd, R. J., & Aggleton, J. P. (2006). The importance of the rat hippocampus for learning the structure of visual arrays. *Eur J Neurosci*, *24*(6), 1781-1788. https://doi.org/10.1111/j.1460-9568.2006.05035.x

Save, E., & Poucet, B. (2000). Hippocampal-parietal cortical interactions in spatial cognition. *Hippocampus*, *10*(4), 491-499. https://doi.org/10.1002/1098-1063(2000)10:4<491::AID-HIPO16>3.0.CO;2-0

Scarborough, J., Iachizzi, M., Schalbetter, S. M., Muller, F. S., Weber-Stadlbauer, U., & Richetto, J. (2024). Prenatal and postnatal influences on behavioral development in a mouse model of preconceptional stress. *Neurobiol Stress*, *29*, 100614. https://doi.org/10.1016/j.ynstr.2024.100614

Scarborough, J., Mattei, D., Dorner-Ciossek, C., Sand, M., Arban, R., Rosenbrock, H., Richetto, J., & Meyer, U. (2021). Symptomatic and preventive effects of the novel phosphodiesterase-9 inhibitor BI 409306 in an immune-mediated model of neurodevelopmental disorders. *Neuropsychopharmacology*, *46*, 1526-1534. https://doi.org/10.1038/s41386-021-01016-3

Schwartzer, J. J., Careaga, M., Chang, C., Onore, C. E., & Ashwood, P. (2015). Allergic fetal priming leads to developmental, behavioral and neurobiological changes in mice. *Translational Psychiatry*, *5*, e543-e543. https://doi.org/10.1038/tp.2015.40

Schwartzer, J. J., Careaga, M., Coburn, M. A., Rose, D. R., Hughes, H. K., & Ashwood, P. (2017). Behavioral impact of maternal allergic-asthma in two genetically distinct mouse strains. *Brain, Behavior, and Immunity*, *63*, 99-107. https://doi.org/10.1016/j.bbi.2016.09.007

Schwendener, S., Meyer, U., & Feldon, J. (2009). Deficient maternal care resulting from immunological stress during pregnancy is associated with a sex-dependent enhancement of conditioned fear in the offspring. *J Neurodev Disord*, *1*(1), 15-32. https://doi.org/10.1007/s11689-008-9000-9

Seligman, M. E., & Maier, S. F. (1967). Failure to escape traumatic shock. *Journal of Experimental Psychology*, *74*(1), 1-9. https://doi.org/10.1037/h0024514

Sertan Copoglu, U., Virit, O., Hanifi Kokacya, M., Orkmez, M., Bulbul, F., Binnur Erbagci, A., Semiz, M., Alpak, G., Unal, A., Ari, M., & Savas, H. A. (2015). Increased oxidative stress and oxidative DNA damage in non-remission schizophrenia patients. *Psychiatry Res*, *229*(1-2), 200-205. https://doi.org/10.1016/j.psychres.2015.07.036

Shan, Y., Lee, M., & Chang, E. B. (2022). The Gut Microbiome and Inflammatory Bowel Diseases. *Annu Rev Med*, *73*, 455-468. https://doi.org/10.1146/annurev-med-042320-021020

Sheng, J. A., Christenson, J. R., Schwerdtfeger, L. A., & Tobet, S. A. (2024). Maternal immune activation by toll-like receptor 7 agonist during mid-gestation increases susceptibility to blood-brain barrier leakage after puberty. *Brain Behavior and Immunity Integrative*, *8*, 100081-100081. https://doi.org/10.1016/j.bbii.2024.100081

Sheng, J. A., & Tobet, S. A. (2024). Maternal immune activation with toll-like receptor 7 agonist during mid-gestation alters juvenile and adult developmental milestones and behavior. *Journal of Neuroendocrinology*, *36*. https://doi.org/10.1111/jne.13417

Shero, N., & Pandeya, D. R. (2022). Impact of Crohn's disease during pregnancy on children with attention deficit hyperactivity disorder: A review. *Annals of medicine and surgery (2012)*, *75*, 103369-103369. https://doi.org/10.1016/j.amsu.2022.103369

Shi, L., Fatemi, S. H., Sidwell, R. W., & Patterson, P. H. (2003). Maternal influenza infection causes marked behavioral and pharmacological changes in the offspring. *Journal of Neuroscience*, *23*, 297-302. https://doi.org/10.1523/jneurosci.23-01-00297.2003

Shipman, S. L., Baker, E. K., Pearlson, G., & Astur, R. S. (2009). Absence of established sex differences in patients with schizophrenia on a two-dimensional object array task. *Psychiatry Res*, *166*(2-3), 158-165. https://doi.org/10.1016/j.psychres.2008.01.012

Silverman, J. L., Yang, M., Lord, C., & Crawley, J. N. (2010). Behavioural phenotyping assays for mouse models of autism. *Nat Rev Neurosci*, *11*(7), 490-502. https://doi.org/10.1038/nrn2851

Smith, S. E., Li, J., Garbett, K., Mirnics, K., & Patterson, P. H. (2007). Maternal immune activation alters fetal brain development through interleukin-6. *J Neurosci*, *27*(40), 10695-10702. https://doi.org/10.1523/JNEUROSCI.2178-

07.2007

Spear, L. P. (2000). The adolescent brain and age-related behavioral manifestations. *Neurosci Biobehav Rev*, *24*(4), 417-463. https://doi.org/10.1016/s0149-7634(00)00014-2

Spini, V., Ferreira, F. R., Gomes, A. O., Duarte, R. M. F., Oliveira, V. H. S., Costa, N. B., Ferreira, A. F. F., Dourado, M. P. B., & Ribeiro-Barbosa, E. R. (2020). Maternal Immune Activation with H1N1 or Toxoplasma gondii Antigens Induces Behavioral Impairments Associated with Mood Disorders in Rodents. *Neuropsychobiology*, *80*(3), 234-241. https://doi.org/10.1159/000510791

Steele, R. J., & Morris, R. G. (1999). Delay-dependent impairment of a matching-to-place task with chronic and intrahippocampal infusion of the NMDA-antagonist D-AP5. *Hippocampus*, *9*(2), 118-136. https://doi.org/10.1002/(SICI)1098-1063(1999)9:2<118::AID-HIPO4>3.0.CO;2-8

Stephens, D. N., Meldrum, B. S., Weidmann, R., Schneider, C., & Grutzner, M. (1986). Does the excitatory amino acid receptor antagonist 2-APH exhibit anxiolytic activity? *Psychopharmacology (Berl)*, *90*(2), 166-169. https://doi.org/10.1007/BF00181234

Su, C., Salzberg, B. A., Lewis, J. D., Deren, J. J., Kornbluth, A., Katzka, D. A., Stein, R. B., Adler, D. R., & Lichtenstein, G. R. (2002). Efficacy of anti-tumor necrosis factor therapy in patients with ulcerative colitis. *Am J Gastroenterol*, *97*(10), 2577-2584. https://doi.org/10.1111/j.1572-0241.2002.06026.x

Sun, K. T., Lam, J. W. Y., Tai, W. C. S., Lau, B. W. M., & Yee, B. K. (2022). Within-subjects vs between-subjects co-variation of prepulse-elicited reaction and the diminution of startle to the succeeding pulse stimulus in the prepulse inhibition paradigm. *Behav Brain Res*, *430*, 113924. https://doi.org/10.1016/j.bbr.2022.113924

Susser, E., & St Clair, D. (2013). Prenatal famine and adult mental illness: Interpreting concordant and discordant results from the Dutch and Chinese Famines. *Social Science & Medicine*, *97*, 325-330. https://doi.org/10.1016/j.socscimed.2013.02.049

Swerdlow, N. R., Benbow, C. H., Zisook, S., Geyer, M. A., & Braff, D. L. (1993). A preliminary assessment of sensorimotor gating in patients with obsessive compulsive disorder. *Biol Psychiatry*, *33*(4), 298-301. https://doi.org/10.1016/0006-3223(93)90300-3

Swerdlow, N. R., Braff, D. L., & Geyer, M. A. (1999). Cross-species studies of sensorimotor gating of the startle reflex. *Ann N Y Acad Sci*, *877*, 202-216. https://doi.org/10.1111/j.1749-6632.1999.tb09269.x

Swerdlow, N. R., Braff, D. L., & Geyer, M. A. (2000). Animal models of deficient sensorimotor gating: what we know, what we think we know, and what we hope to know soon. *Behav Pharmacol*, *11*(3-4), 185-204. https://doi.org/10.1097/00008877-200006000-00002

Swerdlow, N. R., Braff, D. L., Taaid, N., & Geyer, M. A. (1994). Assessing the validity of an animal model of deficient sensorimotor gating in schizophrenic patients. *Arch Gen Psychiatry*, *51*(2), 139-154. https://doi.org/10.1001/archpsyc.1994.03950020063007

Swerdlow, N. R., & Geyer, M. A. (1998). Using an animal model of deficient sensorimotor gating to study the pathophysiology and new treatments of schizophrenia. *Schizophr Bull*, *24*(2), 285-301. https://doi.org/10.1093/oxfordjournals.schbul.a033326

Swerdlow, N. R., Paulsen, J., Braff, D. L., Butters, N., Geyer, M. A., & Swenson, M. R. (1995). Impaired prepulse inhibition of acoustic and tactile startle response in patients with Huntington's disease. *J Neurol Neurosurg Psychiatry*, *58*(2), 192-200. https://doi.org/10.1136/jnnp.58.2.192

Szebeni, B., Veres, G., Dezsõfi, A., Rusai, K., Vannay, Á., Mraz, M., Majorova, E., & Arató, A. (2008). Increased expression of Toll-like receptor (TLR) 2 and TLR4 in the colonic mucosa of children with inflammatory bowel disease. *Clinical and Experimental Immunology*, *151*, 34-41. https://doi.org/10.1111/j.1365-2249.2007.03531.x

Tiede, G. M., & Walton, K. M. (2021). Social endophenotypes in autism spectrum disorder: A scoping review. *Dev Psychopathol*, *33*(4), 1381-1409. https://doi.org/10.1017/S0954579420000577

Treit, D., Menard, J., & Royan, C. (1993). Anxiogenic stimuli in the elevated plus-maze. *Pharmacol Biochem Behav*, *44*(2), 463-469. https://doi.org/10.1016/0091-3057(93)90492-c

Turnbull, A. V., Prehar, S., Kennedy, A. R., Little, R. A., & Hopkins, S. J. (2003). Interleukin-6 is an afferent signal to the hypothalamo-pituitary-adrenal axis during local inflammation in mice. *Endocrinology*, *144*(5), 1894-1906. https://doi.org/10.1210/en.2002-220964

Valls-Sole, J., Valldeoriola, F., Molinuevo, J. L., Cossu, G., & Nobbe, F. (1999). Prepulse modulation of the startle reaction and the blink reflex in normal human subjects. *Exp Brain Res*, *129*(1), 49-56. https://doi.org/10.1007/s002210050935

Vardigan, J. D., Huszar, S. L., McNaughton, C. H., Hutson, P. H., & Uslaner, J. M. (2010). MK-801 produces a deficit in sucrose preference that is reversed by clozapine, D-serine, and the metabotropic glutamate 5 receptor positive

allosteric modulator CDPPB: relevance to negative symptoms associated with schizophrenia? *Pharmacol Biochem Behav*, *95*(2), 223-229. https://doi.org/10.1016/j.pbb.2010.01.010

Vigod, S. N., Kurdyak, P., Brown, H. K., Nguyen, G. C., Targownik, L. E., Seow, C. H., Kuenzig, M. E., & Benchimol, E. I. (2019). Inflammatory bowel disease and new-onset psychiatric disorders in pregnancy and post partum: a population-based cohort study. *Gut*, *68*(9), 1597-+. https://doi.org/10.1136/gutjnl-2018-317610

Vorhees, C. V., Graham, D. L., Braun, A. A., Schaefer, T. L., Skelton, M. R., Richtand, N. M., & Williams, M. T. (2012). Prenatal immune challenge in rats: Altered responses to dopaminergic and glutamatergic agents, prepulse inhibition of acoustic startle, and reduced route-based learning as a function of maternal body weight gain after prenatal exposure to poly IC. *Synapse*, *66*, 725-737. https://doi.org/10.1002/syn.21561

Vorhees, C. V., Graham, D. L., Braun, A. A., Schaefer, T. L., Skelton, M. R., Richtand, N. M., & Williams, M. T. (2015). Prenatal immune challenge in rats: Effects of polyinosinic-polycytidylic acid on spatial learning, prepulse inhibition, conditioned fear, and responses to MK-801 and amphetamine. *Neurotoxicology and Teratology*, *47*, 54-65. https://doi.org/10.1016/j.ntt.2014.10.007

Vorhees, C. V., & Williams, M. T. (2006). Morris water maze: procedures for assessing spatial and related forms of learning and memory. *Nat Protoc*, *1*(2), 848-858. https://doi.org/10.1038/nprot.2006.116

Vuillermot, S., Luan, W., Meyer, U., & Eyles, D. (2017). Vitamin D treatment during pregnancy prevents autism-related phenotypes in a mouse model of maternal immune activation. *Molecular Autism*, *8*. https://doi.org/10.1186/s13229-017-0125-0

Vukovic, J., Borlikova, G. G., Ruitenberg, M. J., Robinson, G. J., Sullivan, R. K., Walker, T. L., & Bartlett, P. F. (2013). Immature doublecortin-positive hippocampal neurons are important for learning but not for remembering. *J Neurosci*, *33*(15), 6603-6613. https://doi.org/10.1523/JNEUROSCI.3064-12.2013

Wagner, A. R., & Brandon, S. E. (1981). SOP: a model of automatic memory processing in animal behaviour. In N. E. Spear & R. R. Miller (Eds.), *Information Processing in Animals: Memory Mechanisms* (pp. 5-47). Erlbaum.

Waterhouse, U., Brennan, K. A., & Ellenbroek, B. A. (2018). Nicotine self-administration reverses cognitive deficits in a rat model for schizophrenia. *Addict Biol*, *23*(2), 620-630. https://doi.org/10.1111/adb.12517

Waterhouse, U., Roper, V. E., Brennan, K. A., & Ellenbroek, B. A. (2016). Nicotine ameliorates schizophrenia-like cognitive deficits induced by maternal LPS exposure: a study in rats. *Dis Model Mech*, *9*(10), 1159-1167. https://doi.org/10.1242/dmm.025072

Weiner, I. (2003). The "two-headed" latent inhibition model of schizophrenia: modeling positive and negative symptoms and their treatment. *Psychopharmacology (Berl)*, *169*(3-4), 257-297. https://doi.org/10.1007/s00213-002-1313-x

Willi, R., Weinmann, O., Winter, C., Klein, J., Sohr, R., Schnell, L., Yee, B. K., Feldon, J., & Schwab, M. E. (2010). Constitutive genetic deletion of the growth regulator Nogo-A induces schizophrenia-related endophenotypes. *J Neurosci*, *30*(2), 556-567. https://doi.org/10.1523/JNEUROSCI.4393-09.2010

Williams, J. H., Wellman, N. A., Geaney, D. P., Cowen, P. J., Feldon, J., & Rawlins, J. N. (1998). Reduced latent inhibition in people with schizophrenia: an effect of psychosis or of its treatment. *Br J Psychiatry*, *172*, 243-249. https://doi.org/10.1192/bjp.172.3.243

Willner, P., Towell, A., Sampson, D., Sophokleous, S., & Muscat, R. (1987). Reduction of sucrose preference by chronic unpredictable mild stress, and its restoration by a tricyclic antidepressant. *Psychopharmacology (Berl)*, *93*(3), 358-364. https://doi.org/10.1007/BF00187257

Wirtz, S., Popp, V., Kindermann, M., Gerlach, K., Weigmann, B., Fichtner-Feigl, S., & Neurath, M. F. (2017). Chemically induced mouse models of acute and chronic intestinal inflammation. *Nature Protocols*, *12*, 1295-1309. https://doi.org/10.1038/nprot.2017.044

Woo, T. U., & Crowell, A. L. (2005). Targeting synapses and myelin in the prevention of schizophrenia. *Schizophr Res*, *73*(2-3), 193-207. https://doi.org/10.1016/j.schres.2004.07.022

Woods, R. M., Lorusso, J. M., Fletcher, J., ElTaher, H., McEwan, F., Harris, I., Kowash, H. M., D'Souza, S. W., Harte, M., Hager, R., & Glazier, J. D. (2023). Maternal immune activation and role of placenta in the prenatal programming of neurodevelopmental disorders. In *Neuronal Signaling* (Vol. 7): Portland Press Ltd.

Woods, R. M., Lorusso, J. M., Potter, H. G., Neill, J. C., Glazier, J. D., & Hager, R. (2021). Maternal immune activation in rodent models: A systematic review of neurodevelopmental changes in gene expression and epigenetic modulation in the offspring brain. *Neurosci Biobehav Rev*, *129*, 389-421. https://doi.org/10.1016/j.neubiorev.2021.07.015

Wu, W. L., Hsiao, E. Y., Yan, Z., Mazmanian, S. K., & Patterson, P. H. (2017). The

placental interleukin-6 signaling controls fetal brain development and behavior. *Brain, Behavior, and Immunity*, *62*, 11–23. https://doi.org/10.1016/j.bbi.2016.11.007

Wusteman, M., Wight, D. G., & Elia, M. (1990). Protein metabolism after injury with turpentine: a rat model for clinical trauma. *Am J Physiol*, *259*(6 Pt 1), E763-769. https://doi.org/10.1152/ajpendo.1990.259.6.E763

Xi, D., Zhang, W., Wang, H. X., Stradtman, G. G., & Gao, W. J. (2009). Dizocilpine (MK-801) induces distinct changes of N-methyl-D-aspartic acid receptor subunits in parvalbumin-containing interneurons in young adult rat prefrontal cortex. *Int J Neuropsychopharmacol*, *12*(10), 1395-1408. https://doi.org/10.1017/S146114570900042X

Yang, C., & Merlin, D. (2024). Unveiling Colitis: A Journey through the Dextran Sodium Sulfate-induced Model. In *Inflammatory Bowel Diseases* (Vol. 30, pp. 844-853): Oxford University Press.

Yang, C. T., Yen, H. H., Su, P. Y., Chen, Y. Y., & Huang, S. P. (2024). High prevalence of vitamin D deficiency in Taiwanese patients with inflammatory bowel disease. *Sci Rep*, *14*(1), 14091. https://doi.org/10.1038/s41598-024-64930-8

Yee, B. K., Balic, E., Singer, P., Schwerdel, C., Grampp, T., Gabernet, L., Knuesel, I., Benke, D., Feldon, J., Mohler, H., & Boison, D. (2006). Disruption of glycine transporter 1 restricted to forebrain neurons is associated with a procognitive and antipsychotic phenotypic profile. *J Neurosci*, *26*(12), 3169-3181. https://doi.org/10.1523/JNEUROSCI.5120-05.2006

Yee, B. K., Chang, T., Pietropaolo, S., & Feldon, J. (2005). The expression of prepulse inhibition of the acoustic startle reflex as a function of three pulse stimulus intensities, three prepulse stimulus intensities, and three levels of startle responsiveness in C57BL6/J mice. *Behav Brain Res*, *163*(2), 265-276. https://doi.org/10.1016/j.bbr.2005.05.013

Yee, B. K., & Singer, P. (2013). A conceptual and practical guide to the behavioural evaluation of animal models of the symptomatology and therapy of schizophrenia. *Cell Tissue Res*, *354*(1), 221-246. https://doi.org/10.1007/s00441-013-1611-0

Yu, A., Friedman, S., & Ananthakrishnan, A. N. (2021). Characteristics and Long-Term Outcomes of Pregnancy-Onset Inflammatory Bowel Disease: A Case-Control Study. *Inflamm Bowel Dis*, *27*(4), 476-481. https://doi.org/10.1093/ibd/izaa096

Zetterstrom, M., Sundgren-Andersson, A. K., Ostlund, P., & Bartfai, T. (1998). Delineation of the proinflammatory cytokine cascade in fever induction. *Ann N Y Acad Sci*, *856*, 48-52. https://doi.org/10.1111/j.1749-6632.1998.tb08311.x

Zhao, X., Erickson, M., Mohammed, R., & Kentner, A. C. (2022). Maternal immune activation accelerates puberty initiation and alters mechanical allodynia in male and female C57BL6/J mice. *Dev Psychobiol*, *64*(5), e22278. https://doi.org/10.1002/dev.22278

Zorrilla, E. P. (1997). Multiparous species present problems (and possibilities) to developmentalists. *Dev Psychobiol*, *30*(2), 141-150. https://doi.org/10.1002/(sici)1098-2302(199703)30:2<141::aid-dev5>3.0.co;2-q

Zuckerman, L., & Weiner, I. (2003). Post-pubertal emergence of disrupted latent inhibition following prenatal immune activation. *Psychopharmacology*, *169*, 308-313. https://doi.org/10.1007/s00213-003-1461-7

Zuckerman, L., & Weiner, I. (2005). Maternal immune activation leads to behavioral and pharmacological changes in the adult offspring. *Journal of Psychiatric Research*, *39*, 311-323. https://doi.org/10.1016/j.jpsychires.2004.08.008